Summer 2019

Historical Floodplain Sedimentation Rates Using Mining Contaminant Profiles, Cesium-137, and Sediment Source Indicators along the Lower Big River, Jefferson County, Missouri

Miranda M. Jordan

Missouri State University, Miranda021@live.missouristate.edu

HISTORICAL FLOODPLAIN SEDIMENTATION RATES USING MINING

CONTAMINANT PROFILES, CESIUM-137, AND SEDIMENT SOURCE INDICATORS

ALONG THE LOWER BIG RIVER, JEFFERSON COUNTY, MISSOURI

A Master's Thesis

Presented to

The Graduate College of

Missouri State University

In Partial Fulfillment

Of the Requirements for the Degree

Master of Science, Geospatial Science

By

Miranda Marie Jordan

August 2019

HISTORICAL FLOODPLAIN SEDIMENTATION RATES USING MINING CONTAMINANT PROFILES, CESIUM-137, AND SEDIMENT SOURCE INDICATORS ALONG THE LOWER BIG RIVER, JEFFERSON COUNTY, MISSOURI

Geography, Geology, and Planning

Missouri State University, August 2019

Master of Science

Miranda Marie Jordan

ABSTRACT

Floodplain sedimentology and geochemistry can indicate the age of sediment layers to evaluate the history of human-caused sedimentation in a watershed. While the Ozark Highlands of Missouri has had a long history of settlement and land disturbance beginning in the early 1800s, there are few studies that have investigated the effects of these anthropogenic activities on river form and legacy sedimentation. The goal of this study is to characterize the sediment properties and geochemical trends in post-settlement floodplain deposits along lower Big River in Jefferson County, Missouri. This study evaluated trends of sediment properties at 3 cm intervals in a 4 m floodplain core. In addition, eleven cores were collected and assessed at 5 to 20 cm intervals from four alluvial landforms including near-channel bench (1 core), floodplain (7), back-swamp (1), and low terrace (2). Stratigraphic indicators used to date the deposits included: (i) Lead and zinc profiles linked to the history of ore production in the Old Lead Belt; (ii) ^{137}Cs activity released by atomic bomb testing in the 1950-60s; (iii) Sand content peaks caused by large floods recorded by a long-term discharge gage; and (iv) Land use records published in the agricultural census. From about 1860 to 1917 floodplain deposition rates were relatively low ranging from 1.6 to 2.4 cm/yr. Deposition rates peaked between 1947 and 1950 averaging 6.7 cm/yr. After 1957, sedimentation rates decreased to an average 0.77 cm/yr through 2018. Peak sedimentation rates in the lower Big River occurred 20-30 years after peak land use disturbance in the watershed suggesting that river response to European settlement occurred later in lower main channel compared to headwaters streams.

KEYWORDS: sediment contamination, mining, Old Lead Belt, Big River, legacy sediment, sedimentation rates

HISTORICAL FLOODPLAIN SEDIMENTATION RATES USING MINING

CONTAMINANT PROFILES, CESIUM-137, AND SEDIMENT SOURCE INDICATORS

ALONG THE LOWER BIG RIVER, JEFFERSON COUNTY, MISSOURI

By

Miranda Marie Jordan

A Master's Thesis
Submitted to the Graduate College
Of Missouri State University
In Partial Fulfillment of the Requirements
For the Degree of Master of Science, Geospatial Science

August 2019

Approved:

Robert T. Pavlowsky, PhD, Thesis Committee Chair

Melida Gutierrez, PhD, Committee Member

Xiaomin Qiu, PhD, Committee Member

Julie Masterson, PhD, Dean of the Graduate College

In the interest of academic freedom and the principle of free speech, approval of this thesis
indicates the format is acceptable and meets the academic criteria for the discipline as
determined by the faculty that constitute the thesis committee. The content and views expressed
in this thesis are those of the student-scholar and are not endorsed by Missouri State University,
its Graduate College, or its employees.

ACKNOWLEDGEMENTS

TABLE OF CONTENTS

LIST OF TABLES

LIST OF FIGURES

INTRODUCTION

Fine-grained floodplains form by the deposition of river sediment over land areas adjacent to the channel during overbank floods (Junk et al., 1989; Lecce, 2000). Overbank floods are generated by relatively high rates of runoff from uplands and slopes into a river system as the result of large rainfall or snowmelt events. The magnitude (or depth) and frequency of overbank floods provide the primary mechanism for the development and structuring of floodplains across the valley floor (Pizzutto, 1987; Thayer and Ashmore, 2016). The amount of sediment available for deposition on a floodplain is controlled by: (i) delivery rate of fine-grained (<250 µm) sediment from the watershed to the channel system, (ii) amount (or load) of suspended sediment being carried by the river, and (iii) depth of inundation and lateral extent of accommodation space for deposition across the valley floor (Wolman and Leopold, 1957; Lecce, 1997; Swennen and Van der Sluys, 1998). Once deposited, floodplain sediment can remain stored for decades to centuries or longer until being remobilized by erosion (Lecce and Pavlowsky, 2001; Macklin et al., 2006). Therefore, floodplains serve as intermediate sediment storages in watersheds, functioning as a sediment sink during periods of floodplain development and sediment source during episodes of bank erosion, mass-wasting, and chute incision when sediment is released back to the channel for downstream transport (Lecce and Pavlowsky, 1997).

Floodplains develop on the valley floor by the progressive deposition of fine-grained overbank sediment over coarser-grained channel deposits over time (Figure 1a). Channel migration across the valley floor erodes stored sediment from the outside of the bend to form a cut-bank and deposit channel material on the inside of the bend to form a point bar (Figure 1b). Therefore, floodplains are created by both lateral accretion of channel sediment across the valley

1

floor and vertical accretion of overbank deposits to build bank height (Wolman and Leopold, 1957; Knox, 1987; Lecce, 1997; Walling and He, 1998; Dean et al., 2011; Hupp et al., 2015) (Figure 2). Oblique accretion is a combination of vertical and lateral accretion and is an important process in low-gradient meandering river floodplains where interbedded layers of mud and sand are deposited when the lateral migration of the river is constrained (Nanson, 1986; Page et al., 2003; Dean et al., 2011).

Geomorphic landscape features associated with floodplain development including levees, back-swamps, chutes, oxbows, and fans indicate the history of channel activity and floodplain deposition along a stream segment (Figure 1b). During overbank flood events, flows carrying excess sediment are dispersed across adjacent floodplains and deposit coarser-grained sediments (sand) closer to the channel as levee deposits and fine-grained sediments out across the floodplain (silt and clay) (Happ et al., 1940). Thus, thicker floodplain deposits tend to be located adjacent to the channel, with thinner deposits located within back-swamp areas near the valley margin. During a flood, channel banks and levee deposits can breach allowing higher velocity flows from the channel to spread laterally and form splay deposits composed of fan-like lobe of sand and fine gravel across the floodplain surface (Happ et al., 1940). Adjacent to levee and splay features and further from the channel are lower elevation landforms known as back-swamps (Nanson and Croke, 1992). Back-swamps are typically inundated during periods of high water and offer areas for flood water storage and downstream drainage at flow velocities lower than those in the channel. Shallow secondary channels formed in back-swamp areas or along the inside of bends on bars and floodplains which convey localized flows of moderate velocity during floods are called chutes (Constantine et al., 2010). Another alluvial landform indicative of the channel migration processes is an oxbow where the channel has eroded through the neck of a

meander bend, effectively shortening channel length, leaving the cutoff channel loop to form a pond and slowly fill in with fine sediment (Constantine et al., 2010).

In general, the width, bank height, and flow capacity of a channel is controlled by the magnitude of peak discharges and associated stream power produced by annual floods (Gomez et al., 1999; Hupp, 2000; James and Lecce, 2013). Alluvial rivers can adjust channel depth by floodplain deposition to increase bank height and/or channel erosion and incision to deepen the channel (Wolman and Brush, 1961; Steel, 1974). In humid regions, floodplains in stable condition tend to form to the stage height (or depth) of the peak discharge of the 1-2 year recurrence interval flood, often called the bank-full flood (Wolman and Miller, 1960). Therefore, sustained increases of the magnitude and frequency of river floods caused by climate change can result in a period of channel enlargement and increased sediment deposition rates on floodplains to produce higher banks over timescales from centuries to millennia (Knox, 1972, 2006) (Table 1 and Table 2). In addition, land use disturbances in a watershed caused by widespread land clearing and agricultural settlement that increase runoff and soil erosion rates can produce larger floods which deposit more sediment on floodplains over periods of decades or longer (Knox, 1977, 1987; Trimble and Lund, 1982; Trimble, 1983; Jacobson and Coleman, 1986) (Figure 3).

Urbanization can also increase the frequency of higher flood peaks in downstream channels. Increased runoff from impervious areas such as compacted soils, roads and parking lots, and roof tops and faster delivery of storm water to local streams via storm drains can cause channel erosion and cross-section enlargement (Hammer, 1972). However, the response of floodplain sedimentation rates will be variable, or even limited, since sediment supply to the channel may become exhausted within a decade after the construction phase as landscaping

matures and channel banks are stabilized by resistant rip-rap and concrete (Wolman, 1967; Wolman and Schick, 1967) (Figure 3a).

Besides the overall tendency of larger floods to increase floodplain deposition rates, the influence of soil erosion and sediment delivery rates to the channel must also be considered and can range over two orders of magnitude according to land use. For example, soil erosion rates from roads, bare soils, and grazed lands can be 50 to 100 times greater than from natural woodland areas (James and Lecce, 2013). Moreover, as flood energy increases, channels will respond by erosion to increase their capacity to contain the larger floods (Knox, 1987). Thus, overbank flood frequency and deposition rates may gradually decrease over time as channel and meander belt capacity expands to contain the larger floods and decrease floodplain inundation frequency overtime (James and Lecce, 2013, Trimble 1983). Therefore, it is widely accepted that land use disturbances in a watershed can change flood routing, sediment transport, and alter channel and floodplain form over timescales of years to decades (Knox, 1987; Lecce and Pavlowsky, 2001; Shepherd et al., 2011).

Legacy Floodplain Deposits

Relatively recent overbank floodplain deposits formed as the consequence of human disturbances in the watershed such as agriculture, mining, logging, and urbanization have been described as Legacy deposits (James, 2013) (Figure 3b). The first studies to recognize the significance of human-induced geomorphic changes on river morphology and sedimentation occurred in the 1800s (Marsh, 1864). Studies in the early 1900s sought to explain sedimentation problems and associated channel disturbances within river systems related to agriculture and logging (Ashley, 1910; Bennett, 1931; Happ et al., 1940). One of the first comprehensive studies

to use the sediment budget approach evaluated the effects of hydraulic mining sediment on downstream sedimentation problems in the Sierra Nevada, California (Gilbert, 1917). More recently, studies of effects of land use changes on river channels and floodplains expanded to include accelerated soil erosion and legacy floodplain deposition in many agricultural regions in the USA (Trimble and Crosson, 2000; Wilkinson and McElroy, 2007), historical channel and floodplain evolution associated with legacy deposition (Knox, 1972, 1977, 1987), and channel responses to a series of land-use changes (Wolman, 1967, Kondolf et al., 2001).

Legacy floodplain deposits can contain an important sedimentary and geochemical record of past human activities in a watershed (Wilkinson and McElroy, 2007; James, 2013). Stratigraphic analysis of floodplain cores can yield information on the timing and source of historical sediment delivery from within the watershed using biological, geochemical, and mineralogical properties that reflect landscape conditions before, during, and after European contact (Miller, 1997; Owens et al., 2005; Macklin et al., 2006; James, 2013). In particular, historical mining activities associated with metal contamination in channel and floodplain sediments have been widely used to evaluate sedimentation trends in watersheds (Lecce and Pavlowsky, 1997, 2001; Gazdag and Sipter, 2008; Acosta et al., 2011; Pavlowsky et al., 2017). In many cases, down-core variations of mining metals reflect the production history of the mine and can be used to determine sediment ages to calculate sedimentation rates (Macklin, 1985; Knox, 1987; Lecce and Pavlowsky, 2001, 2014) (Figure 4). Heavy metal concentrations in legacy sediments also have environmental implications since toxic metals can concentrate within fluvial sediments and harm sediment dwelling organisms and other aquatic life, as well as pose a risk to human health (Macklin et al., 2006; Ciszewski and Turner, 2009) and food chain pathways (Kooistra et al., 2001; Gazdag and Sipter, 2008; Huggins, 2016). Metals do not

5

degrade in the environment and can remain biochemically active. Therefore, floodplains deposits

that store contaminated sediments represent a long-term pollution risk within a watershed

(Macklin, 1985; Knox, 1987; Matschullat et al., 1997; Pavlowsky et al., 2017).

Floodplain Deposition Rates

Understanding the distribution and ages of sediment deposits within floodplains can

provide information about landscape disturbances and geomorphic channel responses that have

affected sediment delivery in the past. Deposition rates on floodplains typically average a few

millimeters to centimeters a year (Wohl, 2014). However, spatial patterns of floodplain

sedimentation rates can vary due to changes in flood characteristics, fluvial processes, and land

use throughout the watershed (Lecce, 1997). Floodplain sedimentation rates have been

determined utilizing geochemical, stratigraphic, and remote sensing analyses (Table 1).

Published sedimentation rates typically range from 0 to 13.4 cm/yr under natural and

anthropogenic conditions within the watershed. The highest rates of sedimentation are associated

with anthropogenic causes such as levee breaches (Florsheim and Mount, 2002) and increased

soil erosion and sediment supply (James, 1989; Lecce and Pavlowsky, 2001; Lecce et al., 2008;

Owen et al., 2011; Lecce and Pavlowsky, 2014). Changes in valley width along a stream

segment can also cause sedimentation rates to vary due to hydro-geomorphic forcing

(Magilligan, 1985). Natural conditions that can affect sedimentation rates within floodplains

include natural levee and splay deposits that range from millimeters to tens of centimeters that

decrease in thickness laterally away from the channel during a single flooding event (Hudson,

2005). Other natural conditions that can have an effect on sedimentation rates include erosion

due to climatic conditions and changes in vegetation density (Hupp, 2000).

Historical sedimentation rates on floodplains can be determined utilizing a variety of methods including geochemical (Goodbred, Jr. and Kuel, 1998), textural (Lecce and Pavlowsky, 2014; Leigh, 2018), and historical records such as flood and mining (Florsheim and Mount, 2002; Bain and Brush, 2005; Lecce et al., 2008). Geochemical methods used to constrain sedimentation rates include X-ray Fluorescence (XRF) (Matschullat et al., 1997; Owen et al., 2011; Pavlowsky et al., 2017) Inductively coupled plasma atomic emission spectroscopy (ICP-AES) (Lecce and Pavlowsky, 2001; Bain and Bush, 2005; Lecce et al., 2008), X-ray diffraction (Swennen et al., 1998), magnetic susceptibility (Gomez et al., 1999), and gamma spectroscopy (McCall et al., 1984; Goodbred, Jr., and Kuehl, 1998; Gomez et al., 1999; Bain and Brush, 2005; Owen et al., 2011). Textural analyses such of particle size (Knox, 1987; Owen et al., 2011, Leigh, 2018), and organic matter (Knox, 1987) can provide data to support sedimentation rates constrained by geochemical results. Finally, historical records have been utilized to further constrain dates of sedimentation by providing records of flooding events linked to coarse sand layers in the floodplain (Florsheim and Mount, 2002) and mining events that increase metal concentrations in floodplain deposits formed during periods of peak ore production (Knox, 1987, Lecce and Pavlowsky, 2001; Owen et al., 2011; Pavlowsky et al., 2017) (Figure 5).

Big River Floodplain

This study analyzes the sedimentological and geochemical properties of legacy floodplain deposits to determine variations in sedimentation rates and how they were linked temporally to the environmental and land use history of the Big River Watershed. The study site is located in northern Jefferson County, Missouri and drains 2,375 km^2 of the Ozark Highlands. The floodplain transect investigated extends for 272 m across the valley floor with bank-full surface

elevations ranging from 136 to 137 masl. The site was chosen based on available information from: (i) flood records at a nearby United States Geological Survey (USGS) discharge gage in operation since 1923 (Gage #07018500), (ii) production records from lead (Pb), zinc (Zn), and barium (Ba) mining activities since 1866 (Pavlowsky et el., 2017); (iii) Population and agricultural census records for the counties drained by Big River since the 1840s (https://www.nass.usda.gov/AgCensus/) and (iv) availability of previous river and sediment investigations due to public health concerns and Superfund regulations since the 1980s (https://cumulis.epa.gov/supercpad/cursites/csitinfo.cfm?id=0705443; https://www.fws.gov/fieldnotes/regmap.cfm?arskey=35501). By combining floodplain core characteristics to the stratigraphic indicators and proxy records above related to watershed disturbances and pollutant tracer inputs, this study aims to link historical watershed disturbances to the timing of floodplain deposition and determine sedimentation rate trends for the post settlement period beginning in the early 1800s.

Early Settlement Land use. The pre-settlement vegetation within the Big River valley region was a mixture of yellow pine, walnut, and post oak forest; pine and oak savannah; and tall-grass prairie (Schoolcraft, 1819; Sauer, 1920). The hillslopes had richer soils and yielded sassafras, buckeye, black walnut, papaw, persimmon, shrubs, wild fruits, and grasses (Schoolcraft, 1819; Sauer, 1920). French settled the area in small communities as early as the mid-1700s, and by early 1819, the watershed contained sixteen grist mills, eight saw mills, and ten distilleries in Washington County and several saw and grist mills and three distilleries in Jefferson County (Schoolcraft, 1819). In the Ozark region in general, the main period of widespread land clearing and agricultural settlement occurred during the mid to late 1800s when valley-bottom forests and upland prairies were converted to cultivated fields and pastures

(Jacobson and Primm, 1994). Most of the conversion of forest and prairie to farmland was completed by 1900 with more than half of the watershed in farms (Jacobson and Primm, 1994) (Figure 6). Row-crop production peaked in 1910 with over two million bushels of corn and 600,000 bushels of wheat produced (Figure 7). Livestock including cattle and horses have increased within the watershed since 1940, indicating a land use change from row cropping to pasture farming (Figure 8).

In general, from 1880 to 1920, commercial timber operations harvested shortleaf pine and oak reducing mature forest cover within the upland portions of the watershed (Jacobson and Primm, 1994). However, timber harvesting on a commercial scale probably started earlier in the 1840s – 1850s in the Big River watershed since dams built during that time had by-pass channels for floating logs (Jacobson and Primm, 1997; Suggs, 2008). The post-timber boom period included upland burning, grazing on open range, and increased land for cultivation creating significant channel disturbances with increased sediment yields (Jacobson and Primm, 1994). In addition to increased sediment yields, five mill dams were installed within Jefferson County at Morse Mill, Cedar Hill, Byrnesville, House Springs, and Byrnes Mill (Meneau, 1997).

Geomorphic response to human activity. The anthropogenic soil and vegetation disturbances driven by land clearing for agriculture and timber harvesting resulted in both coarse- and fine-grained legacy sedimentation in the Big River and generally throughout the Ozark Highlands (Jacobson and Primm, 1994; Owen 2011, Pavlowsky and Meyer, 2018). Land clearing and row-cropping resulted in more runoff across valley floors, increased channel erosion and head-cutting, and higher loads of cherty gravel sediment delivered from tributaries to downstream channels (Jacobson and Pugh, 1997). The excess gravel "choked" the channel system in many segments by filling in pools and forming large bar complexes within

9

"disturbance reaches" beginning in larger tributary streams in the 1880s and attenuating in main valley channels in the 1940s (Saucier, 1983; Jacobson and Gran, 1999; Jacobson 2004). Wilkinson and McElroy (2007) did not recognize rivers of the Ozark Highlands as having legacy floodplain deposits. However, some have been identified along some tributaries and main channels in several river systems including the Osage River (Hajic et al., 2007), Spring River (Carlson, 1999; Trimble, 2001), James River (Rodgers, 2005; Owen et al., 2011), and North Fork of the White River (Benn and Ray, 1996). Pavlowsky et al. (2017) documented legacy deposits typically 1.5 to 3.5 m thick on floodplains along 170 km of Big River from Leadwood to the Meramec River.

Mining history. Mining-metal dating can potentially be used to determine floodplain sedimentation rates along the 170 km of Big River from Leadwood to its mouth on the Meramec River. The Big River Watershed has a long and productive metal mining history including over 200 years of shallow pit mining for Pb, almost a century of large-scale, deep shaft mining in the Old Lead Belt in Saint Francois County, and more than a century of shallow pit and strip mining for barite in Washington County (Pavlowsky et al., 2017; Smith and Schumacher, 2018). Galena (lead) ores were first extracted by shovel from shallow pits by French miners near Potosi in Washington County in the early to mid-1700s (Sauer, 1920). Shallow pit lead mining spread to other locations in St. Francois and Jefferson Counties in the 1800s and continued sporadically at a small-scale into the mid-1900s. Overall, while economically important to the region, relatively low tonnages of lead ore were produced from shallow pit mining (Pavlowsky et al., 2017). Globally important lead production began in the Old Lead Belt (OLB) in the late 1800s, peaked between 1927 and 1942, and the last mine (Federal mine) closed in 1972. Overall, the OLB produced over 9 million Mg of Pb metal (Seeger, 2008; Pavlowsky et al., 2017).

During the deep shaft mining period in the Old Lead Belt, large volumes of metalliferous tailings as fine gravel-sized "chats", sand-sized flotation mill tailings, and silt and clay-sized "slimes" were discharged into the Big River in Saint Francois County (MDNR, 2003; Owen et al., 2011; Pavlowsky et al., 2010, 2017) (Figure 9). As a result, channel sediments and floodplain deposits along 170 km of Big River and 10 km of Flat River Creek, a major tributary, are presently contaminated with metals including lead (Pb), cadmium (Cd), zinc (Zn), and barium (Ba) (Smith and Schumacher, 1991, 1993; Gale et al., 2004; Pavlowsky et al., 2010, 2017; Young, 2011; Hill, 2016; Huggins, 2016) (Figure 10). Concerns about the environmental risk of metal toxicity to aquatic life and human health have been reported by Missouri Department of Natural Resources (MDNR), U.S. Fish and Wildlife Service (USFWS), and U.S. Environmental Protection Agency (USEPA) (Hocutt et al., 1978; EPA 2011, 2012; Meneau, 1997; Gale et al., 2004; MDNR 2007, 2013; Mosby et al. 2009). Contaminated tailings piles at the six major mining sites have been stabilized by Superfund programs to reduce on-site contamination sources (https://www.epa.gov/mo/big-river-mine-tailings-national-priorities-list-npl-superfund-site-st-francois-county-missouri). However, there is significant risk of long-term pollution from the release of stored metals within floodplains and active channel sediment to Big River (Mosby et al., 2009; Pavlowsky et al., 2010; Pavlowsky et al., 2017).

Research Problem

In the Ozark Highlands, there are very few records of land use effects on river systems including sediment supply and transport, channel morphology, floodplain conditions, and water quality. In the absence of monitoring data, sedimentary records stored within floodplain sediments can be used to understand local and regional changes within the watershed (Owen et

al., 2011). Therefore, this study focused on investigating legacy sedimentation on floodplains along Big River by correlating physical and geochemical records of watershed events with specific depositional layers in floodplain cores (Owen et al., 2011; Pavlowsky et al., 2017). Although early documentation of flood events is generally lacking in the US, reconstruction of paleofloods can be an effective method in identifying past flooding utilizing sedimentological features (Baker, 2008; Wang and Leigh, 2012). Moreover, there are five USGS flow gaging stations on the main channel of the Big River including one with a record length of 97 years on the lower river at Byrnesville. Besides mining-metals dating of floodplain deposits, changes in sand content can indicate the timing of large floods (Knox and Daniels, 2002; Knox 2006; Zhang et al., 2015; Leigh, 2018). For example, down core trends in sand grain percentages between 0.25 – 0.50 mm in diameter were a good indicator of floods larger than the 10-year recurrence interval in the upper Mississippi River Valley (Knox and Daniels, 2002). Other studies within the US observed that sand grains >0.25 mm in diameter average about 14% in suspended sediment loads during flood events (Simmons, 1993). The amount of sediment deposited on a floodplain can be independent of the magnitude of the flood, however the increased percentages of sand beds in floodplain cores often indicate flood passage nonetheless (Lecce et al., 2004; Wang and Leigh, 2012).

In the lower Big River watershed, there is a lack in knowledge on interpretation of historical floodplain deposition rates due to land use changes. This study will be the first attempt to link land use history to floodplain deposition and in turn interpret paleo-environmental floodplain records in the eastern portion of the Ozarks. In addition to utilizing flood records and land use records, this study will also utilize geochemical and sedimentological indicators to reconstruct an environmental history in the Ozarks utilizing large scale mining operations

histories. Finally, while previous studies in the Ozarks documented historical gravel waves in the Ozarks (Jacobson and Primm, 1994; Jacobson and Pugh, 1997; Jacobson and Gran, 1999), this study will address the effects of land use change on fine-grained sediment supply and floodplain sedimentation in the Ozark Highland region.

Purpose and Objectives

Legacy deposits have been identified along the 180 km length of the Big River in St. Francois and Jefferson Counties (Pavlowsky et al., 2017). However, analysis of stratigraphic profiles in these legacy deposit dynamics and flow variations due to the influences of land use, flood, and local factors have not yet been studied. Therefore, the goal for this study is to characterize legacy deposits including composition, stratigraphy, and deposition rates from the initial settlement period to present at lower Big River. This site was chosen based on its location to the mouth of Big River on the Meramec River and its proximity to the Byrnesville stream gage with a record extending 94 years (USGS 07018500). Aerial imagery and previous channel records indicate that there has been little channel movement in this reach since the 1930s. Thus, the floodplain deposits are expected to contain a complete sedimentological record that has not been interrupted with channel migration. Further, this site has not had major land use change in over 64 years. Legacy sediment and a stratigraphic record of geochemical tracers were believed to be present along this Big River reach based on previous work and the long and productive history of agriculture since 1850 and mining since 1890 (Pavlowsky et al. (2017). The objectives of this study are to:

(1) characterize legacy deposits using floodplain cores and topographic surveys along a segment of lower Big River in Jefferson County;

(2) quantify and date stratigraphic profiles for texture, organic matter, mining pollutants, flood event deposits, ^{137}Cs, and magnetic susceptibility in a 4 meter core;

(3) Link indicator profiles to historical events in the watershed to determine floodplain sedimentation rate (cm/yr) trends at 10 to 20 cm resolution; and

(4) interpret the land use and geomorphological factors that have controlled floodplain deposition rates along the lower Big River.

Benefits

Information gathered from this study will benefit scientific studies, as well as land management programs. Although studies have provided information on land use effects on stream systems, this study will be the first to link watershed land use and other environmental events to historical deposition trends on floodplains to better understand how humans change river landscapes in the eastern Ozarks (Jacobson, 1995; Owen, 2011; Pavlowsky et al., 2017). Variable trends in sedimentation rates within the core also indicate how watershed disturbances are recorded in floodplain deposits in the Ozarks. Previous studies have provided information on the amount of legacy sediments stored in Big River. However, understanding the storage time of deposits within lower Big River floodplains will benefit management plans considering secondary pollution from the remobilization of stored mining-contaminated sediment (Pavlowsky et al., 2017). Secondary pollution may be affecting endangered mussel populations located downstream from the study site, therefore, this study also aids superfund managers and mussel restoration efforts within the lower portions of the watershed (Mosby, 2009; EPA, 2011, 2012). Overall, this study will inform management plans focused on improvements in fluvial stability and ecosystem health and decreasing the long-term risk for secondary pollution related to mining in the Old Lead Belt.

Table 1. Streams with historical floodplain sedimentation rate >2 cm/yr.

Location	Drainage area (km^2)	Sedimentation Rate Range (cm/yr)	Analyses Performed	Source
Waipaoa River, New Zealand	2,200	<1 - >4	Historical records, flood records, 137Cs, 14C, pollen analysis, magnetic susceptibility	Gomez et al., 1999
River Rhine	185,000	> 1 - 12.6	Aerial photography, elevation, floodplain, hydraulic, and vegetation modeling	Geerling et al., 2008
Mayfair Lake, East Branch Reservoir, Lake Rockwell, Ohio	2.4 - 531	0.3 - 2.4	^{137}Cs, ^{210}Pb, Stratigraphic, particle sizing	McCall et al., 1984
Driftless Area within the Upper Mississippi Valley	27; 450	0.3 - 5	Pb, Zn concentrations; Organic matter; soil horizons; textural; comparison to other studies	Knox, 1987
Bear River, California	1,300	4.7 - 7.4 13.4	Coring, mapping, historical records, cross-sections	James, 1989
Blue River Watershed, Wisconsin	2.4 - 128	> 1 - 2.4	Zn concentrations	Lecce and Pavlowsky, 2001
Lower Cosumnes River, Ca	3,000	4 - 10	Survey, sediment sampling, recording high water marks	Florsheim and Mount, 2002
Gold Hill, North Carolina	254	07. - 2.9	Historical records, particle size, Loss on ignition, ICP-AES	Lecce et al., 2008
Gold Hill, North Carolina	254	0.4 - 7.2	Textural analysis, ICP-AES, heavy metal concentration (XRF), historical records	Lecce and Pavlowsky, 2014
Big River, Missouri	2,473	1.3 – 3.1	Pb, Zn concentrations	Pavlowsky et al., 2017

Table 2. Streams with historical floodplain sedimentation rate <2 cm/yr.

Location	Drainage area (km^2)	Sedimentation Rate Range (cm/yr)	Analyses Performed	Source
Ganges-Brahmaputra	4,900	<1 - >1.6	^{137}Cs, ^{210}Pb	Goodbred, Jr. and Kuehl, 1998
Upper Axe Valley, England	400	0.2 - 1.6	Heavy metal, sedimentological, pollen, historical records, loss on ignition, grain size	Macklin, 1985
Geul River, East Belgium	350	0.11 - 1.06	Textural analysis, atomic absorption spectrometry, mineralogy, XRD, stratigraphic characteristics, historical records, heavy metal concentrations (XRF)	Swennen et al., 1994
Harz Mountains, Germany	6	0.2 - 0.4	Pb, Zn, Cu, Ba, Zr concentrations (XRF), microscopy and microprobe, ^{14}C, Optically stimulated luminescence	Matschullat et al., 1997
Galena River Watershed	526	0.75 - 1.9	Coring, identified paleosols, cross sections	Magilligan, 1985
Baltimore, Maryland	168	0.08 - 1.19	ICP-AES, ^{137}Cs, mining history, cross sections, stratigraphy, Cr	Bain and Brush, 2005
Honey Creek Watershed, Southwest Missouri	176	<1 - 1.8	ICP-AES, sand percentage analysis, loss on ignition, aerial photographs	Carlson, 1999
James River Valley, Missouri	3,770	0.3 – 0.55	Zn concentrations, ^{137}Cs, historical records, particle sizing, metal concentration (XRF), ICP-AES	Owen et al., 2011

a.

Point bar

Overbank
deposits

Channel deposit

Lateral
accretion

b.

Floodplain

Meander Scar

Back Swamp

Bluff

Oxbow Lake

Cutoff

Neck

Natural Levee

Alluvium

Bedrock
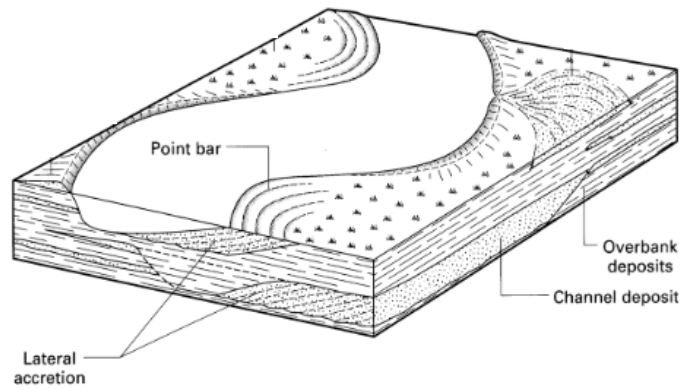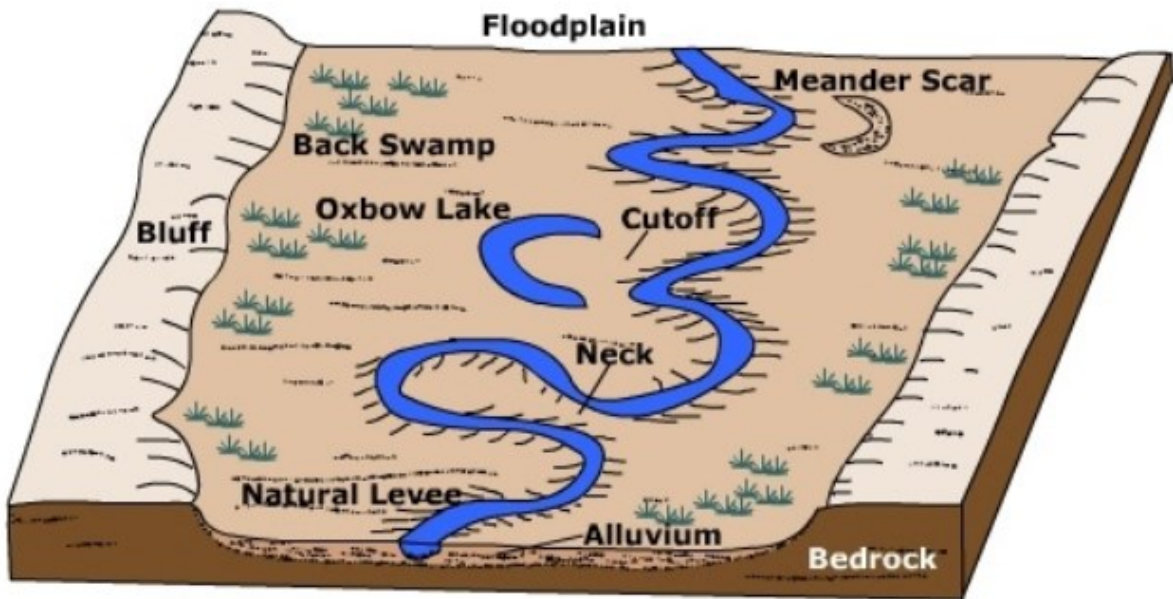
Figure 1. Floodplain accretion (a) lateral accretion of a floodplain (Nichols, 2009) (b) floodplain features (Ritter, 2003).
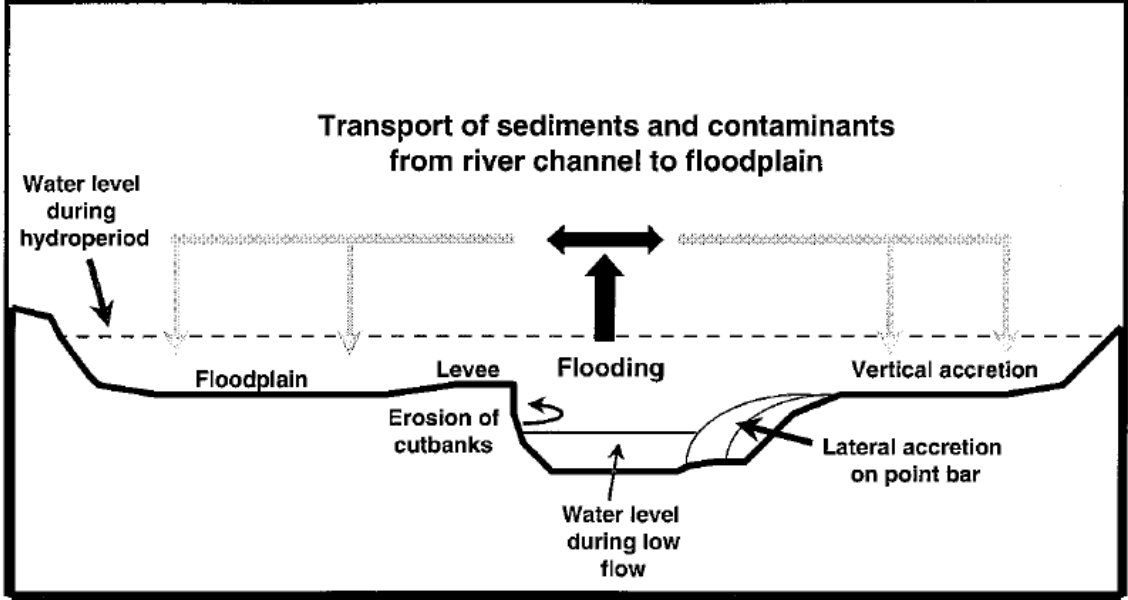
Figure 2. Floodplain deposition processes and landforms (Hupp, 2000).

a.

SCHEMATIC SEQUENCE: LAND USE, SEDIMENT YIELD

AND CHANNEL RESPONSE

FROM A FIXED AREA

b.
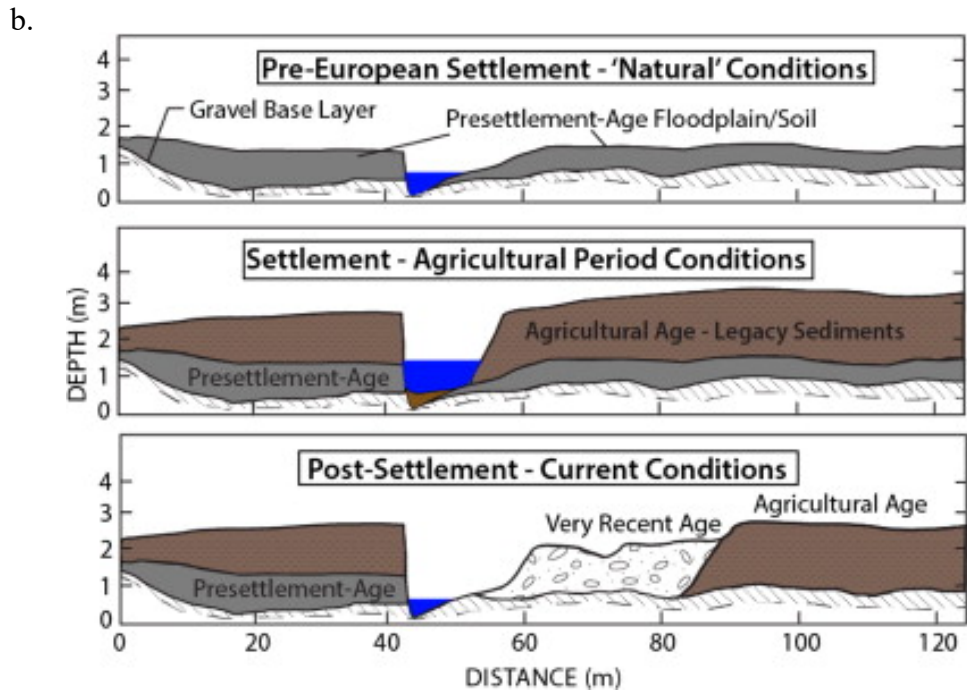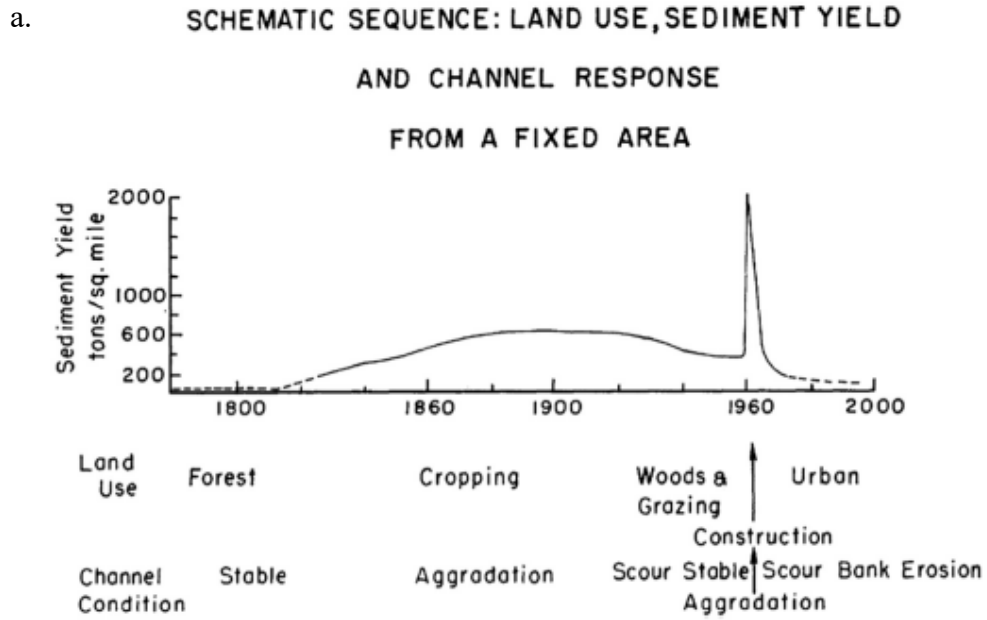
Figure 3. Landscape change effects on sediment yield and deposition (a) Sediment Yield (Wolman, 1967); (b) Legacy Sediment (Donovan et al., 2015).
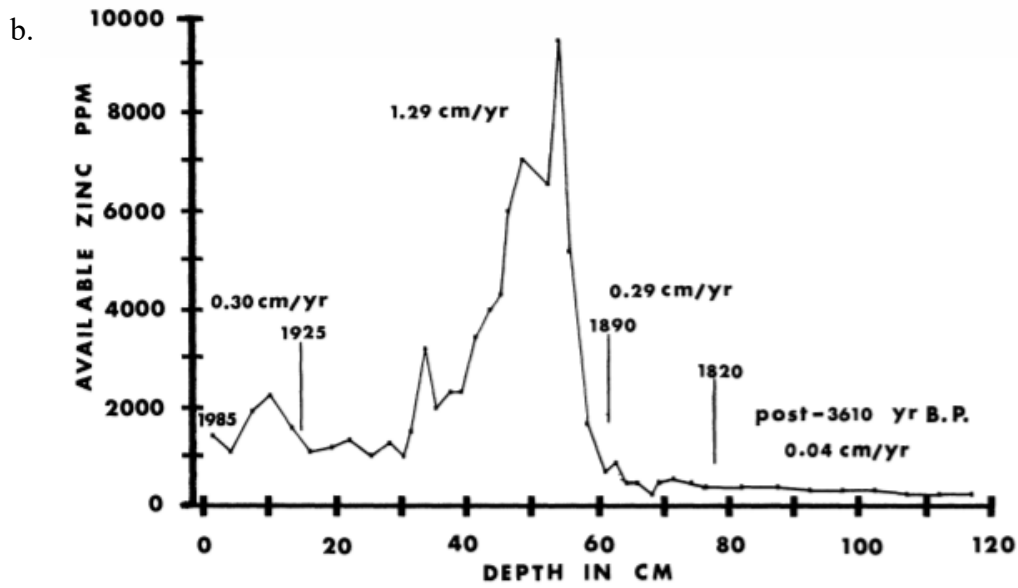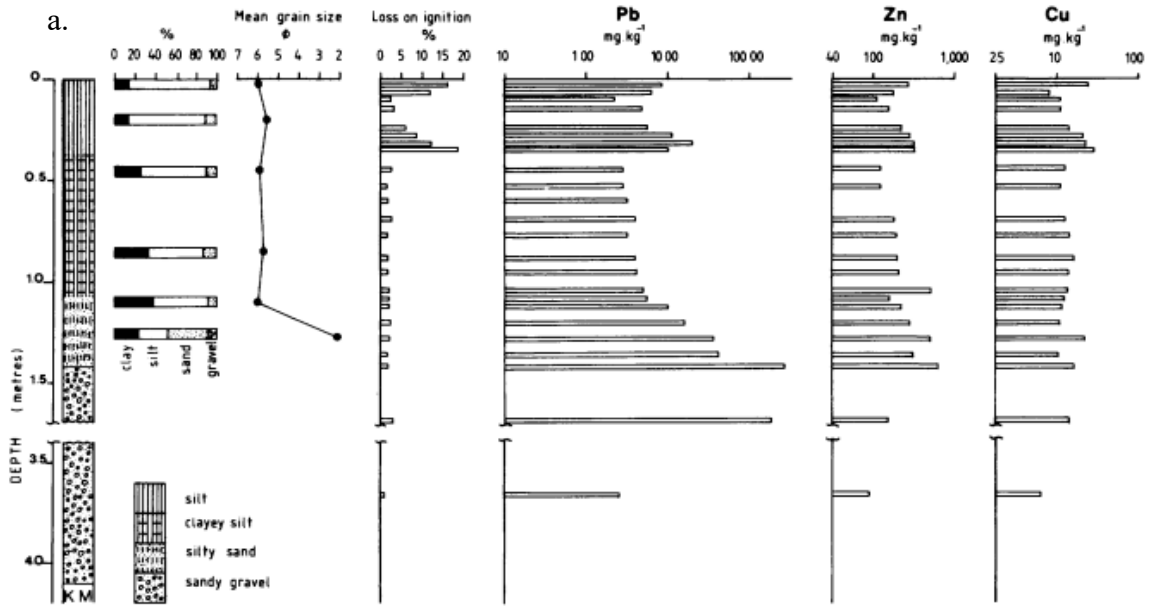
Figure 4. First sedimentation rate studies using mining tracers (a) Heavy metal mining sedimentation rates (Macklin, 1985); (b) Sedimentation rates using geochemical analyses and mining records (Knox, 1987).
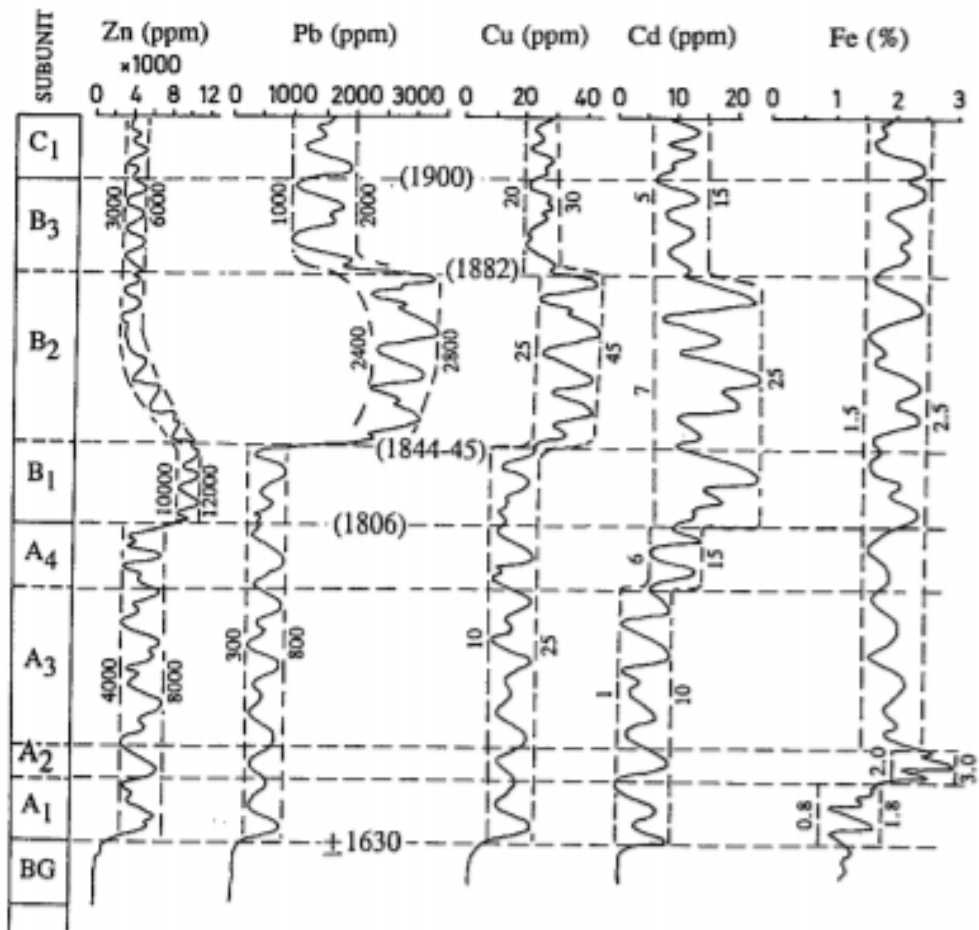
Figure 5. Vertical geochemical trends with sedimentation (Swennen et al., 1994).
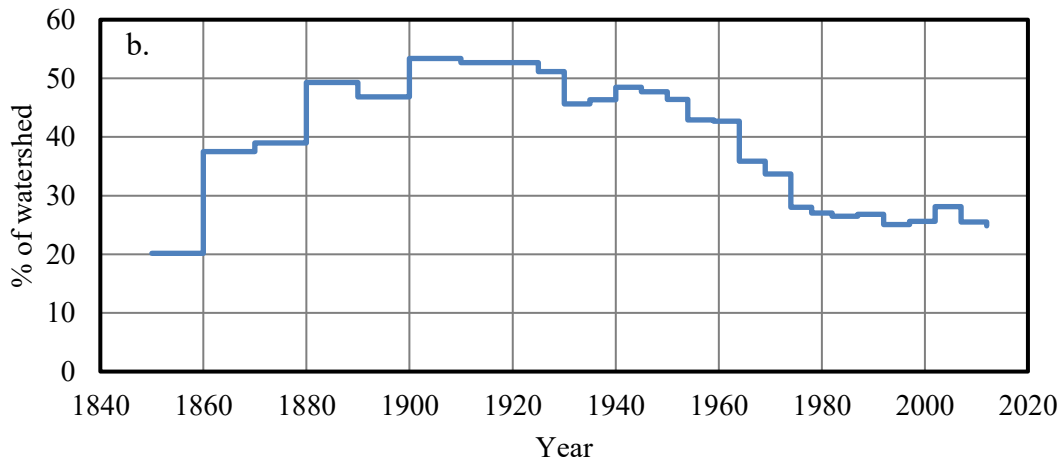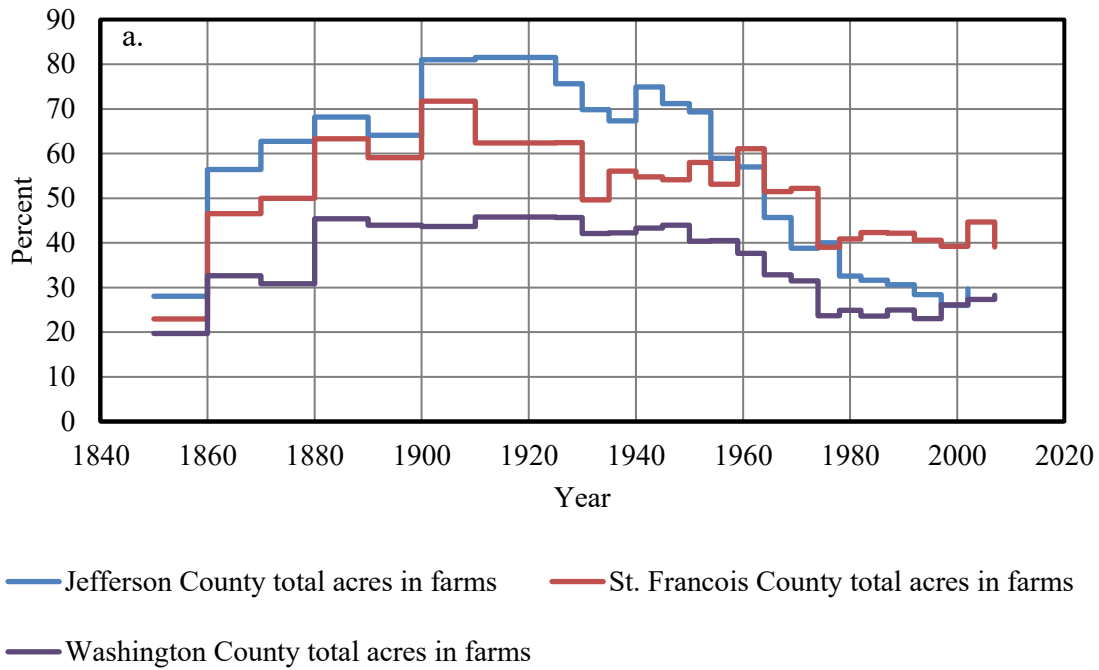
Figure 6. Farm percentages (a) percentage by year for Jefferson, Washington, and St. Francois Counties; (b) percentage of watershed.
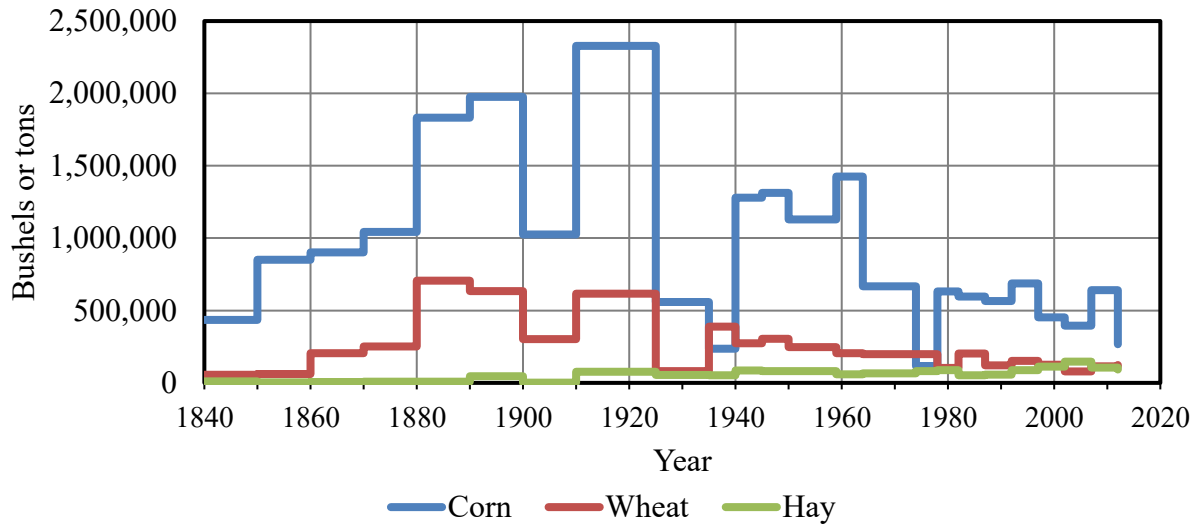
Figure 7. Selected row and pasture crops for Jefferson, Washington, and St. Francois Counties.
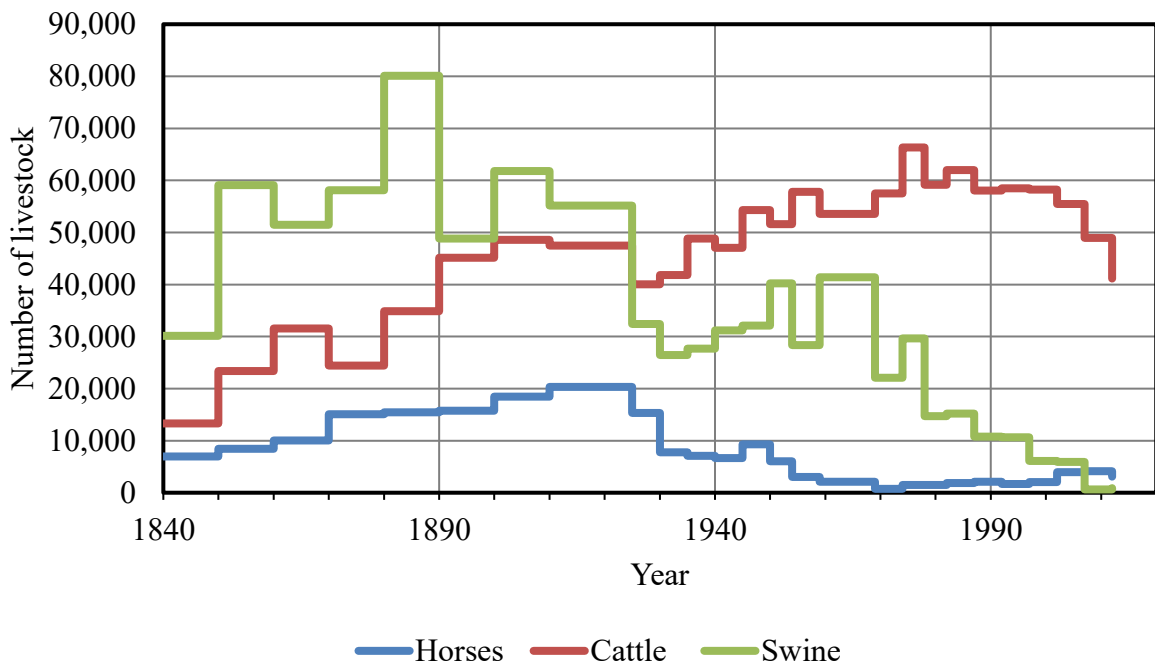
Figure 8. Selected livestock population for Jefferson, Washington, and St. Francois Counties.
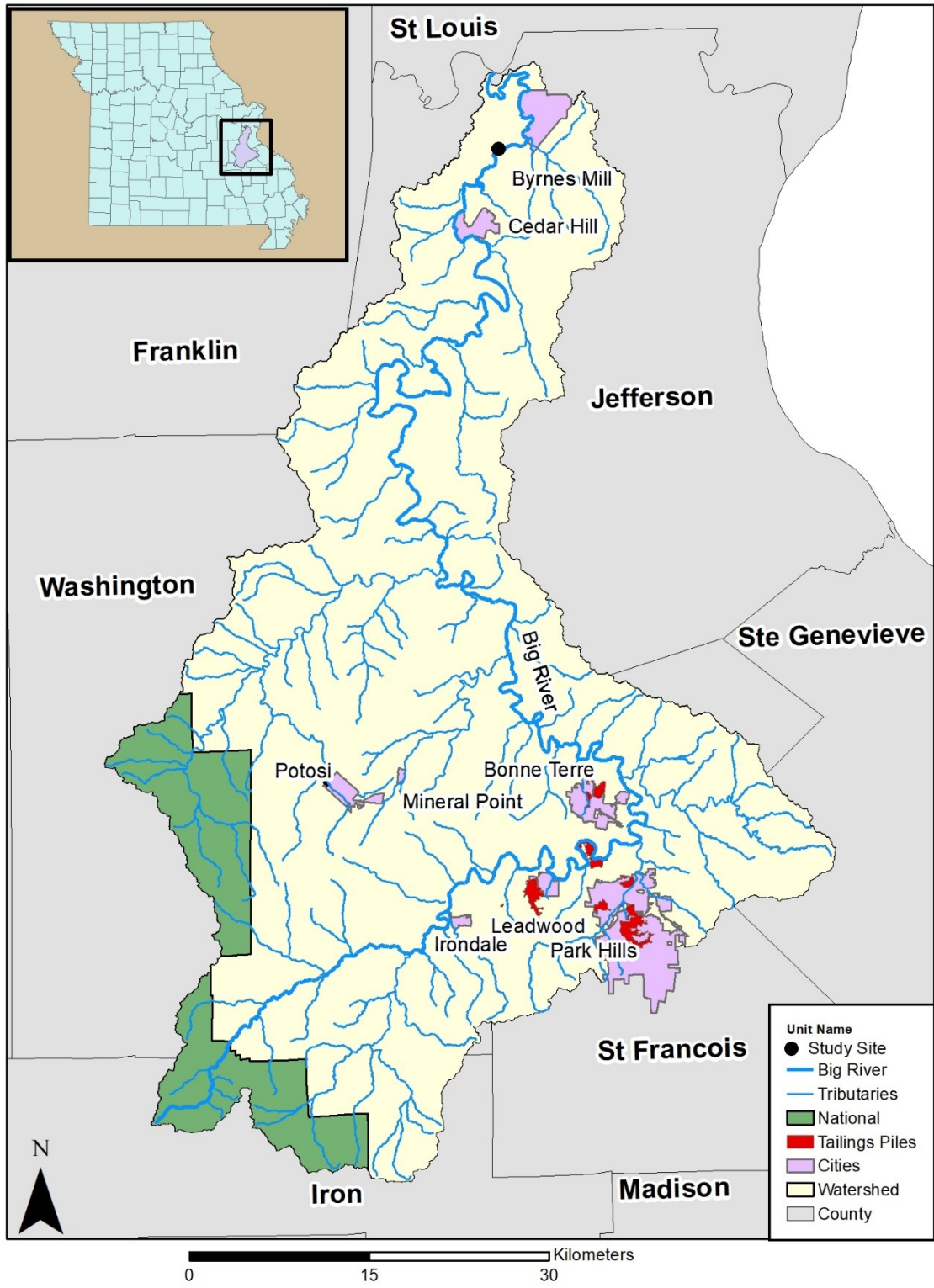
Figure 9. Locations of tailings piles and National Forest land in Big River Watershed.
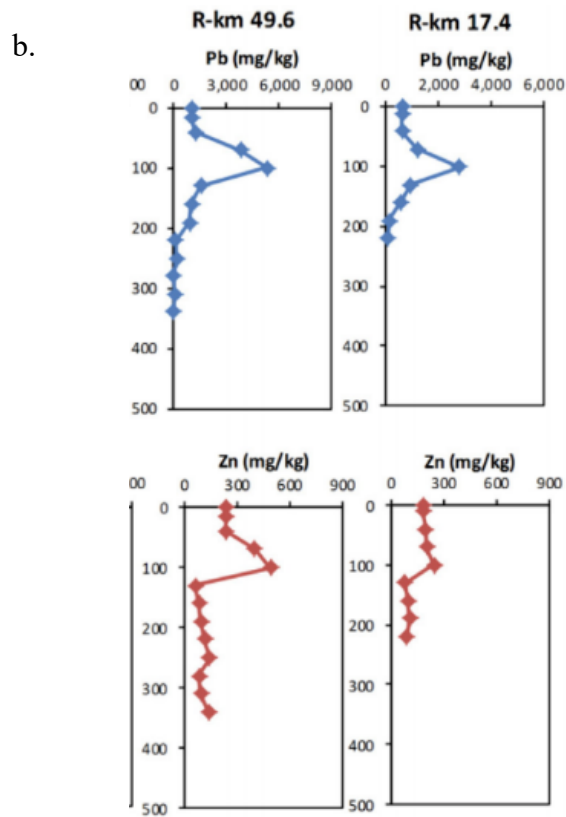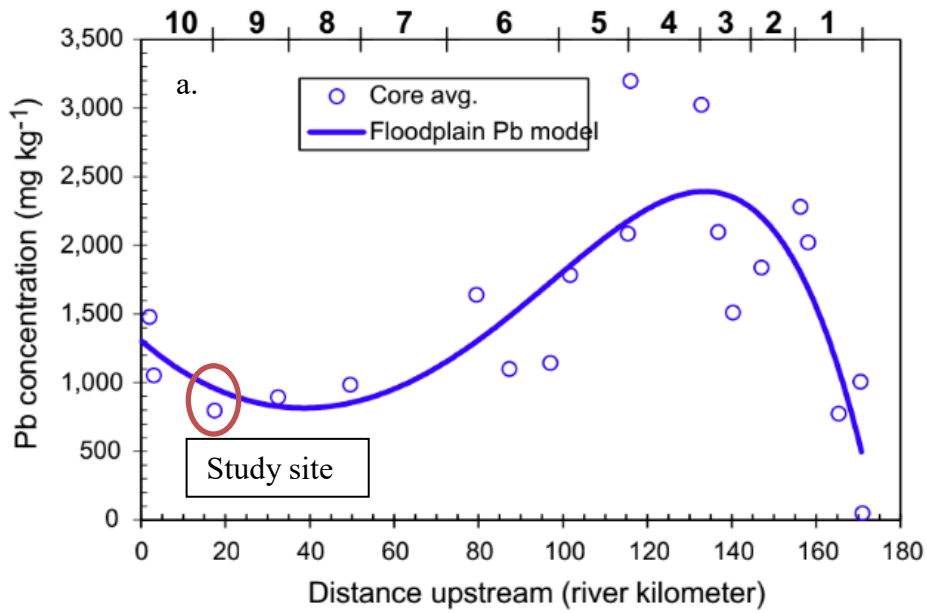
Figure 10. Mining metal contamination in Big River (a) Downstream Pb floodplain trends (Pavlowsky et al., 2017); (b) lower Big River Pb and Zn geochemical core profile (Pavlowsky et al., 2017).

STUDY AREA

The study site (BRB) is location on a floodplain located along Big River below Byrnesville in northwestern Jefferson County, Missouri approximately 3 km downstream from the Byrnesville gage site (USGS gage no. 07018500) and 3 km upstream from Rockford Beach Dam. This site was chosen due to accessibility and the long-term stability of the channel and floodplain landforms since 1937. The floodplain landforms and associated mapped soil series present at this site commonly occur along the main channel of Big River, were previously found to contain legacy sediment, and are contaminated to toxic levels with metals released from Old Lead Belt mines located from 116 to 151 km upstream (Pavlowsky et al., 2010; Huggins, 2016; Pavlowsky et al., 2017).

Regional Physiography, Geology, and Soils

Big River watershed (2,500 km^2) drains the Salem Plateau and the St. Francois Mountains Ozark Plateaus sub-provinces of the Ozark Highlands in eastern Missouri (Meneau, 1997) (Figure 11). Big River flows 225 km from its headwaters at 530 masl in the St. Francois Mountains in Iron County, north through the Old Lead Belt in St. Francois County, and to its confluence with the Meramec River in Jefferson County at 125 masl (Meneau, 1997). Counties within the watershed include St. Francois (19.1%), Washington (44.5%), Jefferson (24.8%), Franklin (1.0%), Iron (7.4%), and Ste. Genevieve (3.2%).

The St. Francois Mountains are formed by uplifted Precambrian igneous rocks including granite, felsite, and rhyolite which form a series of resistant knobs separated by sedimentary valleys of Cambrian age (Brown, 198; Adamski et al., 1995). The majority of the middle and

lower portions of the watershed drain the Salem Plateau with is composed of Cambrian aged sedimentary rocks and Ordovician aged sedimentary rocks consisting mainly of dolomites, chert, sandstones, and limestones with small amounts of shale (Adamski et al., 1995). The geology of the lower portion of the Big River watershed near the study site is composed of near-horizontally bedded sedimentary rocks including cherty limestone and dolomite with some sandstones and shales which contain sinkholes and springs (Jacobson and Primm, 1994; Meneau, 1997) (Figure 11).

Mississippi Valley-type ores located within the watershed were developed through hydrothermal fluid interaction along orogenic belts (Bradley and Leach, 2003). Geological formations in the watershed containing these ore deposits are the Bonne Terre Formations and the Potosi Formation (Gregg and Shelton, 1989; Smith and Schumacher, 1993). The Bonne Terre Formation is approximately 122 meters thick composed primarily of dolomite with hydrothermal minerals including galena, zinc, copper, and silver (Gregg and Shelton, 1989). The younger Potosi Formation is approximately 61 meters thick and contains similar lithology as the Bonne Terre Dolomite (Smith and Schumacher, 1993). Mining operations within the watershed targeted these ore deposits for over 200 years with deep shaft and surface mining in the Bonne Terre Formation in St. Francois County and surface mining in the Potosi Formation in Washington and Jefferson Counties (Gregg and Shelton, 1989) (Table 3).

The upland soils of Big River watershed are mainly comprised of ultisols and alfisoils formed in thin deposits of Pleistocene glacial loess overlying a cherty clay residuum formed from dolomite, limestone, and shale (Jacobson and Primm, 1994; Adamski et al., 1995; NRCS, 2006). Most of the soils on hillslopes throughout the watershed are gravelly silt loams (Sonsac series) and silt loams (Useful series) that are moderately well to well drained and moderately

permeable (NRCS, 2006). Alluvial soils on floodplains with a return frequency of 1 - 2 years are present at the study site consisting of deep to very deep silt loam which occur on poorly- to well-drained positions on floodplains and low terraces (Skaer, 2004; NRCS, 2006) (Figure 12). The landforms associated with these soils are generally classified as Quaternary-age alluvium and include: (i) Kaintuck series, developing floodplains or benches; (ii) Haymond series, present-day floodplain which is slightly higher (0.5-1 m) in elevation than the Kaintuck series; (iii) Wilbur series, poorly drained floodplains including chutes and backswamps; and (iv) Sturkie, low terraces that are slightly higher in elevation than the Haymond series (Skaer, 2004; NRCS 2006) (Figure 13).

Climate, Hydrology, and Flood History

The climate of the Ozark Plateau is moist continental with winters in Jefferson County averaging 0.6°C (33˚F) and summers averaging 23.9°C (75 ˚F). Annual precipitation averages 96.5 cm (38 in) with wettest months in April and May and driest months in January and February (Figure 14). Overall, the Ozarks experience higher temperatures and rainfall amounts than the northern part of the state (Harrington, 2012). There is a consensus among scientists that rainfall totals within the Midwest have increased in recent years (Groisman and Easterling, 1994; Easterling et al., 2000; Wuebbles and Hayhoe, 2004). Annual precipitation data obtained from the Cli-MATE database for the region suggests that there has been an increase in annual precipitation over the past 30 years by 6% on average (https://mrcc.illinois.edu/CLIMATE/) (Figure 15). Previous studies in the Midwest suggested that there were more intense rainfall events between 1948 to 1994 compared to years prior (Angel and Huff, 1997; Foreman, 2014).

The Big River at Byrnesville gage (USGS 07018500; 2,375 km^2) is located 3 kilometers upstream of the study site and has been in operation since 1923. The mean annual discharge for the period of record is 24.83 m^3/s. Mean monthly discharge is highest in April (48.8 m^3/s) and is lowest in August (8.5 m^3/s). Flood recurrence intervals calculated from the annual peak record extending from 1923 to 2018 using PeakFQ software version 7.2 as follows: 1.5-year flood, 366.4 m^3/s; 2-year flood, 484.5 m^3/s; and 5-year flood, 802.2 m^3/s (Figure 16; Appendix A). Long-term trends show fluctuations within the moving average, however, there is an upward trend in discharge over the past 13 years (Figure 17). In 2017, a high magnitude precipitation event flooded small basins throughout the Ozarks that produced record peaks throughout the region and was rated as 0.2 annual exceedance probability in southern Missouri (Heimann et al., 2018). The most recent 60-year record was split into two sets of consecutive 30-year increments to evaluate the difference in average monthly discharge. During the recent 30-year period, monthly discharge increased in average discharge in January (24%), April (10%), May (33%), June (21%), and September (63%) with decreases in February (6%), March (9%), July (21%), and December (26%) (Figure 18). Annual peak discharges with > 10-year recurrence intervals occurred during 1915, 1950, 1957, 1983, 1985, 1993, 2008, 2015, and 2017 (Table 4). This increasing flood trend also correlates with stratigraphic records within Mississippi River floodplains which suggests a shift to more frequent large flood events since 1950 (Knox, 2006).

Historical Land Use

Native American tribes inhabited areas throughout the watershed especially using alluvial terraces (e.g., mapped as Horsecreek, Sturkie, and Razort soil series) along river bottoms for agricultural purposes prior to European Settlement (Skaer, 2004). Most of the land within the

watershed during this time consisted of mostly deciduous forests in the uplands, yellow/shortleaf pines in St. Francois and Washington Counties, and glade, prairie, and bottomland forest communities (Thom and Wilson, 1983). Streams during this time deposited a mixed sediment load of gravel bedload and silty overbank sediment. Although, historical reports frequently noted large quantities of gravel on channel beds and in bank exposures, there were fewer notes of extensive gravel bar deposits in disturbance zones as frequently found today (Jacobson and Primm, 1994).

As settlers began entering the region around 1730s, they noted areas of open woods, with large areas being almost treeless, while sloped regions contained more forested areas (Sauer, 1920). Agricultural changes to the landscape and alluvial changes within the Big River Watershed were documented around the same time (Schoolcraft, 1821). By 1830, many areas within Big River Watershed were being settled and subsequent land clearing for agricultural practices and surface mining increased, thus land use changes were occurring at an accelerated rate (Jacobson and Primm, 1994) (Table 5). In the 1800s, fields of cotton, corn, tobacco, and garden vegetables were planted and livestock were released on the land to open graze and included horses, cattle, mules, and hogs (Brown, 1981). Farming of floodplain soils along the Big River increased after the Civil War, as well as within the uplands (Skaer, 2004). Commercial timber companies began large-scale operations within the Ozarks harvesting both shortleaf pines and oak from 1870 – 1920, however some accounts place timber harvesting in the region as early as 1820 (Jacobson and Primm, 1994). Byrnesville dam was constructed in 1847 and contained a sluice for the passing passage of logs (Suggs, 2008). During the period 1890 – 1900, farmland area as percent of total county area peaked in Jefferson County (81%), St. Francois County (72%), and Washington County (44%) (Figure 6).

Open grazing increased between 1920 and 1960 as well as the use of marginal land for cultivated crops (Jacobson and Primm, 1994). Unmanaged, open-land cattle and hog grazing during this time disturbed riparian vegetation possibly causing more frequent head-cuts in small tributary channels which promoted the erosion and release of stored gravel to downstream channels (Jacobson and Primm, 1994). There were also large fluctuations in corn and wheat production during this time. It was noted through oral history that smaller streams had more discharge for longer periods and were less flashy compared to post 1960 (Jacobson and Primm, 1994). Clusters of cottages were built along the lower Big River, around the study site and upstream, beginning in the 1940s (Meneau, 1997). The population within Jefferson County tripled from 1950 to 1970. Only 17% of the total population of the county lived in incorporated areas (Skaer, 2004).

Run-of-river mill dams are present on Big River in the vicinity of the study site at Byrnesville (3 km upstream) and Rockford Beach (3 km downstream). Byrnesville Dam was constructed in 1847 by David Manchester and was the largest dam along Big River at the time (Suggs, 2008). Byrnesville dam operated until 1936 when operations ceased at the mill during the Great Depression (1993). Rockford Mill was constructed in the 1890s by Henry Vandercrussen (Jefferson County Genealogical Society, 2015). A low head dam was constructed across Big River to impound water for the mill (McLarty, 2016). This mill dam was also closed during the Great Depression and the mill burned down in the 1960s (Jefferson County Genealogical Society, 2015). Jefferson County Parks Department now owns Rockford Beach Park and works with the USEPA on stabilization of the Rockford Dam. The most recent stabilization occurred in 2016 when imminent failure would have released high levels of heavy metals further downstream (McLarty, 2016).

Mining History

Mining activities first began in the region soon after 1717 in Madison County, Missouri when French explorers opened surface pit Pb mines at Mine-La-Motte located 40 km southeast of what later developed as the heart of the Old Lead Belt around the towns of Bonne Terre, Desloge, and Park Hills (Thompson, 1992; Seeger, 2008) (Table 5). The first occurrence of lead mining within the Big River watershed occurred between 1742 and 1762 near Potosi, Missouri where galena was mined in shallow pits or diggings by the French (Buckley, 1909). Ore extracted during this time was burned using a log furnace and only 50% of lead was recovered (Mugel, 2017). During the early 1800s, four major surface mines were active in Big River Watershed including Mine-a-Joe and Mine-a-Burton in St. Francois County and Old Mines and Renault's mines in Washington County (Thompson, 1992). In 1798, ash furnaces were installed to smelt the residual galena ore and collect Pb metal from the ashes in the log furnaces which increased Pb recovery to >50% (Mugel, 2017). By 1818, Gray's Mines and McKane's Mines were established near the mouth of Big River on Dry Creek in Jefferson County (Thompson, 1992). Surface mining operations continued throughout the Old Lead Belt region until the mid-1860s when most of the surficial galena deposits were depleted (Smith and Schumacher, 1993). The Scotch hearth replaced log and ash furnaces by the mid-1870s which improved Pb metal recovery during smelting up to 90% lead (Mugel, 2017).

In 1866, modern mining operations began in Bonne Terre (Pavlowsky et al., 2017). After the introduction of diamond drilling technology by the St. Joseph Lead Company at Bonne Terre around 1869, exploration by core drilling indicated that large amounts of ore were concentrated under the towns of Bonne Terre, Flat River, Leadwood, Desloge, and Elvins and large-scale mining expanded rapidly in the Old Lead Belt after 1895 (Smith and Schumacher, 1993).

Metallic ores were sent to Herculaneum, Missouri for smelting during the 20th century mining era. From the 1890s to early 1930s, the primary milling processes separated ore by wet and dry jigging processes which produced tailings in the size of 2 to 16 mm typically containing 3,000 to 5,000 ppm Pb (Pavlowsky et al., 2017). Shaking table methods were instituted in the OLB in the early 1900s which created tailings in the sand range from 0.125 to 0.5 mm and typically contained less than 1200 ppm Pb (Coghill and O'Meara, 1932; Pavlowsky et al., 2017). Flotation methods skimmed the surface of chemically treated materials to recover the concentrate and slimes were discharged to either large tailings or slime ponds near mills measuring less than 0.074 mm and contained 27,000 to 60,000 ppm Pb (Jackson et al., 1935; Pavlowsky et al., 2017). Peak years of production of lead occurred in 1917, 1925, and 1942 which included wet and dry jigging (1917) as well as flotation (1925, 1942) milling processes (Pavlowsky et al., 2017). An overall increase in mining from 1890s until 1930 produced large quantities of tailings and ultra-fine slimes (<63 um), some of which have been deposited as legacy sediments within the channels and floodplains of Big River (Gilbert, 1917; Macklin et al., 2006, Pavlowsky et al., 2017).

Barite mining began in Washington County around 1860 by extracting barite from surface and float deposits in Potosi and Eminence Dolomites with cleaning and separation in washer plants (Smith and Schumacher, 1993; Adamski et al., 1995; Mugel, 2017). Wastes from the extraction process was diverted to tailings ponds in Mineral Fork and Mill Creek watersheds that enter the main channel of Big River about 100 km above the study site (Smith and Schumacher, 1993). Open-pit hand mining for barite in residuum began in the 1920s and mechanized mining began in 1937 using gas, steam, or electric powered shovels (Mugel, 2017) (Table 5). Large quantities of water were used to mine barite from either recirculation, dammed

streams, or pumped from wells (Mugel, 2017). In 1978, there were a total of nine mines in Washington County, of which the largest producer extracted 25% of the total barite mining in Missouri (Arndt., 1979). In 1981, there were ten operations that extracted 185 thousand short tons and in 1982 there were eight operations that extracted 107 thousand short tons (Minerals Yearbook, 1982). By 1987, there were only 3 operations still extracting barite for an annual total of 18 thousand short tons (Minerals Yearbook, 1987). The last barite extraction operation closed in Missouri in 1998, however, one processing plant for barite operated within the watershed in 2011 (Mugel, 2017).

Recent Land Use

Agriculture within the watershed has been on a decline since the 1940s, however an upward trend in farm acreage not pastured of 1.5% has occurred in the watershed within the recent 10 years. Total production of corn has decreased within the watershed, however hay has maintained a steady production over the past 50 years in Washington County, St. Francois County, and Jefferson County between 30,000 and 40,000 tons per year. The number of livestock within the watershed has decreased 6% within the past 20 years, especially dairy cattle. Changes in agriculture over the years within Big River Watershed has an inverse relationship with population, especially in Jefferson County. Land use within the watershed in 2006 was 72% forest, 18% grassland, 1% row crops, and 7% urban/developed (MDNR, 2013). More recent land use trends in 2018 report 75% forest, 16% pasture, 1% row crops, <1% water, and 7% urban/developed (National Agricultural Statistics Service (NASS) Crop Database (https://www.nass.usda.gov/AgCensus/).

Table 3. Geology of Big River Watershed: rock types.

Unit Name	Geologic Age	Primary Rock Type	Secondary Rock Type	% area
Tertiary and Quaternary				0
Osagean Series	Mississippian	Limestone	Chert, Dolomite, Shale	2
Pennsylvanian System	Pennsylvanian	Shale	Limestone, Sandstone, Coal	0
Devonian System	Devonian	Limestone	Sandstone, Shale, Chert	0
Maquoketa Group and Kimmswick Limestone	Ordovician	Limestone	Shale	1
Decorah and Plattin Groups	Ordovician	Limestone	Shale	2
Joachim Dolomite and Dutchtown Formation	Ordovician	Dolomite	Limestone, Shale, Sandstone, Siltstone	1
St. Peter Sandstone and Everton Formation	Ordovician	Sandstone / Dolomite	Sandstone, Limestone; Shale, Siltstone, Sandstone, Limestone	1
Cotter and Jefferson City Dolomite	Ordovician	Dolomite	Sandstone, Shale, Chert, Conglomerate	11
Roubidoux Formation	Ordovician	Sandstone	Chert, Dolomite	2
Gasconade Dolomite	Ordovician	Dolomite	Sandstone	8
Eminence and Potosi Dolomite	Cambrian	Dolomite	Chert	39
Elvins and Bonneterre Dolomite	Cambrian	Dolomite	Conglomerate	26
Lamotte Sandstone	Cambrian	Sandstone		4
Precambrian Volcanics	Precambrian	Rhyolite	Trachyte	2
Precambrian Intrusives	Precambrian	Granite		1
Precambrian Mafics	Precambrian	Diorite	Gabbro	0

35

Table 4. Important land use and large flood dates.

Year	Event	Article
1811	European Settlement begins	Sauer, 1920
1830	Large-scale land clearing within the watershed begins	Jacobson and Primm, 1994
1847	Byrnesville Dam constructed with log sluice	Suggs, 1993
1857	St. Louis and Iron Mountain Railroad built	Brown, 1981
1870	Large scale timber production begins in the Ozarks	Jacobson and Primm, 1994
1890	Rockford Mill constructed	Jefferson County Genealogical Society, 2015
1900	Peak Farm Acreage 53%	USDA
1910	Peak Horse and Row Crop (2,328,352 bushels)	USDA
1915	Historical peak 2265 m3/s discharge August 21	USGS
1920	Prescribed burning instituted, 15% of southwest portion of watershed	Jacobson and Primm, 1994
1950	January 4 - 6 overbank flood 977 m3/s	USGS
1957	July 1053 m3/s overbank flood	USGS
1974	Peak Number of Cattle 66328 total cattle	USDA
1978	50% of St. Francois County cleared for pasture, hay, and corn	Brown (USDA), 1981
1983	May 1135 m3/s overbank flood	USGS
1985	November 1053 m3/s overbank flood	USGS
1993	September 23 - 27 1637 m3/s and November 14 - 18 1328 m3/s overbank flood	USGS
2008	March 20 1260 m3/s overbank flood	
2015	December 27 - 31 overbank flood 1175 m3/s	USGS
2017	May 1 - 6 overbank flood 1688 m^3/s	USGS

Table 5. Important mining dates.

Year	Event	Article
1725	Small Lead Surface Mines in SE Mo	Showalter, 1963
1798	Ash furnaces used to separate Pb	Mugel, 2017
1819	first sinking of shallow shafts - Valles Mines	Schoolcraft, 1819
1824	Valles Mines highest lead production in state	State Historical Society of Missouri, 2013
1850	Increased lead production	Winslow, 1894
1855	30 shafts and 3 mines in St. Francois County	Mugel, 2017
1860	small scale Barite mining begins in SE Mo	Showalter (1963)
1864	organized lead mining begins in OLB at Bonne Terre	Pavlowsky et al., 2017
1870s	Wet and dry jigging (4 - 8 mm tailings)	Pavlowsky et al., 2017
1880	21 mines between Washington, St. Francois, and Jefferson Counties	Winslow, 1894; USDA
1905	Barite mining increases - hand mining	Showalter (1963)
1906	Lead mining ceased in Washington County	Buckley, 1908
1914	Flotation Methods begin (< 0.074 mm)	Pavlowsky et al., 2017
1917	Valles Mines decreased operations; peak in Pb Production in OLB	Kiilsgaard et al., 1967; Pavlowsky et al., 2017
1925	Peak in Pb production in OLB	Pavlowsky et al., 2017
1930	1932- end of chat milling, Flotation milling dominants production	Pavlowsky et al., 2017
1930's	peak in Barite hand mining	Showalter (1963)
1940's	Return of Barite mechanized mining methods	Harness and Barsigian (1946)
1942	Peak Pb production	Pavlowsky et al., 2017
1940 - 1945	Increase in milling for war supply; release of fine grained heavy metal into stream from Valles Mines	Mugel, 2017
1957	April 4 - 6; May 18 - 25 overbank flood; Barite mining peak 382,000 tons	USGS; Mugel, 2017
1969	30 processing plants for Barite	Wharton et al., 1969
1971	15 Barite mines open in Washington County	Wharton, 1972
1972	Lead mining ceased in Old Lead Belt	Pavlowsky et al., 2017
1998	Barite last mined in Missouri	MDNR, 2012
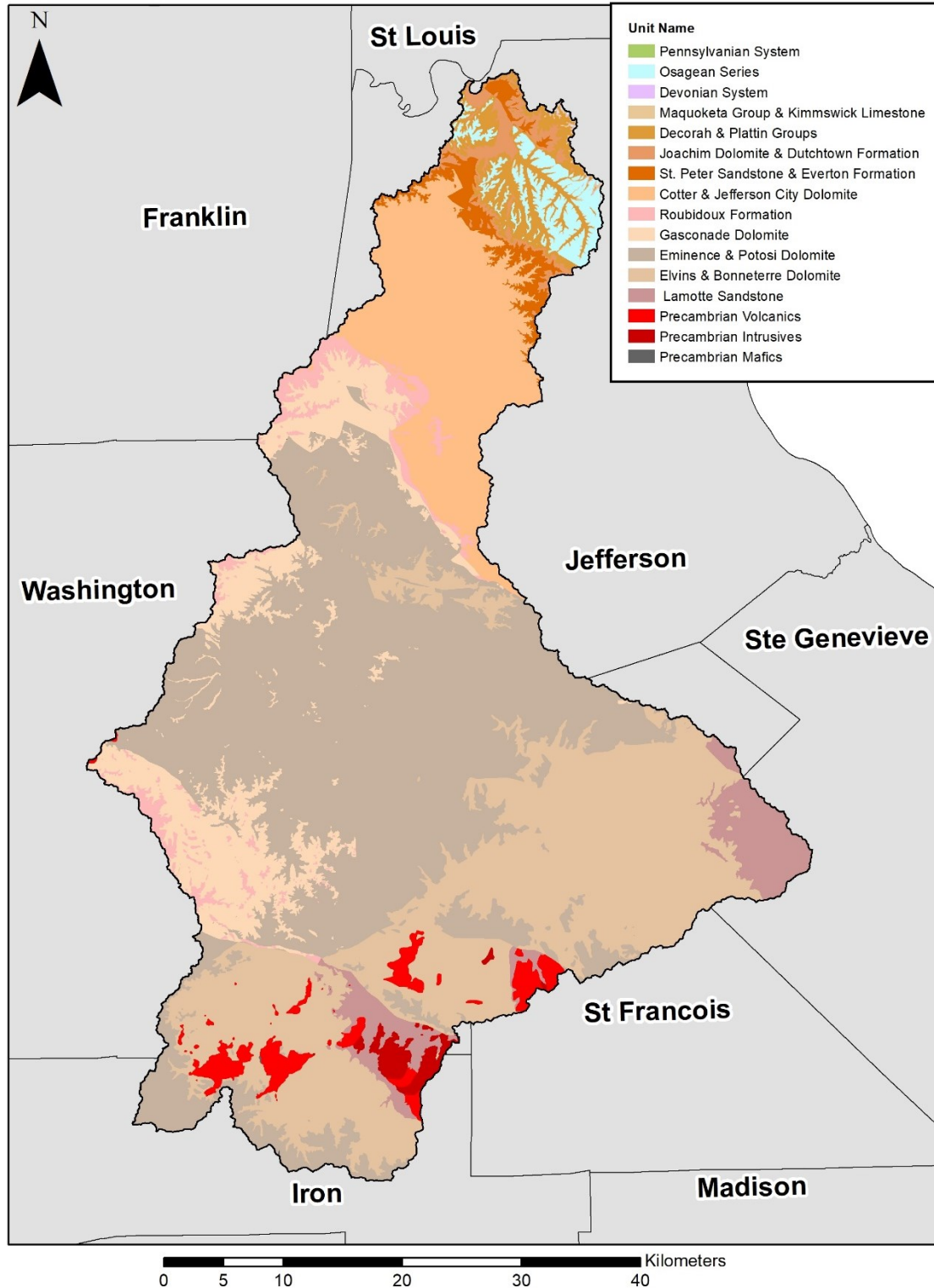
Figure 11. Geology of Big River Watershed, Missouri.

39
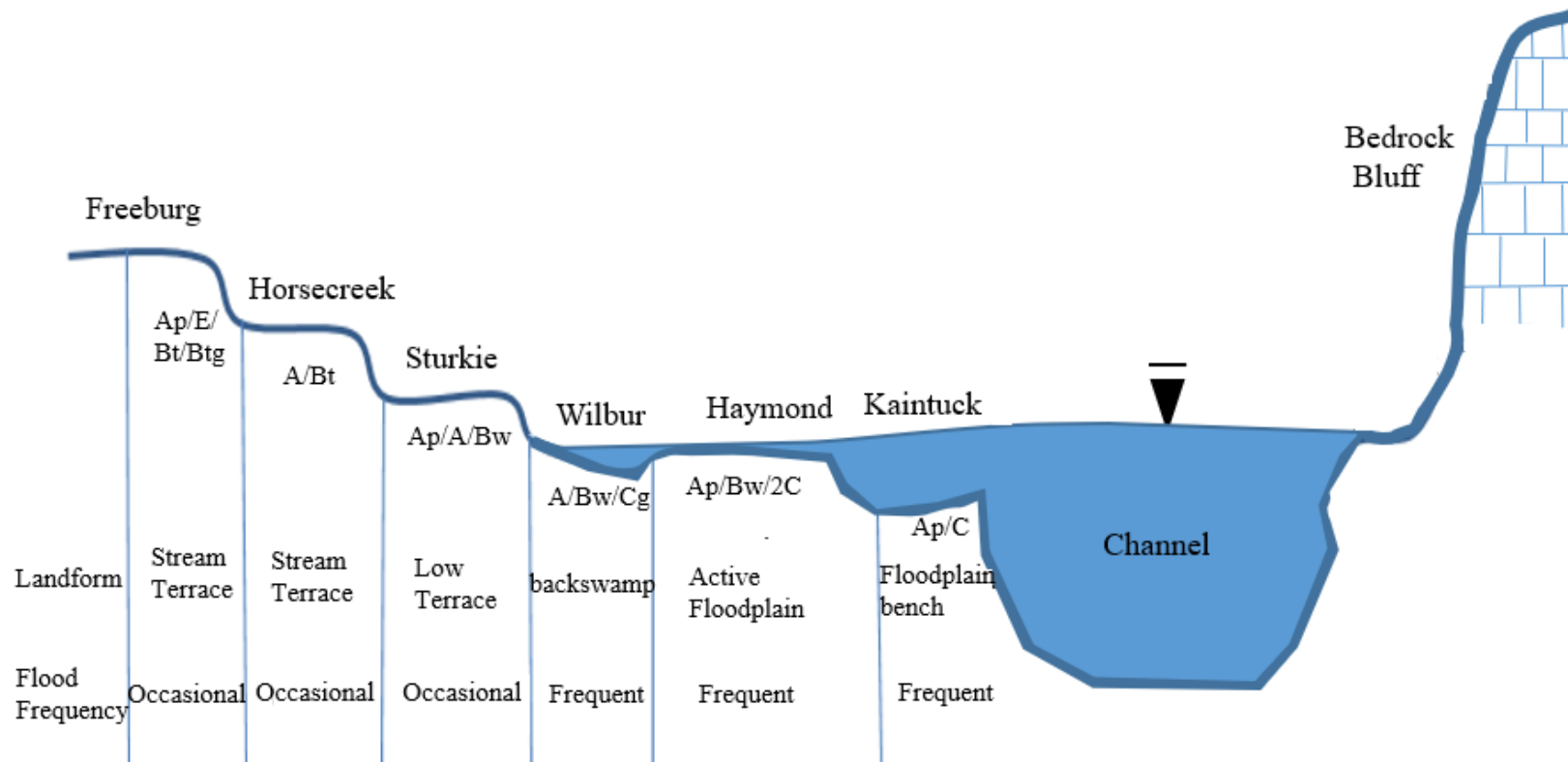
Figure 12. Big River soil series cross section.
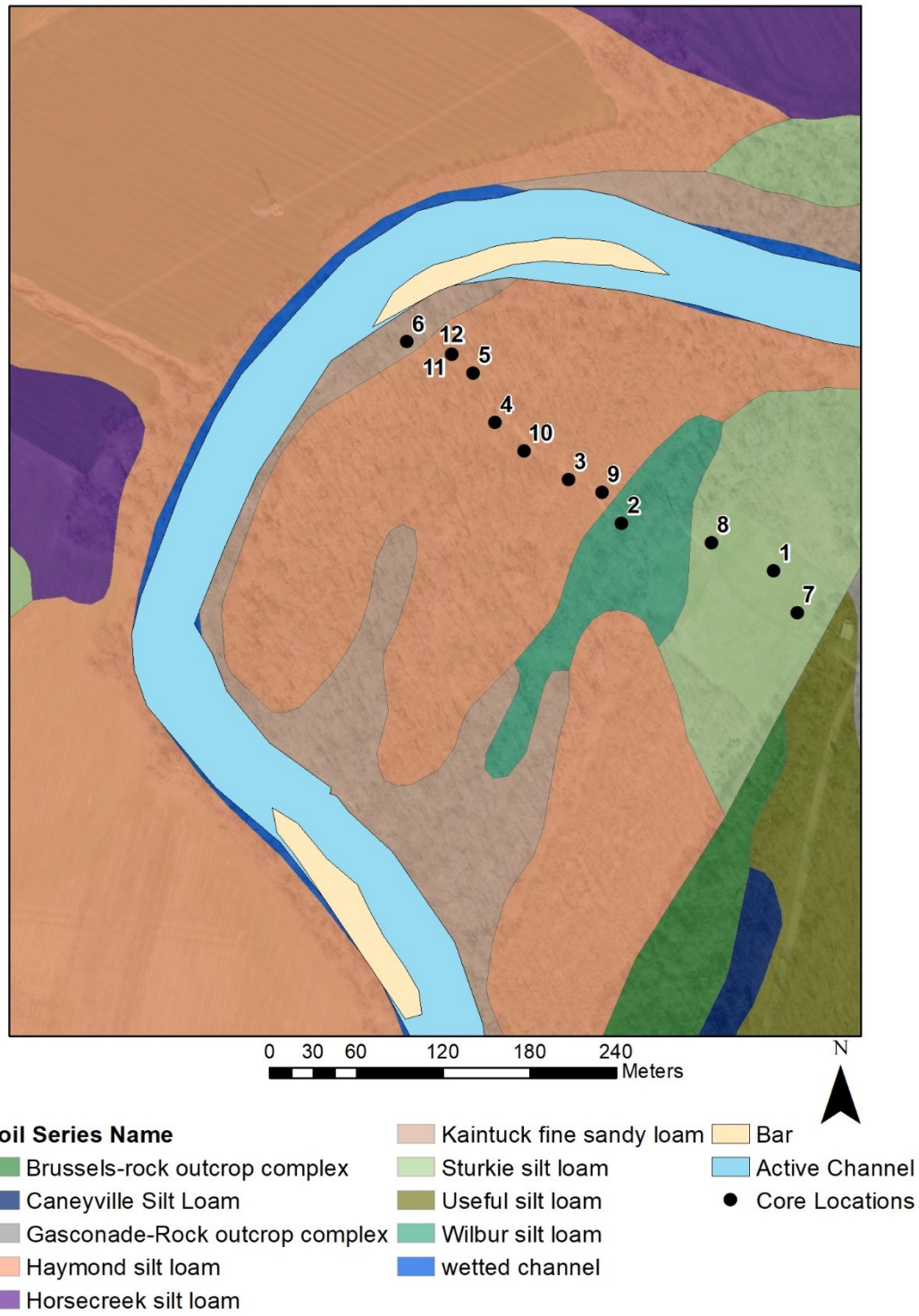
Figure 13. Soil series map for study site.
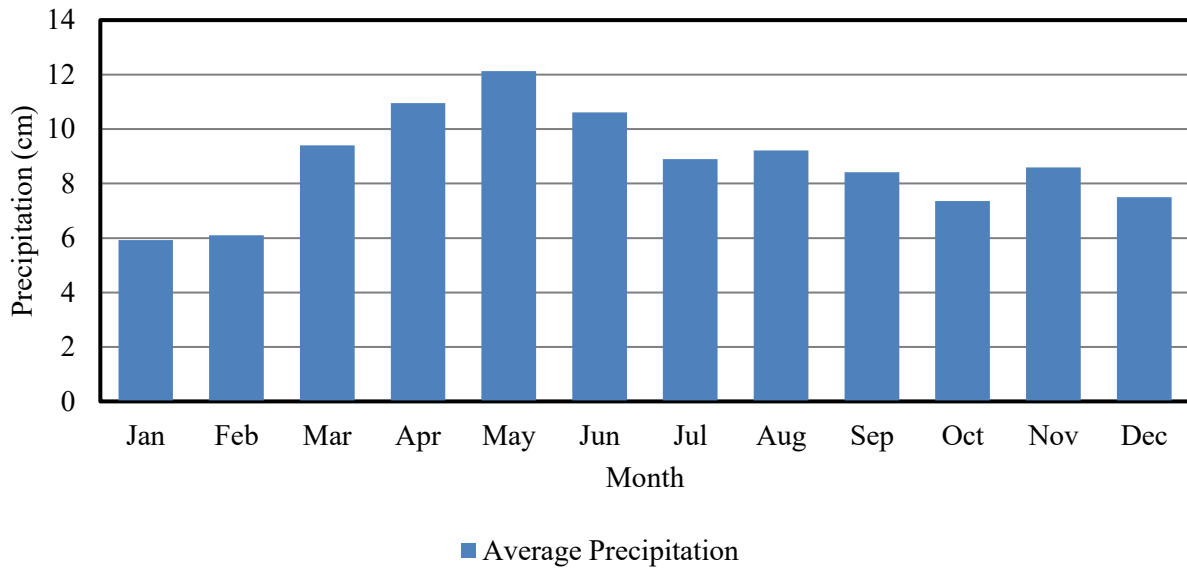
Figure 14. Average monthly precipitation 1937 - 2017.
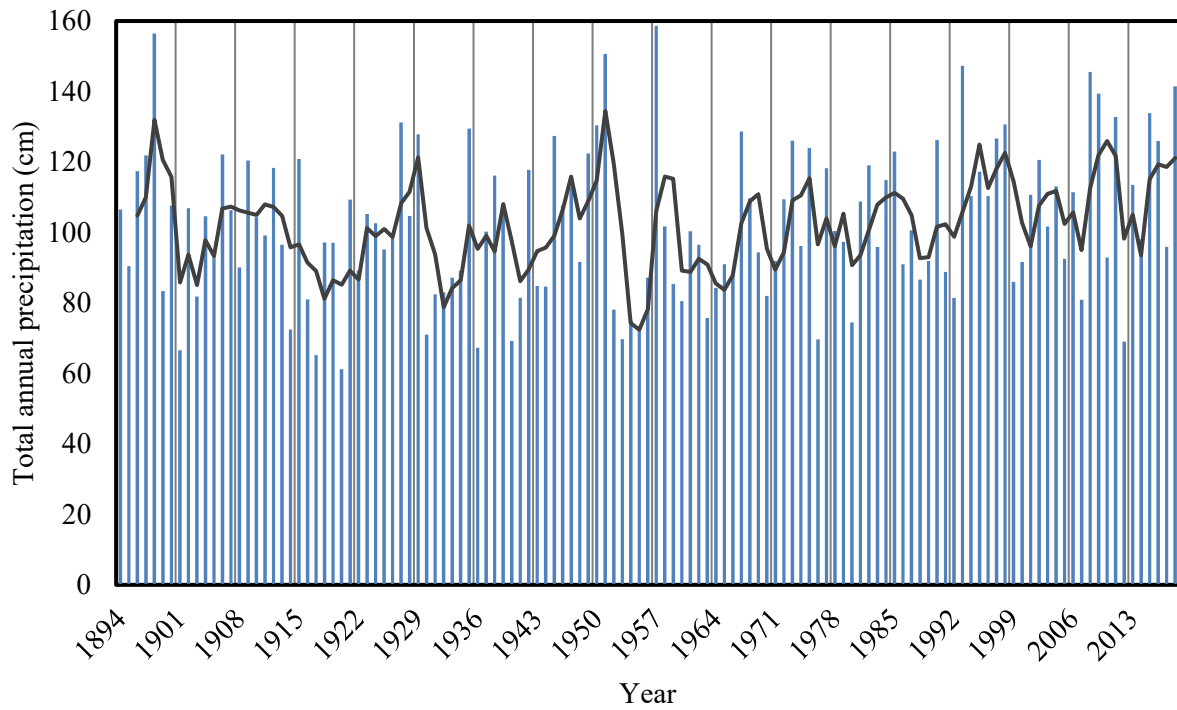
Figure 15. Big River at Byrnesville total annual precipitation.
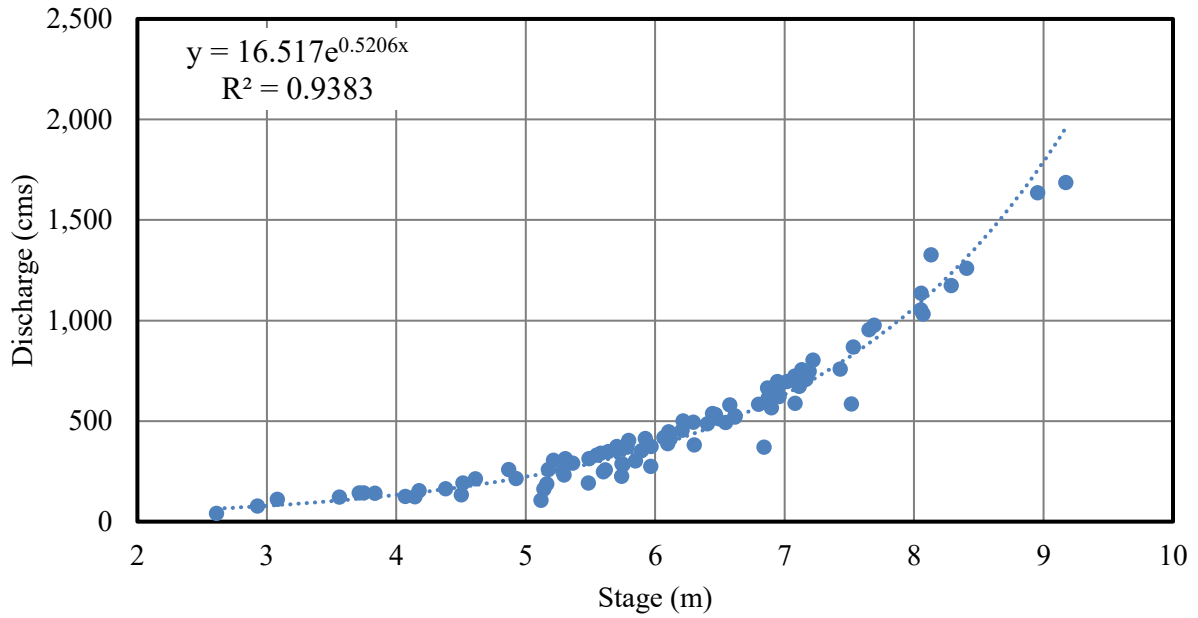
Figure 16. Stage-discharge rating curve at Byrnesville.

The equation shown on the chart: $y = 16.517e^{0.5206x}$, $R^2 = 0.9383$.
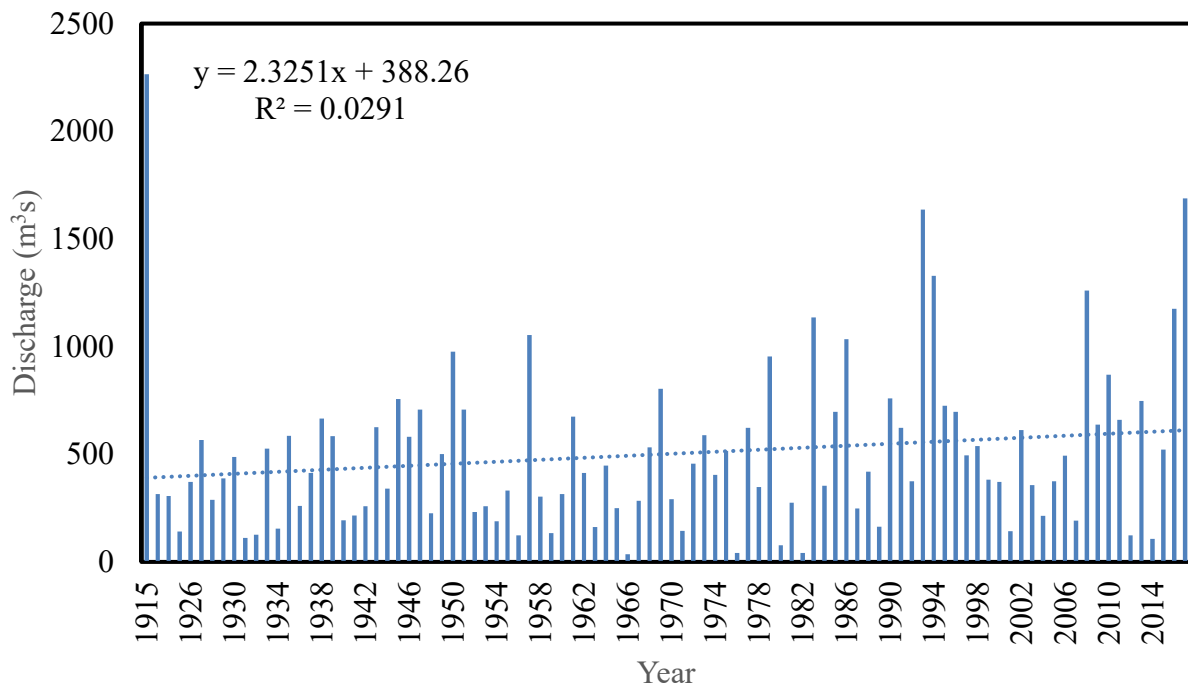
Figure 17. Annual peak discharge at Byrnesville.

The equation shown on the chart: $y = 2.3251x + 388.26$, $R^2 = 0.0291$.
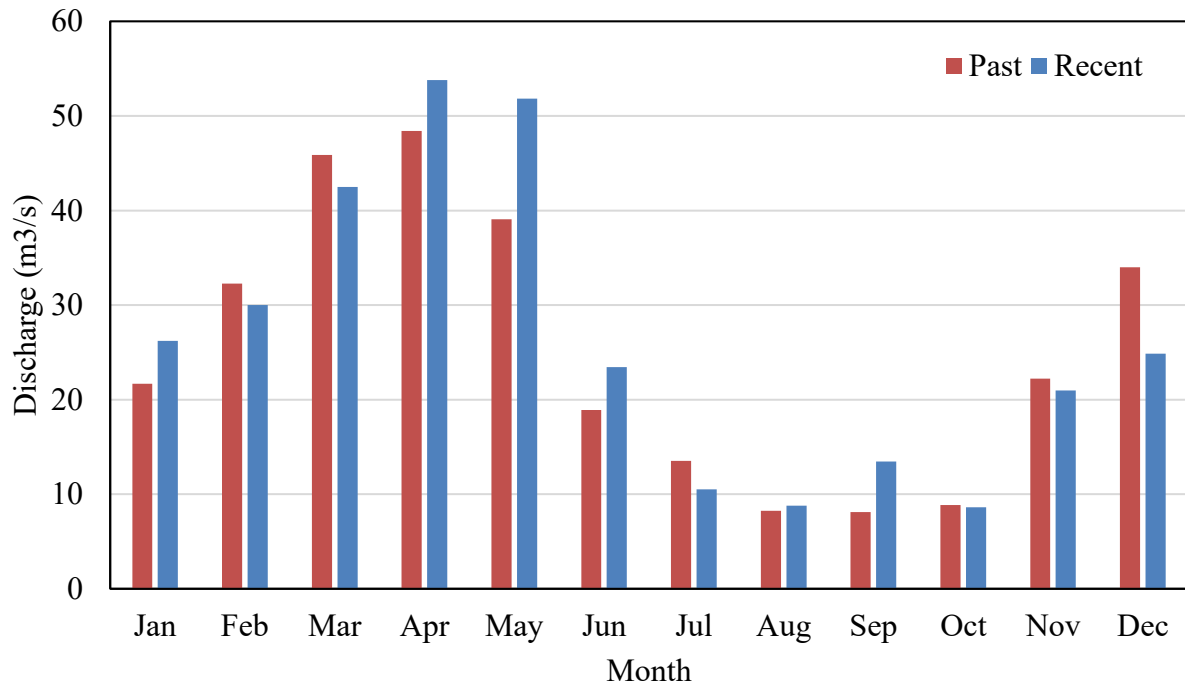
Figure 18. Past-30 yr and recent-30 yr average monthly discharge trends at Byrnesville.

METHODS

This study used a combination of field, laboratory and Geographic Information Systems (GIS) methods. Cores were extracted and returned to the Ozarks Environmental and Water Resources Institute (OEWRI) geomorphology laboratory at Missouri State University for analyses. Sediment samples collected in the field were subjected to sedimentological and geochemical analysis with trends evaluated against historical land use, mine production, and flood records and results from previous studies in this region (Pavlowsky et al., 2010; Young, 2011; Huggins, 2016; Pavlowsky et al., 2017).

Field Methods

The study site was selected primarily due to the downstream location along Big River and mining areas, accessibility of aerial photographs from 1937, 1956, 1970, 1990, and 2006, and a discharge gage located 3 kilometers downstream that spans over 94 years of record. Core locations were selected based on property accessibility, floodplain landform, and proximity to the Big River channel. Field maps containing soil and landform data were created and utilized in the field to determine preferred coring locations throughout a single transect. Soil and elevation profile mapping provided information on geomorphic characteristics such as floodplains, terraces, and benches for proposed study sites. A total of 12 coring sites were chosen along a 110 meter transect running perpendicular to the channel downstream of the USGS stream gage at Byrnesville (07018500).

Topographic surveys. Cross sections provide information about bankfull width, channel depth, and area that can all be utilized to determine overbank flooding conditions (Rosgen, 1996;

Bartley and Rutherford, 2005). In this study, topographic surveys were used to determine changes in surface elevations and relationship to the present-day channel bed as well as to identify alluvial geomorphic features along the study transect. A Topcon HiPer Lite+ Real-Time Kinematic (RTK) GPS unit and a Topcon GTS-225 total station were utilized to complete the cross section of the study transect from the road surface to the left bank of Big River. The OEWRI standard operating procedure (SOP) was used to setup and operate the RTK system and the Topcon instrument manual was used to setup and operate the total station using one prism pole (OEWRI, 2016; Topcon, 2007). The RTK was used to develop a cross sectional survey along the study site to note elevation changes and to compare surface conditions at extracted core sites. A total station was used to complete the cross section from bank to bank including thalweg location. GPS surveys were also completed along the bank top edge along the reach to compare to digitized bank locations. LiDAR data with 1 meter resolution collected between December 10, 2010 and April 6, 2011 was downloaded from Missouri Spatial Data Information Service for visualizing topographic changes along the study transect in the field and for core collection purposes.

  Core collection. Previous studies used sediment cores collected along Big River to provide information on the sedimentology and geochemistry of floodplain and terrace deposits (Pavlowsky et al., 2017; Smith and Schumacher, 2018). For this study, sediment cores were collected at 12 locations across the valley floor by a Giddings truck-mounted push tube and auger to assess subsurface trends across the cross section on March 12 – 13, 2018 (Table 6; Figure 12 and Figure 19; Appendix B). The core length and the hole depth were measured with a tape measure after each core segment to determine percent recovery of the material. The average core length was 3 m ranging from 1 m on a higher terrace to 4.11 m in an active floodplain near

the river bank. Each core segment was placed on half sections of PVC pipes and arranged in order with depth measured with folding rulers (Figure 20). Soil and sediment characteristics were described in the field including soil horizons, sedimentary units, texture changes, and color changes (Owen et al., 2011). Core tube refusal typically occurred at depths > 2 m in sand beds or gravelly materials. A handheld tile probe was used to determine the depth to refusal which indicated the total depth of fine-grained sediments over coarser channel deposits or bedrock. If present, the water table was measured at the depth of the stable water surface in the hole. Finally, sedimentary changes were noted in the cores which included color, water table depth, sand lenses and silt/clay textures, and sand mineralogy. Probe depths ranged from 3 m to 6 m and water table depths were ranged from 2 m to 3 m from the floodplain surface.

Core description and sampling. Sand lenses were visible in 11 of the 12 cores at depths ranging from 1 m to 4 m and organic debris layers were noted in 10 of the 12 samples at depth of 0 m to 4 m. Cores 1 through 11 were subjected to field XRF analysis described below to identify where the high resolution research core would be collected. Any changes within the core were noted and photographs were taken at a 13 cm scale using a Geological Society of America ruler. The core was then split into 3 cm segments using a small spade, which was rinsed and wiped clean between each split to reduce cross contamination of samples. The 3 cm segment was then placed in a labeled Ziploc bag and sealed for transportation to the OEWRI geomorphology laboratory.

Source sediment sampling. The geochemistry of background or source sediments within the watershed can be used to compare with core trends to evaluate the provenance of sediment in floodplain deposits (Oldfield et al., 1985). This study used source sediments to identify geochemical similarities between core 12 sediments and sediments from Big River tributaries.

The primary geologic rock type in the watershed is Cambrian-aged Eminence and Potosi Dolomite (39%) and Cambrian-aged Elvins and Bonne Terre Dolomite (26%) with minor Cotter and Jefferson City Dolomite (11%) and Gasconade Dolomite (8%) (Table 7). The secondary rock types include sandstone, conglomerate, and chert. Fifty samples were obtained from tributaries of Big River including Big River at Belgrade (3), Belews Creek (5), Big River at Bootleggers Access (7) Cedar Creek (7), Heads Creek (3), Terre Bleue upstream and downstream (7), Mill Creek (7), Mineral Fork (7), and Big River at Irondale (4) (Figure 21). Big River at Irondale is underlain by the Precambrian volcanics which represents the oldest geological area sampled for this study. Terre Bleue, Big River at Belgrade, and Big River at Bootleggers Access drains the Cambrian-aged Elvins and Bonne Terre Dolomite. Younger Cambrian- aged Eminence and Potosi Dolomite is drained by Mill Creek and Mineral Fork. Terre Bleue upstream and downstream drains the Cambrian-aged Lamotte Sandstone. Belews Creek drains Ordovician-aged Cotter and Jefferson City Dolomites. Finally, Heads Creek drains the Ordovician-aged Decorah and Plattin Groups. For this study, floodplain samples gathered from overbank deposits will be compared to geochemical results in core 12 (Table 7).

Laboratory Methods

   Sample preparation. Core 12 samples were also processed in the OEWRI Geomorphology laboratory at Missouri State University. The Ziploc bags were opened and placed in ovens and dried at 60°C for 72 hours. Once dried, the samples were disaggregated with a mortar and pestle and sieved using 2 mm, 250 um, and 63 um sieves and each sample fraction was placed in a labeled lead-free bag for storage. Mineralogy, geochemical, and textural data were obtained for each sample to determine trends within the 4 m core.

Percent organic matter by LOI. Loss on ignition (LOI) techniques have been utilized in studies to determine organic carbon and carbonate carbon concentrations within sediments to determine buried soils, sedimentation environment, and potential sorption capacities of sediments (Dean Jr., 1974; Abella and Zimmer, 2007; Downing et al., 2008; Akpomie et al., 2015). Percent organic matter was determined by using LOI techniques defined by combining steps from published procedures (Heiri et al., 2001; OEWRI, 2007a; Konare et al., 2010; Owen et al., 2011). This analysis is completed by heating pre-washed crucibles at 105˚C for four hours in an oven to remove moisture. Each crucible was tare weighed and 5 grams (g) of material was added with the total weight recorded. The loaded crucibles were then placed back in the oven at 105˚C for two hours to remove moisture. After 8 hours, the crucibles were placed in a desiccator lined with drierite anhydrous calcium sulfate to cool while preventing rehydration. After thirty minutes, each crucible was weighed for total pre-burn weight and placed in a muffle furnace at 600˚C for 8 hours. The muffle furnace was then turned off and the samples cooled for 45 minutes in the furnace before they were placed in the desiccator for 30 minutes after which they were weighed again for the post-burn weight. The LOI percentage is calculated as the difference between the pre-burn sample weight and the post-burn weight divided by the pre-burn weight and multiplied by 100. Each analysis included two racks of 14 samples and one duplicate for a total of 30 samples. All laboratory duplicates were < 7% relative percent difference (RPD).

Percent sand. Particle size analysis has been utilized in previous research to determine the effects of particle size and metal sorption potential on heavy metal concentrations (Lecce and Pavlowsky, 1997). Utilizing the same methodology, this analysis can identify increased sand percentages throughout the core as well as heavy metal concentration differences which produce floodplain stratigraphy and suggest changes in sediment supply and transportation with flooding

events (Magilligan, 1992; Florsheim and Mount, 2002). Sand analysis was completed by drying samples at 60˚C and disaggregating the samples using a mortar and pestle to pass through a 250-micrometer sieve. Prewashed 250 mL beakers were placed in an oven at 105˚C for four hours to remove any excess moisture. The beakers were then weighed and 20 g of samples were added. Total weight was recorded and the beakers were places in the oven at 105˚C for 2 hours to remove excess moisture. The samples were then cooled in a desiccator for 30 minutes and the total weight was recorded, 125 mL of sodium hexametaphosphate was added to each sample, stirred with a glass rod, and soaked for 24 hours. The sand percentage was measured by wet sieving the samples through a 63-micrometer sieve, drying the remaining sample in the oven at 105˚C overnight, and recording the weight of the dried sample and beaker. RPD values ranged from 0 to 10% between all samples. The remaining sample was placed in labeled lead-free Ziploc bags for mineralogical and geochemical analyses. Sand percentages in each sample was used to correct XRF results by removing the effect of dilution by quartz sand present.

Mineralogy and anthropogenic materials. Mineralogy changes throughout core profiles can indicate changes within land use and location of sediments (Koinig et al., 2003). Changes throughout the core can indicate changes in sediment source, as well as identify pre-mining surfaces and pre-settlement surfaces (James, 2013). Sand particles from the sand percentage analyses were analyzed under a microscope to note quartz, feldspar, and lithic composition of each sample. The samples were cleaned from all silt and clay particles, which made mineralogical identification more precise. Samples weighing up to 5 grams were placed in plastic dishes and placed under the microscope at 5x and 10x. The presence of anthropogenic material was noted in the form of plastic microbeads and broken glass (<1 mm in size) (Figure 22).

XRF analysis. X-ray Fluorescence (XRF) analysis is routinely used to determine metal profiles in alluvial sediments (Macklin and Dowsett, 1989; Matschullat et al., 1997; McComb et al., 2014). This study uses XRF analysis to determine metal profiles in lower Big River cores to characterize sediment composition and for mining metal dating purposes (Pavlowsky et al., 2010; Huggins, 2016; Pavlowsky et al., 2017; Smith and Schumacher, 2018). Field analyses were conducted on cores 1 – 11 to determine the depths of heavy metal concentrations across the floodplain. Each core segment was placed on table top holders to analyze for geochemical and sedimentary changes throughout the profile. The outside of the extracted core is disturbed during the coring process as it slides against the core barrel, therefore cores were split lengthwise with a spade to expose the undisturbed portion and a flat surface was created for XRF analysis (Smith and Schumacher, 2018). A lead-free bag was placed between the XMET3000 analyzer and the samples to keep the analyzer free of sediment contamination. Samples were analyzed every 30 centimeters for 60 seconds. Duplicates, blanks, and standards were run every 10 samples to reduce variability and validate the calibration of the analyzer as well as maintaining quality assurance and quality control (QA/QC). X-ray fluorescence analyses were taken at the same increment in each core in order to remain consistent. The metals of concern for this study were lead (Pb), zinc (Zn), iron (Fe), manganese (Mn), and calcium (Ca). Relative percent difference values for duplicates under field condition the 11 cores were Pb (13%), Zn (10%), Fe (4%), and Ca (14%). In all, 36 duplicates were measured in the field (Appendix C).

The < 250 um fraction of samples from core 12 were analyzed in the OEWRI geomorphology laboratory and took place in 90 second increments per sample to collect elemental concentrations of Pb, Ca, Fe, and Zn utilizing the same portable XRF that was used in the field analyses. Duplicate samples were taken every ten samples, as well as blanks and

standards, yielding 14 total duplicate analyses under laboratory conditions. The RPD for core 12 were: Pb (3%), Zn (6%), Fe (2%), and Ca (9%). The metal concentrations were then corrected by eliminating sand percentages within each sample. This was completed by dividing the metal concentrations by the fraction of fine-grained material in the bulk sample.

Barium (Ba) concentrations could not be obtained utilizing the XRF at MSU therefore, core 12 samples were taken to the U.S. Fish and Wildlife Service (USFWS) in Columbia, Missouri and analyzed by Thermo scientific Niton XL3t XRF for Ba concentrations. The same procedures were followed as in the MSU laboratory. Maximum RPD for Ba concentrations were 11% (14 duplicate samples) and 12% for Pb. Results from XRF analyses in the OEWRI laboratory were compared to the USFWS Niton XL3T XRF. Relative percent difference values for the samples ranged from 0% to 11.7% for Pb suggesting that low variability between the two XRF instruments.

Three surface samples were also collected parallel to the river channel 5 m upstream and downstream of the original core sites as well as at the core site to determine variabilities within surface concentrations of metals (Appendix D). These samples were analyzed using XRF techniques and compared to their respective core. The coefficient of variation (CV%) of the triplicate samples sets was relatively low for all core sites (1, 2, 3, 4, 5, 6, 9, 10, and 11/12). The highest CV% value was 11% for Pb at core 1. Errors for the other metals were also relatively low with maximum CV% values for Zn at 3% and Ca at 15%.

Magnetic susceptibility. Variations in magnetic susceptibility (MS) can be related to variations in ferrimagnetic minerals and particle sizes in core profiles (Le Borgne, 1955; Mullins, 1977). These changes can reflect erosional processes on specific lithologic and soil source areas and land use changes in a catchment (Turner, 1997). Previous studies have determined

differences between pre-mining surfaces and surfaces that contain Pb, Zn, and Ca using MS

(Petrovsky et al., 2001). Typically, MS values and concentrations of heavy metals have a

significant relationship possibly due to the magnetically harder grains from Pb industrial

processes (Petrovsky et al., 2001). MS analyses were conducted utilizing OEWRI SOP (OEWRI,

2013). Even numbered core samples (every other one) were analyzed utilizing the Bartington

MS3 magnetic susceptibility meter and Trimble nomad 900 GL handheld model. Small plastic

cups were weighed, and ten grams of material were added and sealed for analysis. Each sample

was then analyzed for low frequency and high frequency changes in frequency dependent

susceptibility. Blanks, standards, and duplicates were conducted every ten samples for QA/QC

and RPD. Samples were measured before the destructive loss of ignition analysis and after loss

on ignition to note changes in susceptibility. Due to the loss of mass with loss on ignition

analysis, post LOI sediment results must be corrected by taking the measured value, multiplying

it by 10, and dividing it by the sample mass to account for the differences between the 10 g of

required material and the actual sample mass. There are some potential problems with utilizing

MS including migration of ferrimagnetic grains throughout the profile and differences in

sediment mineralogy during flooding events (Petrovsky et al., 2001). The range of RPD for pre-

burn magnetic susceptibility at low frequency was between 0.0% to 0.7% and 0.0 to 0.3% for

high frequency. The range of RPD for post-burn magnetic susceptibility low frequency was

between 0.1% to 8% and 0.0 to 7.6% for high frequency.

Mining metals dating. Pb and Zn concentrations have been used in previous studies to

identify changes within sediment profiles as well as constrain dates of sedimentation through

comparing geochemical records to historical mining records (Macklin, 1985; Knox, 1987;

Swennen et al., 1994). Macklin (1985) was the first to use heavy metal concentrations within a

floodplain to determine depositional events. Knox (1987) combined geochemical mining metal analyses with Pb/Zn mining records to determine sedimentation rates within a floodplain due to land use change over time. This study primarily used Pb and historical mining records to constrain dates of sedimentation as mining production history is recorded in floodplain sediments (Macklin, 1985; Knox, 1987; Owen et al., 2011) (Figure 23). Secondary elements used to date historical mining peaks include Zn, Ba, and Ca. Constraining sedimentation dates utilizing mining metals only gives a minimum age for sedimentation due to time delays in transportation from the mining site to the floodplain in lower portions of the watershed (Macklin, 1985).

Cesium-137 dating. Cesium 137 (^{137}Cs) can be used to determine the age of recent sediment deposits (<70 years). Nuclear weapons testing began in the early 1950s and contained ^{137}Cs as a radioactive isotope (Walling and Woodward, 1992). Therefore, ^{137}Cs can be utilized as a marker in core analyses for sedimentation beginning in the 1950s (Walling and He, 1999; Owen et al., 2011). There are some potential errors in utilizing ^{137}Cs due to bioturbation within the floodplain profile (Walling and He, 1993). However, the ^{137}Cs peak can be utilized to approximate the 1963 surface as this was the peak year of nuclear testing and the 1954 surface as this was the first year for worldwide nuclear testing (Walling and He, 1994).

Spatial Data Analysis

Light Detection and Ranging Data (LiDAR). LiDAR is often used to create a high resolution topographic map of watershed features (McKean et al., 2008). For this study, LiDAR data (2011) from MSDIS with 1-meter resolution was obtained through the OEWRI database at MSU to create a map of alluvial landform changes. Landforms were constrained by breaks in slope and digitized of distinct landforms were performed. A total of five landforms were

identified including channel, bench/bar, active floodplain, backswamp, and low terrace (Figure 24). The bench/bar surface was identified by the elevated surfaces within the wetted channel. The active floodplain was identified by the change in elevation from the bench deposit to the increase in elevation at the low terrace. The backswamp was identified as a depression within the active floodplain. Finally, the low terrace was identified as the increase in elevation from the active floodplain.

Soil series and landform associations. Soils reflect both natural processes and human interactions by weathering, erosion, sedimentation, as well as soil development and degradation (Renschler and Harbor, 2002). Previous studies in the watershed have identified certain soil series that are more likely to contain geochemical profiles from mining and land use changes (Pavlowsky et al., 2017). Understanding the soil horizons present within the study site can provide insights into landform characteristics as well as provide information on where to extract cores. Soil data were gathered from the USDA-NRCS gateway for Jefferson County, St. Francois County, and Washington County (Brown, 1981; Skaer, 2004).

Aerial photography. Historical aerial photographs analysis is useful for identifying planform river channel changes (Surian, 1999). Historical planform channel analysis involves the co-registration of aerial photos and maps from different years so a sequence of past channel positions can be overlain and analyzed (Hughes et al., 2006) (Figure 25 and Figure 26). Aerial photographs from 1937, 1954, 1970, 1990, and 2006 were utilized to understand geomorphic and topographical changes on the landscape by downloading data from USGS Earth explorer, MSDIS, OEWRI server, and the USDA-NRCS geospatial gateway. Big River Watershed was delineated from files stored in the OEWRI server. Data were then analyzed in ESRI ArcGIS

software to determine spatial and temporal variability within the study site. The compiled information aided in field navigation and interpretations.

Historical Data

Discharge records and analysis. Stream gage information has been used in previous research to determine geomorphic responses of channels to human disturbance including dam construction (Juracek and Fitzpatrick, 2009). This study utilizes data from the Big River at Byrnesville gage (USGS 07018500) which is located 3 km upstream of the study site. Annual peak flood data were gathered from the USGS website to determine if magnitude of floods have increased in recent times (https://waterdata.usgs.gov/usa/nwis/uv?07018500). The top ten stream flows recorded were from 1915, 1950, 1957, 1983, 1986, 1993, 1994, 2008, 2016, and 2017 with values ranging from 1,045 m^3/s (1950) to 2,265 m^3/s (1915). The average peak discharge for the record is 579 m^3/s. Daily discharge records were then used to determine overbank flood duration from 1923 to 2018. The average days of overbank flows for the entire record is 2 days per year ranging from 1 day to 8 days in May 1957 (Figure 27).

Population census. Population census information was gathered from the social explorer website to determine population trends in Jefferson, St. Francois, and Washington Counties from 1840 to 2012 (www.socialexplorer.com). There is a gap in population data from 1954 and 1974 between all counties that may skew the actual population in the counties during this time period.

Agriculture census. Agricultural census data were obtained from the USDA agricultural census, to obtain historical information on farm acreage, livestock numbers, and bushels of grains (https://www.nass.usda.gov/AgCensus/). Historical trends in these land use indicators were used to evaluate timing and intensity of early land clearing and settlement and subsequent

agricultural practices in the watershed. Underreporting in agricultural census data as well as changes to terminology used such as improved/unimproved from 1850 – 1910 to pastured/not pastured from 1940 – 2012 can cause misinterpretation (Gallman, 1972). A gap in information exists in 1925 for livestock and crops as well as acreage pastured/not pastured in 1890,1900, 1920, 1940, and 1969.

Other historical sources. Historical documents, news articles, and personal accounts can fill in gaps and help identify core profiles, flood records, and land use change within the study area (Deacon, 1999). This study used historical records obtained by Schoolcraft which provided general land use information during early 19th century in the Ozarks including mining, agriculture, and landscape data (Schoolcraft, 1819). Historical documents provided by Jefferson County Library provided information on Rockford Mill construction and ownership (Jefferson County Genealogical Society, 2015). Information on the construction and maintenance of Byrnesville dam was obtained from George Suggs' book on water mills as well as the current owners website (Suggs, 2008; https://www.thelalumondiere.com/). Finally, Sauer's 1920 publication provided general information on conditions within the Ozarks as well as early settlement and mining operations in the Big River area (Sauer, 1920).

Table 6. Study site soil associations.

Soil	Landform	Recurrence Interval (yr)	% of site
Kaintuck	bench/bar active	2	8
Haymond	floodplain	2	62
Wilbur	backswamp	2	8
Sturkie	low terrace	2 - 50	22

Table 7. Source sediment location and geology.

Site	Geology	Stream	County	Latitude	Longitude
Big River (Belgrade)	Elvins and Bonne Terre	Big River	Washington	37.780849	-90.846329
Cedar Creek	Lamotte Sandstone	Cedar Creek	Washington	37.76074	-90.7417
Big River (Bootleggers)	Elvins and Bonne Terre	Big River	Washington	37.812395	-90.772109
Big River (Irondale)	Volcanics	Big River	Washington	37.830509	-90.696067
Mill Creek	Eminence and Potosi Dolomite	Mill Creek	Washington	37.99427	-90.66089
Mineral Fork	Eminence and Potosi Dolomite	Mineral Fork	Washington	38.05410	-90.77987
Terre Bleue Creek (smaller drainage area upstream site)	Lamotte Sandstone	Terre Bleue Creek	St. Francois	37.919536	-90.41746
Terre Bleue Creek (larger drainage area – downstream site)	Elvins and Bonne Terre	Terre Bleue Creek	St. Francois	37.92876	-90.49273
Belews Creek	Cotter and Jefferson City Dolomite	Belews Creek	Jefferson	38.292444	-90.60002
Heads Creek	Decorah and Plattin Group	Heads Creek	Jefferson	38.381343	-90.5297

Figure 19. Giddings core rig.

Figure 20. Field XRF of core segment.
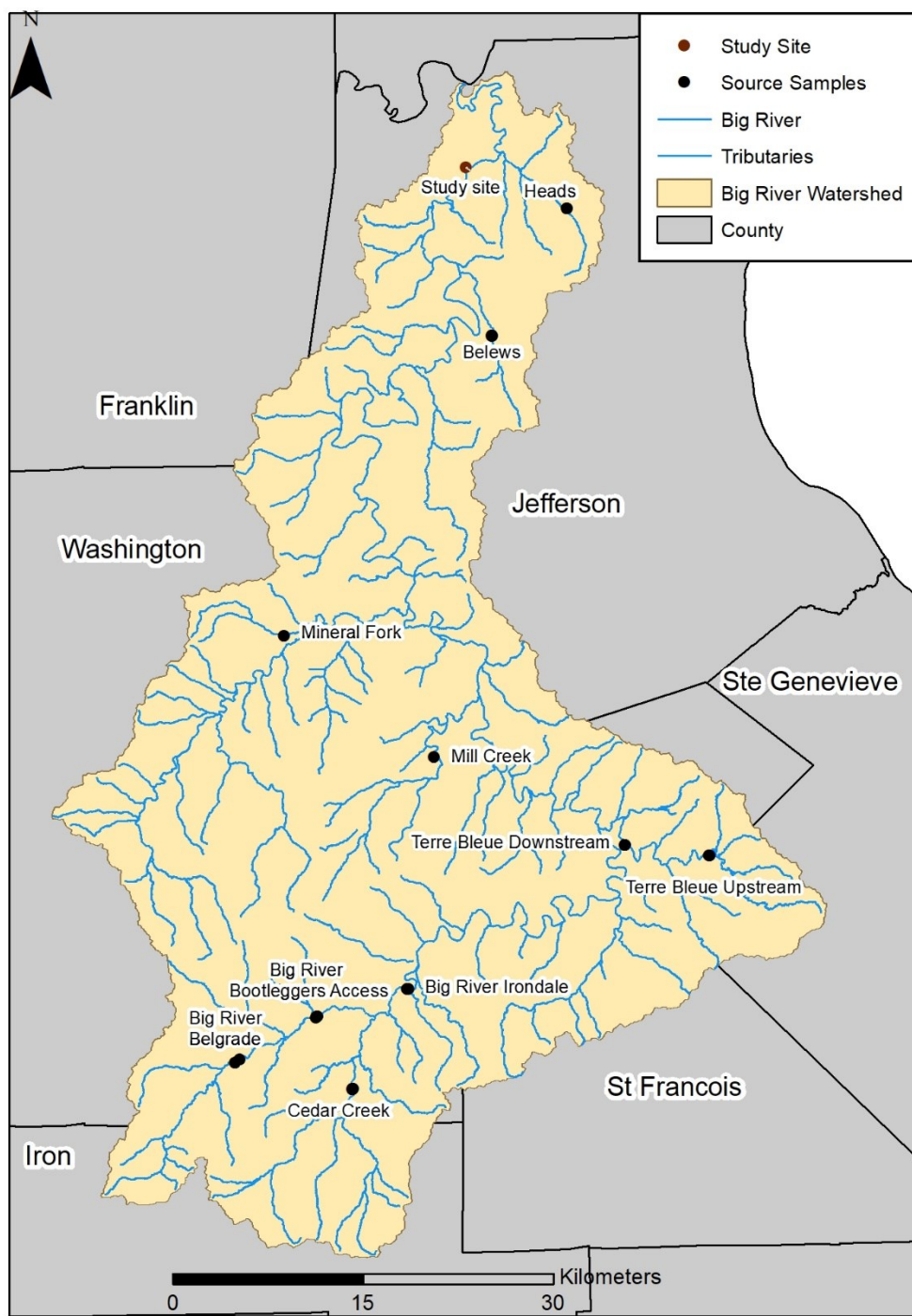
Figure 21. Source sample locations.

a.

b.

Figure 22. Anthropogenic material in surface sample (a) microplastic bead and (b) broken glass.
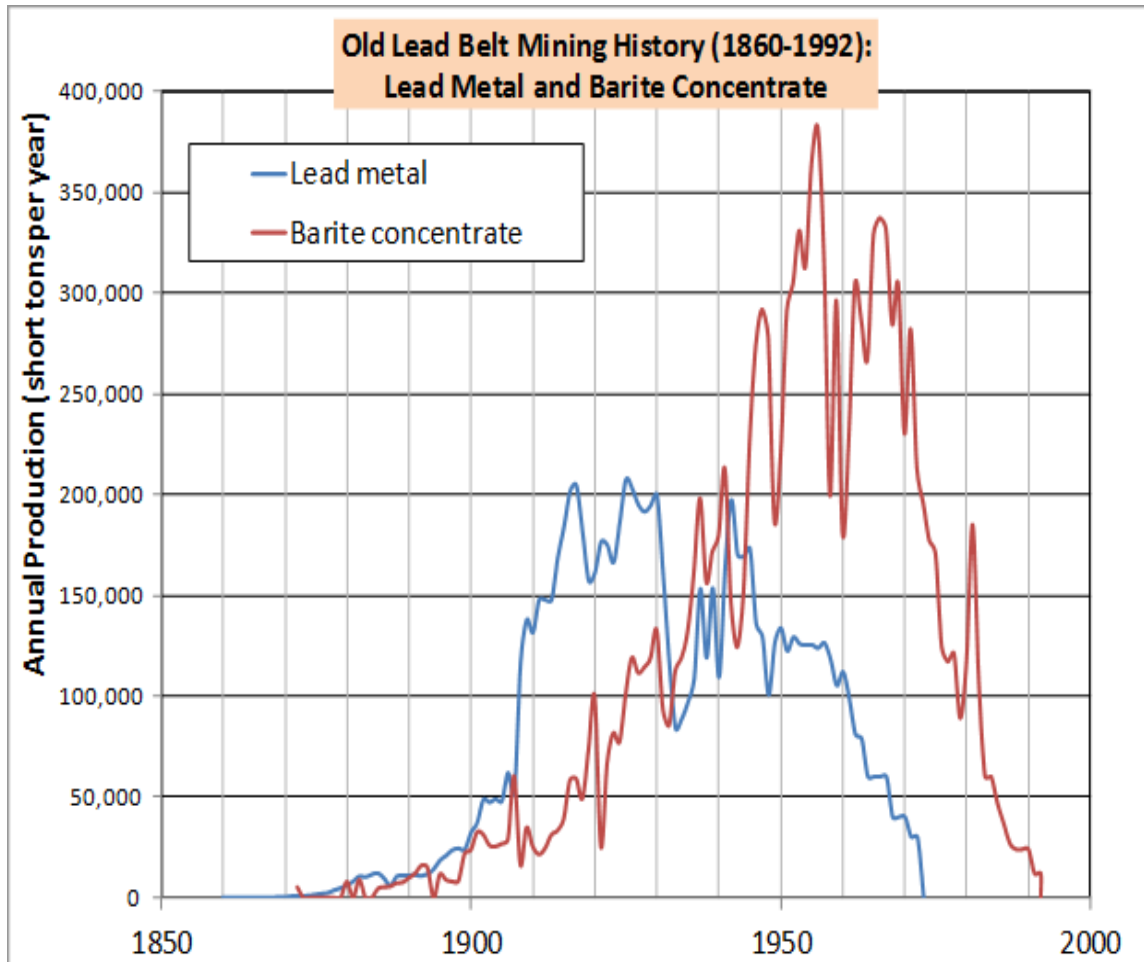
Figure 23. Pb and Ba annual production (courtesy of Robert T. Pavlowsky; data from Minerals Yearbooks, all years).
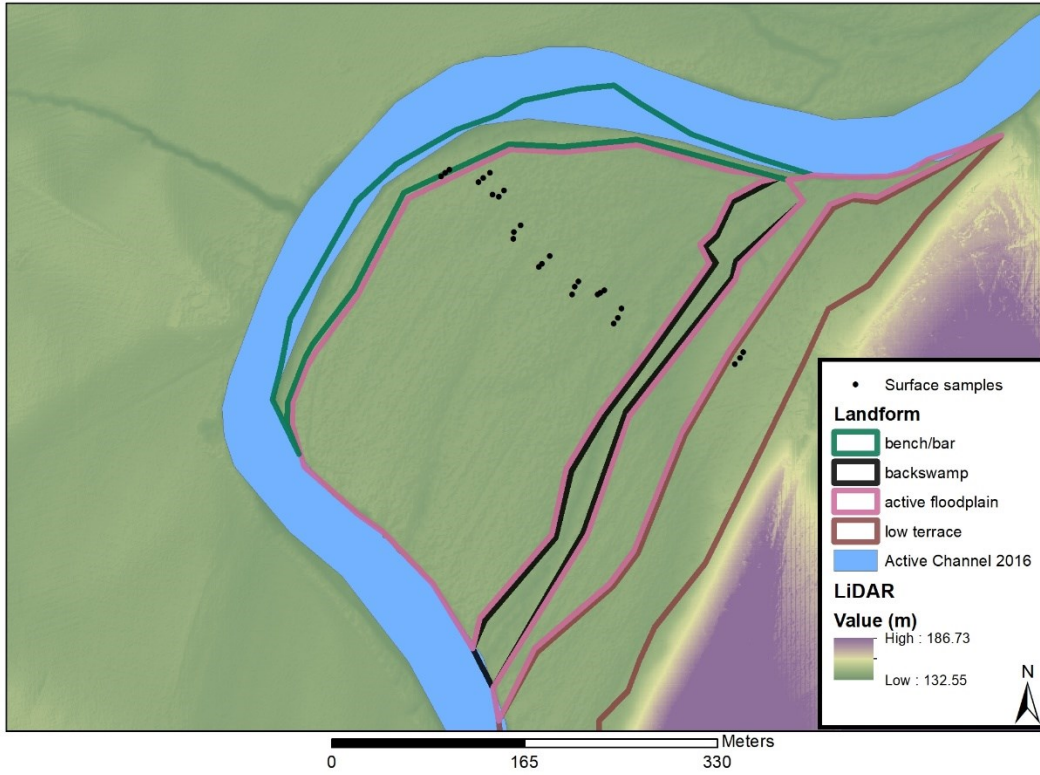
Figure 24. Geomorphic landforms and surface samples for error analysis.
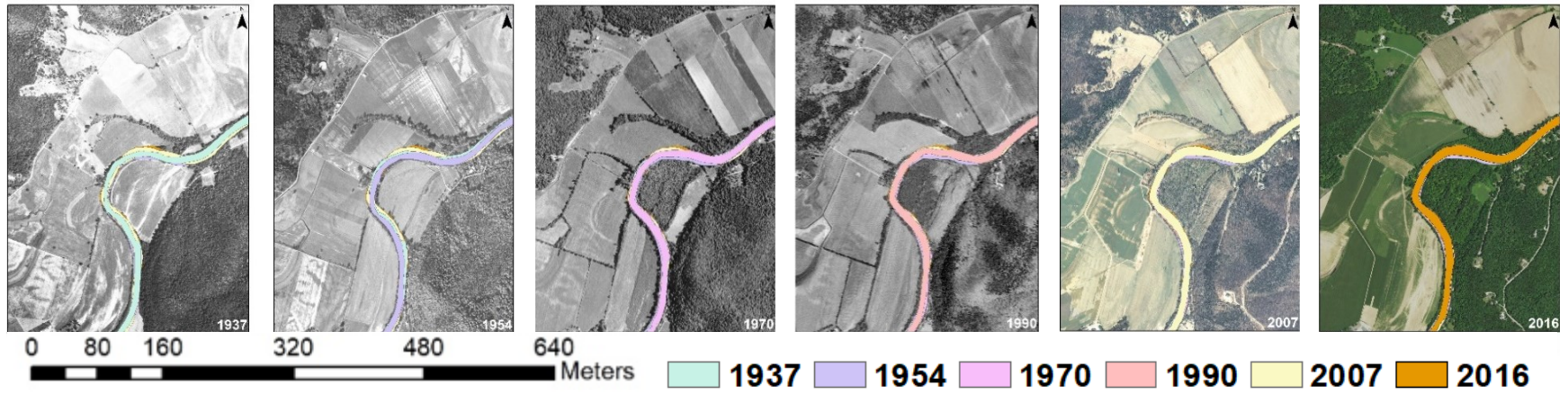
Figure 25. Big River Byrnesville active channel migration.

64

Figure 26. Big River Byrnesville bar migration.
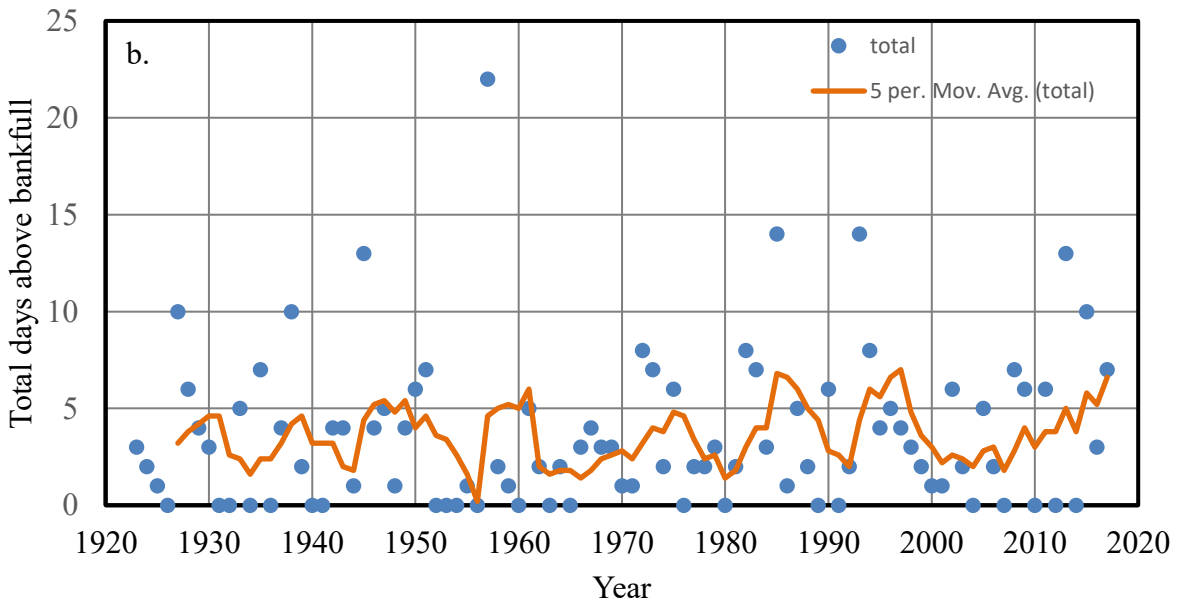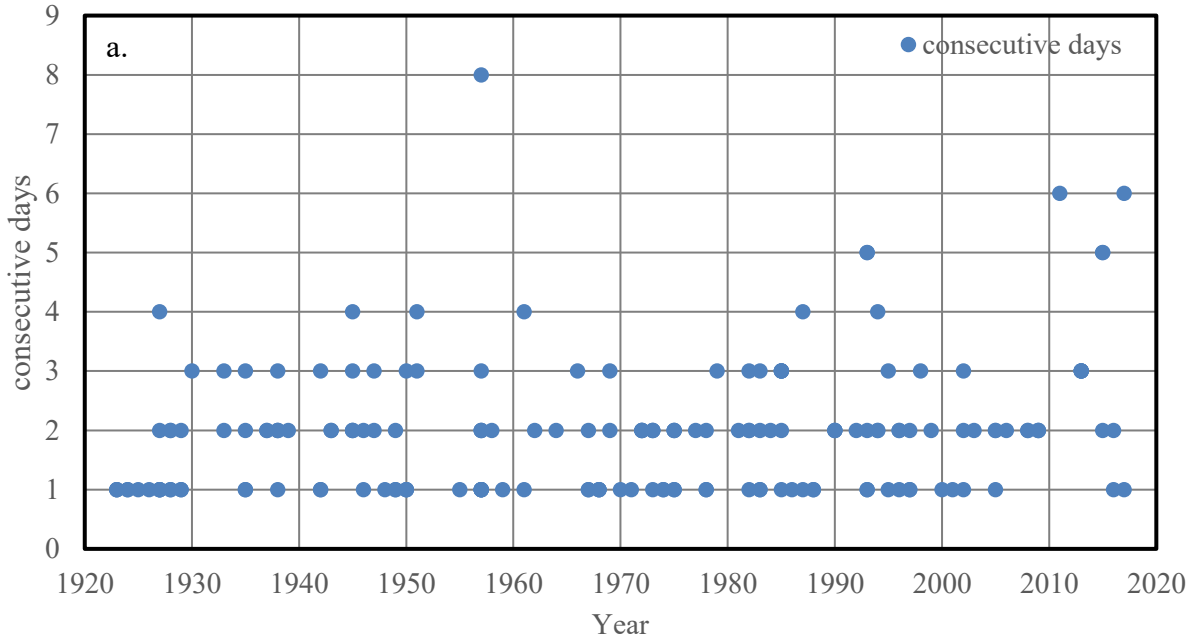
Figure 27. Consecutive and total days of overbank conditions (a) consecutive days each year and (b) total days each year.

RESULTS AND DISCUSSION

The goal of this chapter is to report and interpret geochemical and sedimentological core records to relate them to the environmental history of the watershed and floodplain sedimentation rates along lower Big River. To evaluate the stability of the site, aerial photographs were used to assess the historical locations of the active channel banks and bars in Big River. In March and December 2018, twelve cores were collected, described, and analyzed for XRF-metals in the field. One hundred sixty-five samples from core 12 were brought back to the laboratory and later analyzed to determine percent organic matter and sands, mining metal concentrations, ^{137}Cs activity, and magnetic susceptibility in core samples. Inflections in the geochemical and sedimentological profiles (i.e. peaks and troughs) were linked to land use, flood, and mining records to date sediment layers and calculate Post-European settlement sedimentation rates. Historical sedimentation rate trends were interpreted to evaluate land use and geomorphological factors that have influenced floodplain deposition rates along the lower Big River since European settlement began.

Site History

Active channel widths and gravel bar areas within a three-kilometer river segment including the study area were digitized on aerial photographs from 1937, 1954, 1970, 1990, 2007, and 2016 (Table 8). The river segment was split into three one-km long reaches: upstream reach at river km 21, study reach at river km 20, and downstream reach at river km 19. Only minor geomorphic changes related to localized channel migration and bar aggradation occurred within

66

the segment since 1937 (Table 8). More importantly, the land areas along the core transect have not been affected by channel migration and bank erosion since at least 1937.

In the upstream reach, channel width averaged 48 m since 1937 and bars were present between 1954 and 1970, only covering about 5% of the active channel. Bar area in the upstream reach peaked at 7% in 2007 and decreased to 4% in 2016. In the study reach, the average channel width since 1937 was 48 m. Between 1970 and 1990, the location of bank lines fluctuated laterally across a range of 12 m on the left bank and 4 m on the right bank, with average channel width decreasing by 2 m overall (Table 8). By 2007, the range of channel bank adjustments decreased to 4 m on the left bank and 7 m on the right bank. Bars were first observed in the study reach in 1990, covering 3% of the total channel. However, bar area expanded to cover 11% of the active channel by 2007 and remained at 12% bar area in 2016 (Table 8). Average channel width increased by an average of 6 m throughout the study segment between 2007 and 2016 possibly due to a series of large floods during that period (Figure 25). In the downstream reach, the average width of the channel was 51 m and no bars were observed in the downstream reach since 1937.

Historical photography analysis indicates minimal land use changes within the study area during the past 79 years (Figure 26). The 1937 land use within the study reach was mainly agricultural land to the west of the river (left side), with forest and grassland/pasture on the east side of the river, with no structures on the valley floor. In 1937, the study site was in pasture/grassland with trees growing on the study site between 1954 and 1970 (core locations 2-6 and 9-12). Between 1970 and 1990, some of the forested areas were again converted to grassland within the northeast portion of the study site (core locations 2, 9, 3). Rivermont Road was constructed along the right valley side between 1990 and 2007 with more forest growth across

the study site overall. A building was constructed on the property 34 m to the east of core seven between 2007 and 2016. The higher terraces were cleared of trees near core one and core eight, however, grass was still visible on the aerial photograph in 2007.

Valley Floor Transect

     Geomorphic Setting. The study transect consists of 12 cores: two were located on a low terrace associated with the Sturkie soil series (cores 1 and 7); one was within a back-swamp mapped as the Wilbur soil series (core 8); eight were collected from the active floodplain with the Haymond soil series (cores 2 - 5 and 9 - 12); and one was within the bench or Kaintuck soil series (core 6) (Table 9; Figure 28). Surface elevations ranged 1.47 m from 137.07 meters above sea level (masl) at the low terrace (core 7) to 135.6 masl at the back-swamp landform (core 6) (Figure 28). Probe refusal depth varied along the transect from 3.7 m to 6.6 m. Average depths from the top of the floodplain surface were 1.3 m to the top of the channel bar and 4.5 m to the current channel bed at the thalweg (Figure 28).

     Core analyses indicated that the sedimentology of the alluvial landforms of Big River were typical of low to moderate gradient, mixed sediment load rivers in the Midwest USA (Knox, 1987). Young floodplain or bench deposits with silt and loam textured deposits overlying a coarser unit with sand lenses and silty mud drapes were found near the channel close to the modern bank. In addition, thick layers of organic matter (leaves, twigs, seeds) were often interbedded between sand lenses as found in channel- or chute-fill deposits where burial rate was relatively rapid (Leigh, 2018). Floodplain cores were mainly composed of silty overbank sediment with some fine sand. Organic matter, reduced colors, and sand lenses are found at depth indicating buried channel bar deposits concentrations which increased at lower depths (Knox,

68

1987). Back-swamp chute deposits consisted primarily of poorly-drained silt, organic deposits in varying states of decomposition, and occasional sand beds. The low terrace deposits contained silt and clay-sized grains and evidence of argillic horizon development in the solum. However, there were gravel-sized particles present within the upper 5 cm as well as at the bottom of the core suggesting sporadic coarse colluvial inputs from nearby hillslopes during the Holocene and modern surface wash from the nearby road.

Geochemistry. Samples from cores 1 – 11 were described by color, texture, and other sedimentary features and analyzed by field XRF for mining-related and other metals. A transect from right bank of Big River to the low terrace feature was sampled to determine surface and subsurface variability in metals with respect to distance from the channel (Table 9; Figure 28 and 30). A total of 219 samples were analyzed in the field among the 11 cores. Floodplain Pb trends and refusal depths reflect the typical stratigraphy expected for alluvial deposits along rivers draining historical mining areas (Knox, 1985) (Figure 29).

Geochemical analyses on cores 1 – 12 indicate significant peaks in Pb, Zn, and Ca between 90 cm and 150 cm depths within the floodplain cores as well as the bench and back-swamp cores. However, both low terrace cores did not contain high concentrations of Pb depth suggesting that low terrace surfaces were not flooded as often as the floodplains (0.5-1 m lower). Mean Pb concentration of all the samples collected was 1,056 ppm with the highest concentration found in a floodplain deposit (core 12, 108 cm depth, 5,648 ppm Pb) and the lowest concentration found in the low terrace (core 7, 30 cm depth, below detection for Pb) (Figure 29). The mean Zn concentration was 162 ppm with the highest concentration found in the bench deposit (core 6, 120 cm depth, 408 ppm Zn) and the lowest concentration being found in the lower portions of the floodplain (core 3, 320 cm depth, 32 ppm Zn). The mean value for

Ca is 2,479 ppm with the highest concentrations found in a bench sample at 12,320 ppm and the lowest concentrations (below detection) found in the lower portions of the floodplain, low terrace, and back-swamp cores.

Each core was divided into background (uncontaminated) and contaminated segments (Table 9; Figures 29 and 30). Recall, that the coefficient of variation (CV%) The average (CV%) for contaminated core samples (n =184) was: 1,246 ppm (89%) for Pb, 174 ppm (38%) for Zn, and 3,543 ppm (70%) for Ca. For uncontaminated core samples (n = 19), the average (CV%) was 35 ppm (24%) for Pb, 100 (21%) for Zn, and 1,641 ppm (24%) for Ca. Calcium concentrations in pure mine tailings from the Old Lead Belt average about 18% Ca (Pavlowsky et al.2017). Assuming a simple dilution process, post-mining legacy floodplain deposits along lower Big River contain only about 1-2% tailings sediment with the most heavily contaminated sediment layers containing up to 6% tailings.

Spatial Error Analysis

The coefficient of variation (CV%) of sediment and geochemical properties among triplicate surface samples was used to estimate potential sampling errors for core sediment analyses for sand %, LOI%, and metals (Table 10 and Table 11). The three samples were collected at a depth of 0-3 cm: (i) 1 m away from the field core hole; (ii) 5 m upstream from the first sample; and (iii) 5 m downstream from the first sample. Average sand content for surface soils increased in the following order: low terrace, 7.9%; floodplain, 9.2%, and bench, 14.4% with the CV% ranging from 12 to 21% (Table 10) Average percent LOI decreased slightly across the valley floor in the following order: low terrace, 6.2%; floodplain, 5.5%, and bench, 5.2% with the CV% ranging from 6 to 10% (Table 10). In general, surface sand content

decreased across the floodplain from 12-14 % near the channel to 6-8% at the valley margin This

trend for Big River compares well with previous studies that report a lateral fining of sediments

away from the channel (Wolman and Leopold, 1957; Knox, 1987; Lecce and Pavlowsky, 2004;

Dean et al., 2011; Hupp et al., 2015) (Table 2). Average Pb concentrations in the surface

samples ranged from 663 ppm to 1,219 ppm, all exceeding the toxic threshold concentration of

400 ppm (EPA, 2015). Metal concentrations varied randomly across the valley with no lateral

trends observed with average CV% values as follows: Pb, 5% (max, 11%); Zn, 3% (max, 6.4%);

and Ca, 15% (max, 50.4%) (Table 11).

Summary. Floodplain areas along the coring transect have been stable since 1937

indicating that the profiles stored sediments for at least 80 years. The maximum channel

migration occurred between 1937 and 1954 within the study segment, which correlates with

previous studies that suggest sand and gravel waves migrated downstream during this time

(Jacobson, 1995). Core trends reflect those typical for alluvial floodplains by exhibiting a fining

upwards sequence from laterally-accreted coarse channel deposits upward into vertically-

accreted fine-grained overbank deposits (Happ et al., 1940). Lateral fining from the channel to

core seven reflect typical alluvial landform formation (Happ et al., 1940; Knox 1987; Hupp et

al., 2015). Field geochemical analyses on the cores suggest that trends are present in surface soils

and subsurface sediments with respect to Pb and Zn concentrations and are similar to previous

studies in Big River Watershed (Pavlowsky et al., 2010; Huggins, 2016; Pavlowsky et al., 2017).

Coefficient of variation analyses on the surface samples indicate that there is relatively low

spatial error present at this site with Pb, Zn, and Ca concentrations. Therefore, it is assumed that

the geochemical analyses produced for this study have similar ranges of low-variability at depth

and over sampling distances of 10 m (Table 11). Previous research has identified high

concentrations of mining metals stored within floodplains throughout the watershed (Pavlowsky et al., 2017). Floodplain deposits were found to be heavily contaminated at depths between 100-150 cm and, therefore, were assumed to reflect the timing of peak mining periods for sediment dating purposes (e.g., Macklin, 1985; Knox, 1987) (Figure 30).

Floodplain Core 12

Sand profile. Sand percentages were determined for 137 samples ranging in value from 1% at 0.27 m to 63% at 2.76 m in Core 12 (Appendix E). Although the overall average percentage was 17%, there is a distinct increase in sand percentages in the core below 2 m. The average from 0 m to 2 m is 7 % sand while the average between 2 m and 4.11 m is 28 % sand. As mentioned about, this fining-upward sequence from sandy bar deposits formed by lateral accretion to overbank floodplain deposits is typical for fine-grained floodplains (Happ et al., 1940; Knox 1987; Hupp et al., 2015) (Figure 31). In general, the mineralogy of the sand fraction is rich in quartz with traces of feldspar, limestone, and dolomite throughout the depth of the core. While higher sand percentage in the lower portion if the floodplain core is predictable based on sedimentological evidence, there is the possibility that the transport rate of sand sediment by the Big River was greater than present in the past. Soil conservation land management began in the Ozarks in the 1930s when government agencies purchased large tracts for recreation and timber harvesting (Jacobson and Primm, 1994). Therefore, sediment supply for floodplain deposition before the 1930s may have had higher sand content due increased sand availability as a result of active land clearing and soil disturbance well as lack of soil conservation practices (Jacobson and Primm, 1994). In addition, sand and gravel waves may have migrated down Big River and through the study segment during periods prior to 1910, 1945 – 1955 and 1980 - 1990 (Jacobson,

1995). Increased sand deposition within the channel during these periods may have raised bed elevations and thus increased frequency of overbank floods and sedimentation rates on floodplains (James, 2010).

LOI. Due to the lack of fine-grained material <250 um in some samples, only 100 out of the 137 samples were analyzed for organic matter percent utilizing loss on ignition techniques (Appendix E). Organic matter content ranged from 2.0 – 14.2% with the maximum located at 3.54 m depth (Figure 31). Organic material within the surface soil (0 - 6 cm) was 8.9% and decreased to an average of 5.5% LOI from 6 to 30 cm depth. The Average LOI% from 0 to 2 m was 4.7% with a CV of 23% while the average LOI% from 2 to 4 m was 5.1% with a CV of 40% indicating more variability below 2 m depth. Peaks in organic matter within the lower portion of the core represents layers of poorly decomposed leaves and twigs interbedded with sand lenses suggesting relatively rapid burial early on.

^{137}Cs results. Recall, peak levels of ^{137}Cs indicate the 1963 surface layer, with the first presence of ^{137}Cs below that representing the 1954 surface layer (Walling and Woodward, 1992; Walling and He, 1993). A total of ten samples were analyzed by Dartmouth University for peaks in ^{137}Cs activity. The peak activity of ^{137}Cs was located at 30 cm depth at 10.6 Bq/kg (1963) with the first initial presence at 50 cm depth measuring 0.9 Bq/kg (1954) (Table 13 and Figure 32).

Source sediments comparison. Background sources within the watershed from previous work suggest that metal concentrations can vary with soil, mineralogy, and bedrock type (Pavlowsky et al., 2017). The upper Big River and tributaries were sampled to evaluate the geochemistry in some areas not affected by OLB mining. For this study, background concentrations in pre-mining sediments were estimated by averaging concentrations of metals from background sediment sources that were not exposed to mining events in the watershed to

determine the 95% confidence limit (+2 s) for Pb (73 ppm) and Zn (159 ppm) as suggested in previous studies in the watershed (Pavlowsky et al., 2017).

All source sample averages were below background concentrations for Pb except for Big River Irondale, Mill Creek, Mineral Fork, and Belews Creek (Table 12). Lead mines were present at Irondale in 1902 and local contamination could account for these concentrations (Buckley, 1908). Surface mines in the Potosi Formation for both Pb and Ba and some crude smelting furnaces were located along both Mineral Fork, Mill Creek, and Belews Creek beginning in the 1800s and extending into the middle 1900s (Buckley, 1908; Mugel, 2016). Zinc concentrations are above background concentration only in Mill Creek and Mineral Fork samples. Calcium concentrations are higher at all source sites compared to core 12 sediments except for between core depths of 66 cm to 111 cm when mining inputs occur at the highest level (Figure 33). Mill Creek and Mineral Fork contain relatively high concentrations of Pb and Zn due to releases of metal-rich sediment from the erosion of naturally mineralized soils as well as historical surface mining activities in Washington County (Table 12) (Mugel, 201). The high Pb and Zn concentrations in core 12 indicate mining source inputs from the watershed above 123 cm depth for Zn and 258 cm depth for Pb. This depth profile of mining metals has been found previously by other workers in Big River floodplains (Young, 2011; Pavlowsky et al., 2017). Source fingerprinting analysis could offer more insight to sources, but was not completed for this study (Haddadchi et al., 2013).

Geochemical dating results. Geochemical results for the 137 samples from XRF analysis suggests that peaks in the historical mining record can be used to constrain dates of deposition within core 12 (Table 14). Lead peaks correlate well with the highest concentrations of Zn in the core as well as Ca and Cu (Figure 33 and Figure 34). In the upper 2 m of the core, all

three metals (Pb, Ca, and Zn) are positively correlated due to the strong association of these elements in mining sediment contaminated by ore and tailings particles with Pearson correlation coefficients as follows: Pb – Zn (0.62), Pb – Ca (0.77), and Zn – Ca (0.83) (n= 67) (Figure 33). Lead and Ca are positively correlated throughout the samples since the primary host rock for the Pb is the Bonne Terre Dolomite which typically contains 21% Ca (Jackson et al., 1935; Pavlowsky et al., 2017). Previous studies have also noted strong relationships between Pb and Zn concentrations on mining contaminated sediments in Big River (Smith and Schumacher, 1993; Pavlowsky et al., 2017). However, correlations noticeably decrease in the samples below 2 m depth as follows: Pb – Zn (-0.04), Pb – Ca (0.43), and Zn – Ca (0.28) (n= 70) (Figure 33). Lower core sediments were presumably deposited prior to large-scale mining in St. Francois County and reflect background or uncontaminated sediment-metal associations and not the geochemistry from mining wastes.

Barium concentrations increase slightly in the lower core in response to the start of surface pit Ba mining and overall effect of agricultural soil disturbance on increased soil erosion in Washington County. Barium concentrations in the whole core ranged from 144 ppm to 712 ppm with most of the samples measuring between 400 ppm to 600 ppm Ba. There is an obvious increase in Ba concentration above 3 m depth below which Ba averages 420 ppm and above which Ba averages 566 ppm (1.35 times increase) (Figure 35). The CV% of Ba concentrations is similar between core segments, with 13% for the upper 3 m and 19% for the >3 m core segment. This result is similar to other geochemical studies in this portion of the watershed that indicate Ba concentrations in Big River sediment are not as sensitive to mining history as Pb and Zn concentrations (Pavlowsky et al., 2017; Smith and Schumacher, 2018).

Old Lead Belt mining-related metal trends can be used to date floodplain sediments in core 12 assuming that periods of peak Pb production also produce higher tailings pollution loads to Big River (e.g., Macklin, 1985; Knox, 1987; Owen et al., 2011; Lecce and Pavlowsky, 2014). The highest peak in the sand-corrected Pb was 5,943 ppm at 111 cm depth and this sample was consequently assigned the year 1942 which was the final and largest Pb mining peak in the watershed (Figure 33 and Figure 34). Copper (Cu) sulfide minerals were associated with galena mineralization on the Old Lead Belt (Smith, 1988). Therefore, Cu concentration trends in the core between 81cm and 195 cm can be used to specifically identify the depths of mining peaks in the core (Figure 34). Other noticeable peaks in Pb were at 195 cm (2,903 ppm) and 219 cm (1,424 ppm) and these were assigned dates of 1927 (195 cm) and 1917 (219 cm) (Figure 33). The decrease in Pb concentrations at 159 cm was assigned the date of 1933 due to the drop in Pb production due to the Great Depression. The depth at which Pb concentrations in the core begin to increase over 50 ppm (250 cm) was assigned the year 1896 as this was the first year of large-scale mining operations in the watershed when first contamination began. There was an increase in Ba at 303 cm that was determined to be the 1860 surface as 32% of Washington County was farm land and barite surface mines were active within the watershed.

Correlation of sand layers with floods. Eleven sand peaks were identified within core 12 with differences between peaks and neighboring percentages ranging from one to two percent by mass. Peaks in sand percent were compared to days over bankfull per year to try and link the core record to flood events of known dates. The first year identified through this process was 1927 which had 10 total days over bankfull at this site and was previously identified using Pb geochemical data. A 6% sand percentage peak at 147 cm represents 1935 which experienced 7 days over bank conditions and 2 consecutive days of 2.33 year RI flood. Sand peak at 133 cm

correlates to 1938 which experienced 10 days over bankfull that included two consecutive days (3) and three consecutive days (1) which was a 2.33 recurrence interval flood (Table 15). Although the 1942 sediment layer was identified using Pb peaks, the sand percent peak at 111 cm also helped to date this layer as it correlated with a 2.33 recurrence interval flood that was overbank for three consecutive days. Sand peak at 96 cm of 7% was assigned the year 1945 as there were a total of 13 days over bankfull including events that had two consecutive days over bankfull (3), three consecutive days over bankfull (1) and four consecutive days over bankfull (1). The 1947 surface layer was assigned at 90 cm with a 4% sand percentage and five total days of overbank including one day of 2.33 year RI flood (number 18 on record). The 1950 surface layer was assigned at 70 cm depth with a 3% sand percentage and six total days overbank with the highest discharge representing the number ten flood on record. The 1957 layer was assigned at 42 cm with a 3% sand percentage and a total of 22 days overbank with 8 consecutive days overbank with the highest discharge representing the number eight peak on record.

A recent increase in magnitude of floods over the past 40 years may have increased the sand percentages within the top 15 cm of the core. Seven of the ten top floods on record have taken place since 1983, with the most recent flood in 2017 being number two on record. The 1983 surface was assigned at 15 cm with seven days total overbank and three consecutive days with the maximum discharge representing the number seven flood on record. The 1993 surface layer is located at 12 cm depth with a total of 14 days overbank with four floods lasting three consecutive days and one of the floods was rated as a 50-year recurrence interval (number three on record). Further, sand content remains high for 12 cm to the surface as a result of five floods over the 10 year recurrence interval since 1993. The last year assigned using sand percentages was 2008 at 9 cm depth with a 9% sand percentage. There were seven days overbank including

one day of a 10 year RI (number five on record). Although sand percentages helped to assign

years of deposition, this process was only possible by the primary geochemical dating method.

Further research is needed to understand the relationship between floods and sand percentages at

this site.

Historical Trends in Floodplain Sedimentation Rates

      Sedimentation rates. Applying sedimentation rates using historical, geochemical, and

sedimentological records can provide valuable information on how land use change effects

sedimentation within the Big River Watershed. Beginning in 1860 at 303 cm depth in core 12,

sedimentation rates were 1.47 cm/yr, similar to those previously reported for the Midwest which

ranged from <1 cm to 1.9 cm (Magilligan, 1985; Knox, 1987; Lecce and Pavlowsky, 2001;

Owen et al., 2011). At the lower Big River site, significant increases in overbank sedimentation

rates >2 cm/yr began to occur around 1927, peaking between 1927 and 1935 at 6 cm/yr, and then

decreasing to an average 4.5 cm/yr until 1950 (Figure 36). While these rates are generally similar

given core variability, the reduced sedimentation rate between 1935 and 1938 may indicate the

decrease in agriculture during the Great Depression. In addition, there was also relatively lower

Pb concentrations and fewer days over bankfull for these years. The period of highest deposition

rates occurred from 1950 – 1954 (6.7 cm/yr). Higher sedimentation rates in the 1940s and 50s

may have been partially related to gravel waves moving through the study reach causing a rise in

channel bed elevation and more frequent flooding events. However, this effect is not repeated

later as decreasing floodplain sedimentation rates occur during the passage of a second gravel

wave in the 1980s (Jacobson, 1995). Although the highest floods of record have occurred since

1993 resulting in higher sand concentrations in recent floodplain deposits, the deposition rates

generally decreased to 0.2 cm/yr until recently when there was an increase to 0.6 cm/yr since 2008 suggesting that grain size distribution in the river sediment load may not correlate with sand deposit thickness or deposition rate.

The theory of sediment wave propagating through a watershed was proposed by Gilbert (1917) when he studied sediment waves within a heavily mined watershed. Sediment waves were shown to flatten out and deposit on floodplains where channel widths were not adequate enough to hold the material (Gilbert, 1917). These sediment waves may continue to migrate through the channel long after channel elevations have recovered (James, 2010). Within the Ozarks, studies have used USGS gage records to track coarse-grained sediment waves through rivers including Big River (Jacobson, 1995). In this study, there appears to be a 20 to 30 year time lag between the highest rates of land clearing for farms and row-crop production in the period from 1880 to 1925 and highest fine-grained overbank sedimentation rates on floodplains along the lower Big River between 1927 and 1953 (Figure 36). This finding compares well with previous studies suggesting that sediment eroded from headwater drainages during agricultural settlement may take decades or more to move downstream from hillslopes and tributaries to become deposited on floodplains as legacy sediment (Knox, 1977, 1987; Meade, 1982; Jacobson and Primm, 1994; Lecce and Pavlowsky, 2001).

Although ^{137}Cs profiles were not determined for cores 1 – 11, Pb signatures can be used to estimate sedimentation rates from 1896 – 1942 and from 1942 - 2018. Recall, the first recorded concentration of Pb > 50 ppm was assigned the year 1896 as this was the beginning of large-scale mining in the watershed and the peak Pb concentration was assigned the 1942 surface as this was the last major peak in production. Average sedimentation rates for the ten floodplain cores was 4.1 cm/yr from 1896 to 1942. However, floodplain sedimentation rates tended to

decrease away from the channel from about 6 cm/yr in cores 6, 12, and 11 to 3 cm/yr in cores 10, 3, 9, and 2 (Table 16). Floodplain sedimentation rates for the post-1942 period were lower in all cores compared to the <1942 period, averaging 1.5 cm/ yr. There were no lateral trends in deposition rate for the later period, with highest sedimentation rates >1.7 cm/yr observed in cores 6, 4, 10, and 2 and lowest sedimentation rates <1.2 cm/yr in cores 5 and 9 (Table 16).

Environmental Risk due to Historical Mining Contamination

The study site is located within Southwest Jefferson County Mining National Priorities List superfund site that includes most of Jefferson County (EPA, 2012). Concerns for this site includes human health risk due to Pb in residential soils and threats to the environment due to remobilization of Pb in the soils (EPA, 2012). Overall, the average Pb concentration was 1,056 ppm Pb for all the core samples evaluated for this study. Lead concentrations in recent sediments being deposited on floodplains today still remain elevated over the toxic threshold of 400 ppm Pb at locations >120 km below the core mining areas (EPA, 2015). This fact suggests that there is significant environmental risk associated with mining-related soil contamination on floodplains along Big River even after 50 years has passed since the last mine closed in the Old Lead Belt. The average depth of peak Pb concentrations in cores varied by landform at 130 cm for the near-channel floodplain bench, 112 cm for floodplains, 65 cm for back-swamp, and 35 cm for stream terraces. Moreover, the average depth to uncontaminated sediment (< 50 ppm Pb) was 400 cm in the bench, 294 cm in floodplain deposits, 160 cm in the back-swamp, and 35 cm in the low terrace. The only landform that contained Pb concentrations below the toxic threshold for soils was the low terrace. Results from this study support other research findings within the watershed suggesting that management practices should focus reducing the bioavailability of Pb

in bench deposits (Kaintuck soil series) and floodplain soils (Haymond and Wilber soil series) along Big River for 171 km from Leadwood, Missouri to its confluence with the Meramec River at Eureka, Missouri (Gale, 2004; Pavlowsky et al., 2010; Huggins, 2016; Pavlowsky et al., 2017).

Table 8. Aerial photography geomorphic assessment.

Aerial Photography year	R-km 21 Average channel width (m)	Bar area (m^2)	% of channel area	R-km 20 Average channel width (m)	Bar area (m^2)	% of channel area	R-km 19 Average channel width (m)	Bar area (m^2)	% of channel area
1937	36	0	0	39	0	0	46	0	0
1954	49	2,490	5	42	0	0	51	0	0
1970	54	2,633	5	48	0	0	46	0	0
1990	49	1,371	3	47	1,251	3	53	0	0
2007	48	3,506	7	42	4,651	11	54	0	0
2016	50	2,077	4	54	6,295	12	58	0	0
Average	48			45			51		

Table 9. Physical and geochemical characteristics of cores 1 to 11.

Site number	Landform	Soil series	Surface elevation (masl)	Distance from near bank edge (m)	Core depth (cm)				Concentration (ppm)				
					Total length	Tube refusal	Probe refusal	Depth to < 50 ppm Pb	Peak Pb depth	Pb min	Pb Peak	Zn Peak	Ca Peak
7	Low terrace	Sturkie	137.1	341.3	100	240	660	30	10	BD	355	159	6,014
1	Low terrace	Sturkie	136.8	311.6	110	110	660	40	5	BD	401	178	3,848
8	Backswamp	Wilbur	135.6	264.5	210	231	563	160	65	BD	1,010	234	3,411
2	Floodplain	Haymond	136.2	207.3	370	370	478	280	135	BD	4,067	294	7,941
9	Floodplain	Haymond	136	183.9	315	320	569	220	90	19	3,406	299	7,046
3	Floodplain	Haymond	136.3	161.5	320	329	368	250	110	BD	3,672	303	7,028
10	Floodplain	Haymond	136.3	125.1	310	326	597	280	150	24	2,339	246	4,958
4	Floodplain	Haymond	136.5	95.1	385	347	588	347	130	17	3,286	265	7,485
5	Floodplain	Haymond	136.4	63	270	354	630	220	80	BD	3,817	296	7,871
11	Floodplain	Haymond	136.3	41.9	400	410	604	370	100	BD	4,537	349	9,611
6	Bench	Kaintuck	136.4	14.3	400	410	664	330	130	423	3,497	408	12,320

Table 10. Surface sample texture and magnetic susceptibility results for triplicate surface samples.

Core	Landform	Number of samples	Sand %		Magnetic Susceptibility (SI)		LOI %	
			Average	CV%	Average	CV%	Average	CV%
1	Low terrace	3	7.9	12.4	0.00050	7.0	6.2	10.3
2	Floodplain	3	9.4	9.1	0.00039	0.9	5.2	6
9	Floodplain	3	8	11.4	0.00041	3.1	5.3	11
3	Floodplain	3	6.1	15.7	0.00044	3.5	5.1	10.7
10	Floodplain	3	11	4.6	0.00039	4.5	5.6	9.8
4	Floodplain	3	9.9	39.3	0.00040	3.6	6.3	8.6
5	Floodplain	3	8.4	24.1	0.00040	8.7	5.6	13.8
11	Floodplain	3	11.7	24.4	0.00040	4.3	5.3	9.6
6	Bench	3	14.4	21.3	0.00038	1.9	5.2	6.3
Average			9.6	18.0	0.00041	3.7	5.5	9.6

Table 11. XRF results for triplicate surface samples.

Core	Average concentration (ppm)						CV%					
	Pb	Zn	Ti	Fe	Sr	Ca	Pb	Zn	Ti	Fe	Sr	Ca
1	663	260	4,038	22,029	97	6,405	11.0	3.7	6.9	4.2	4.2	15.2
2	1,078	333	3,691	19,881	97	11,533	6.5	6.4	8.4	3.8	5.2	25.2
9	1,129	323	3,955	19,998	97	8,281	2.7	4.0	1.6	2.8	1.2	7.7
3	1,219	359	4,290	21,137	99	7,308	2.5	4.2	2.8	1.6	5.3	2.8
10	1,155	356	3,945	20,881	100	10,817	1.0	1.8	6.9	1.9	2.3	50.4
4	1,142	344	3,910	20,504	95	8,917	1.5	1.8	5.3	0.7	6.9	6.0
5	1,214	340	4,099	20,456	93	8,399	4.4	4.7	1.9	3.6	5.9	15.5
11	1,090	322	3,722	19,413	88	8,207	8.2	3.4	2.6	2.3	5.7	7.9
6	978	312	3,588	18,711	90	7,956	3.2	1.1	3.4	1.8	6.4	4.6
Average	1,074	328	3,915	20,334	95	8,647	5	3	4	3	5	15

Table 12. 137Cs results for core 12.

Sample	Depth below surface (cm)	Cs-137 Bq kg-1	Deposit Date
MJ091418-01	0 – 3	2.4	
MJ091418-03	6 – 9	4.2	
MJ091418-05	12 – 15	5.9	
MJ091418-07	18 – 21	5.6	
MJ091418-09	24 – 27	10.8	
MJ091418-11	30 – 33	10.5	1963
MJ091418-13	36 – 39	5.3	
MJ091418-15	42 – 45	1.8	
MJ091418-17	48 – 51	0.9	1954
MJ091418-19	54 – 57	0.2	

Table 13. Source sample XRF results.

Site	number of samples	Soil Series	average metal concentrations (ppm)				range of metal concentrations (ppm)			
			Pb	Zn	Ca	Fe	Pb	Zn	Ca	Fe
Big River (Belgrade)	3	Cedargap	41	116	10,027	13,690	BD - 70	43 - 168	4,843 - 14,746	5,478 - 22,188
Cedar Creek	7	Cedargap	46	54	4,639	20,801	BD - 104	48 - 98	2,814 - 6,288	18,298 - 28,902
Big River (Bootleggers)	7	Cedargap	63	138	10,769	20,516	BD - 119	70 - 232	6,591 - 16,596	16,306 - 25,268
Big River (Irondale)	4	Huzzah	135	132	12,736	19,849	97 - 112	98 - 177	11,011 - 12,722	18,162 - 21,445
Terre Bleue Creek (smaller drainage area upstream site)	3	Kaintuck	22	21	1,911	15,481	BD - 36	10 - 39	1,697 - 2,588	6,884 - 20,955
Terre Bleue Creek (larger drainage area – downstream site)	4	Kaintuck	23	19	1,869	11,302	BD - 92	6 - 39	BD - 3,972	5,184 - 19,453
Mill Creek	7	Cedargap	417	893	12,005	41,107	370 - 666	737 - 1,034	4,551 - 29,641	25,092 - 55,810
Mineral Fork	7	Cedargap	211	332	22,714	22,532	131 - 327	226 - 397	3,552 - 49,139	17,322 - 28,077
Belews Creek	5	Gladden	201	126	15,424	24,153	49 - 397	44 - 197	7,881 - 20,768	22,255 - 26, 073
Heads Creek	3	Fishpot-Urban	12	65	16,745	16,592	BD - 38	54 - 91	4,298 - 25,743	18,294 - 19,484
Average mining-effected			241	371	15,720	26,910				
Average background			35	69	7,660	16,397				
Core 12 > 73 ppm	124	Haymond	1,247	207	5,335	18,648	62 - 5,648			
Core 12 < 73 ppm	13	Haymond	54	114	2,580	13,325	32 - 48			

Table 14. Sedimentation rates and stratigraphy for core 12.

Depth (cm)	Year	Sedimentation rate	Data utilized
3	2018	0.60	Surface elevation
9	2008	0.20	Flood event sand %
12	1993	0.30	Flood event sand %
15	1983	0.75	Flood event sand %
30	1963	2.00	peak ^{137}Cs Atomic bomb testing
42	1957	2.67	Flood event sand %
50	1954	5.00	Initial 137Cs
70	1950	6.67	Flood event sand %
90	1947	3.00	Flood event sand %
96	1945	5.00	Flood event sand %
111	1942	5.50	Pb/Zn peak and Sand %
133	1938	4.67	Flood event sand %
147	1935	6.00	Flood event sand %
159	1933	6.00	Pb decrease
195	1927	2.40	2nd Pb Peak and Sand %
219	1917	1.48	First Pb peak
250	1896	1.47	initial over background Pb)
303	1860		Increase in Ba census records

Table 15. Flood record for assigned dates from sand lens analyses in core 12.

Flood Year	Discharge Q (m³/s)	Rank	Sand %	Total days overbank	Max Consecutive days overbank	Cross Data	Core Depth (cm)
2008	1260	5	9	7	3		9
1993	1637	3	4	14	4		12
1983	1136	7	4	7	3		15
1957	1053	9	4	22	8		42
1950	977	10	4	6	3		78
1947	708	17	4	5	3		90
1945	756	16	7	13	4		96
1942	589	(not ranked)	5	4	3	Pb/Zn peak	111
1938	665	24	8	10	3		133
1935	651	31	6	7	3		147
1927	566	35	47	10	4	Pb Peak	195

Table 16. Sedimentation rates pre- and post- 1942 at the site.

Core number	Landform	Distance from bank edge (m)	Initial mining 1896	Production Peak 1942	Sedimentation Rates (cm/yr)		
					1896 - 1942	1942 – 2018	1896 – 2018
7	Low terrace	341	30	10	0.43	0.13	0.25
1	Low terrace	312	40	5	0.76	0.07	0.33
8	Backswamp	265	160	65	2.07	0.86	1.31
2	Floodplain	207	280	135	3.15	1.78	2.30
9	Floodplain	184	220	90	2.83	1.18	1.80
3	Floodplain	162	250	110	3.04	1.45	2.05
10	Floodplain	125	280	150	2.82	1.97	2.30
4	Floodplain	95	347	130	4.72	1.71	2.84
5	Floodplain	63	220	80	3.04	1.05	1.80
11	Floodplain	42	370	100	5.87	1.32	3.03
12	Floodplain	42	387	102	6.20	1.34	3.17
6	Bench	14	400	130	5.87	1.71	3.28
Average			249	92	3.40	1.21	2.04
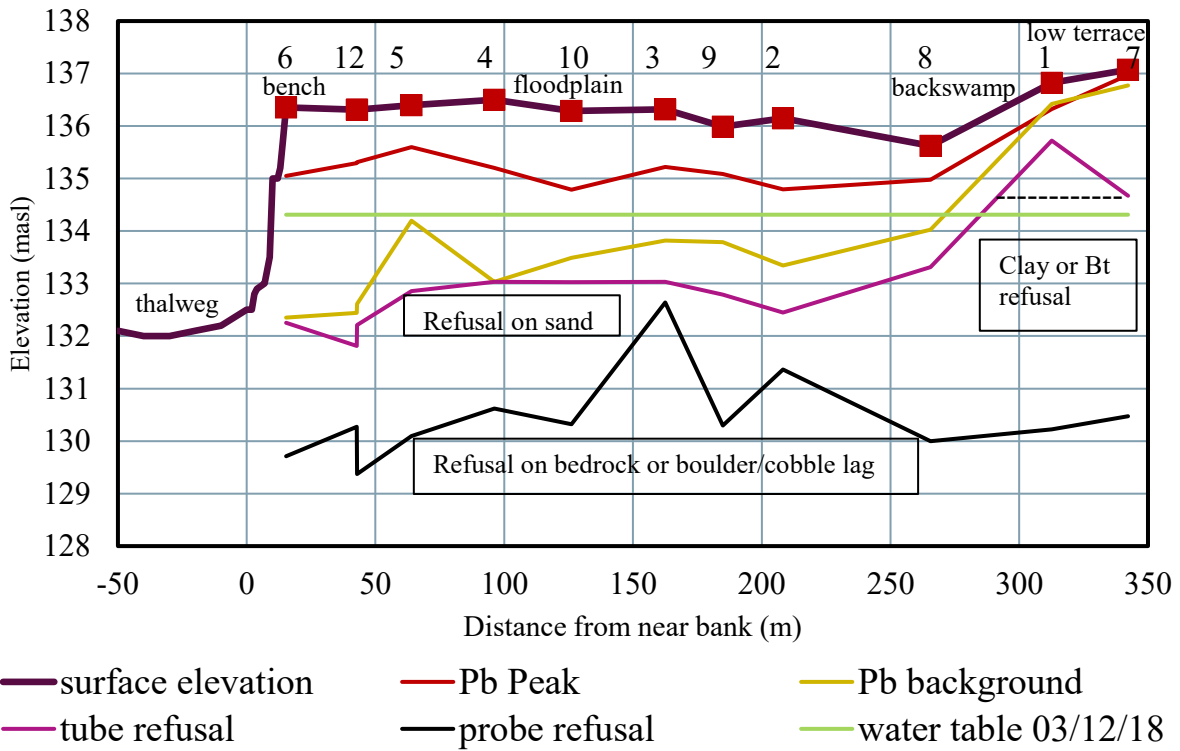
Figure 28. Cross section data for the study transect.
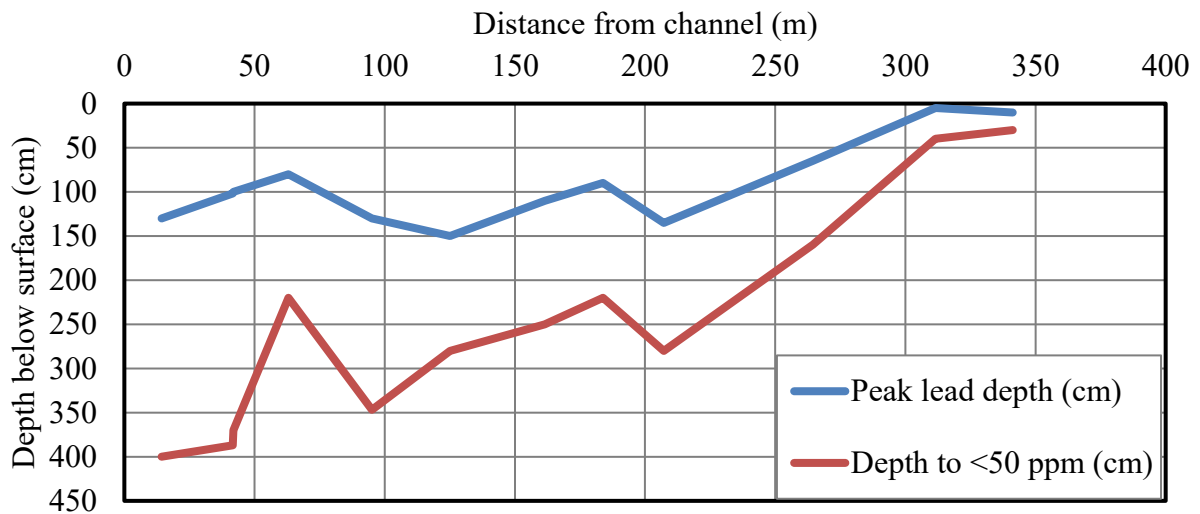
Figure 29. Pb geochemical trends for cores 1 – 11.
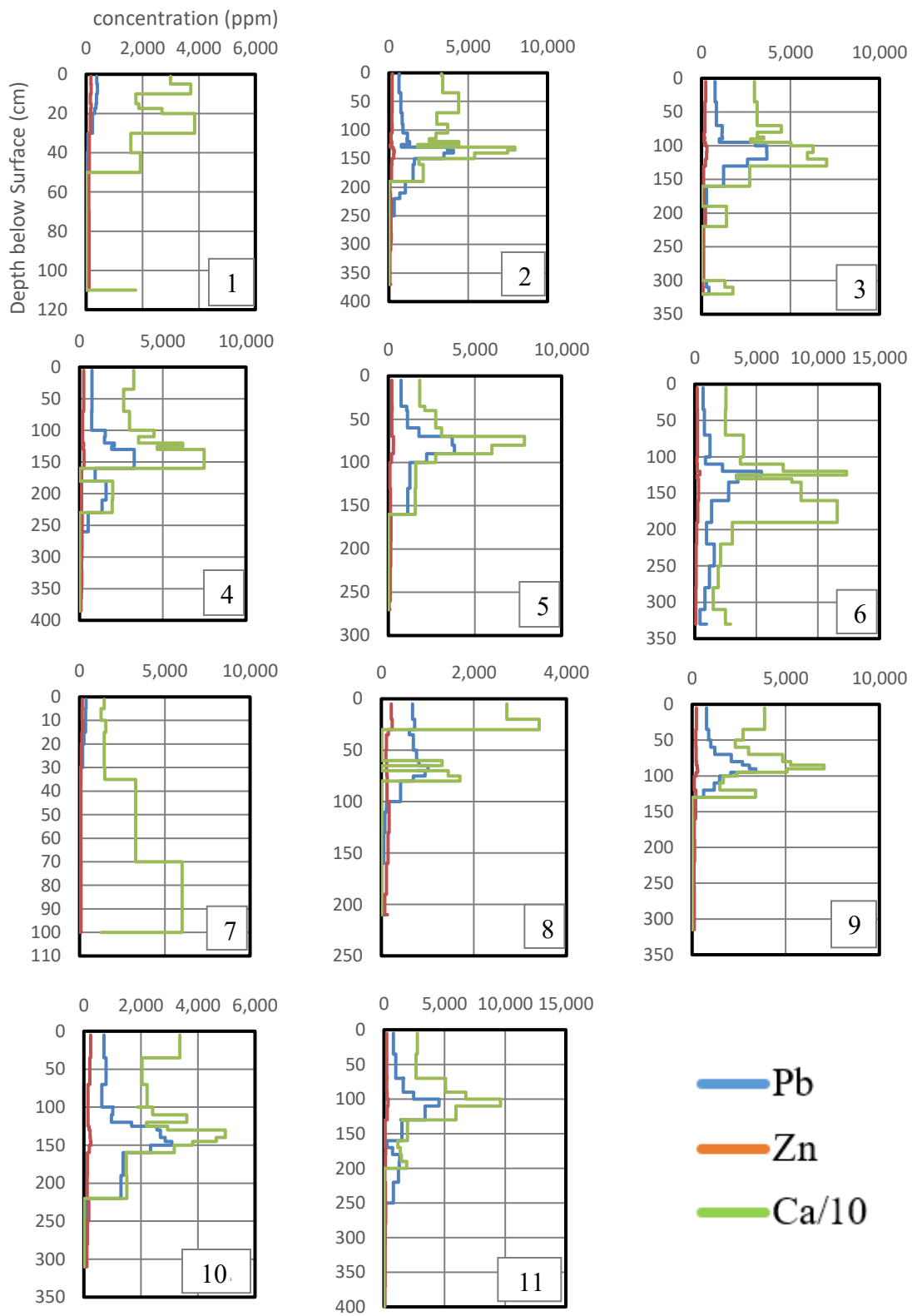
Figure 30. Mining metal geochemistry for cores 1 – 11.
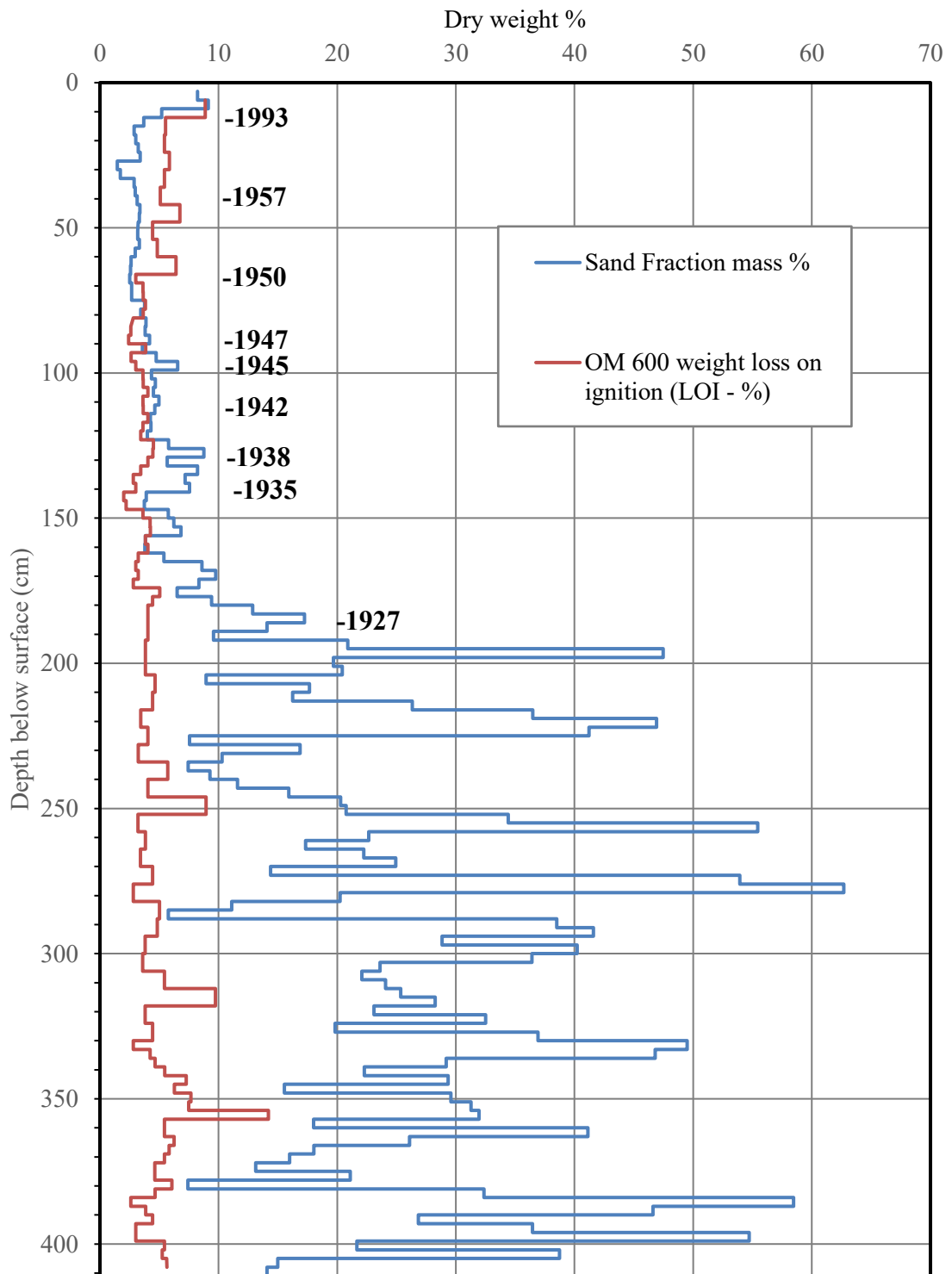
Figure 31. Sand and organic matter percentages for core 12.
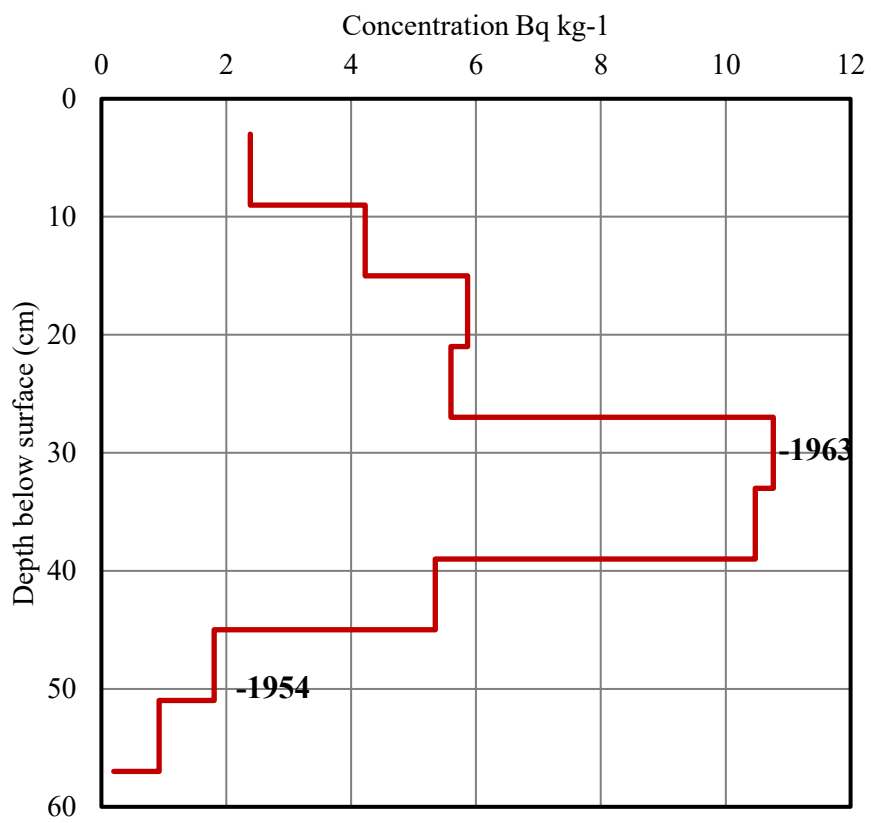
Figure 32. [137]Cs results for core 12.
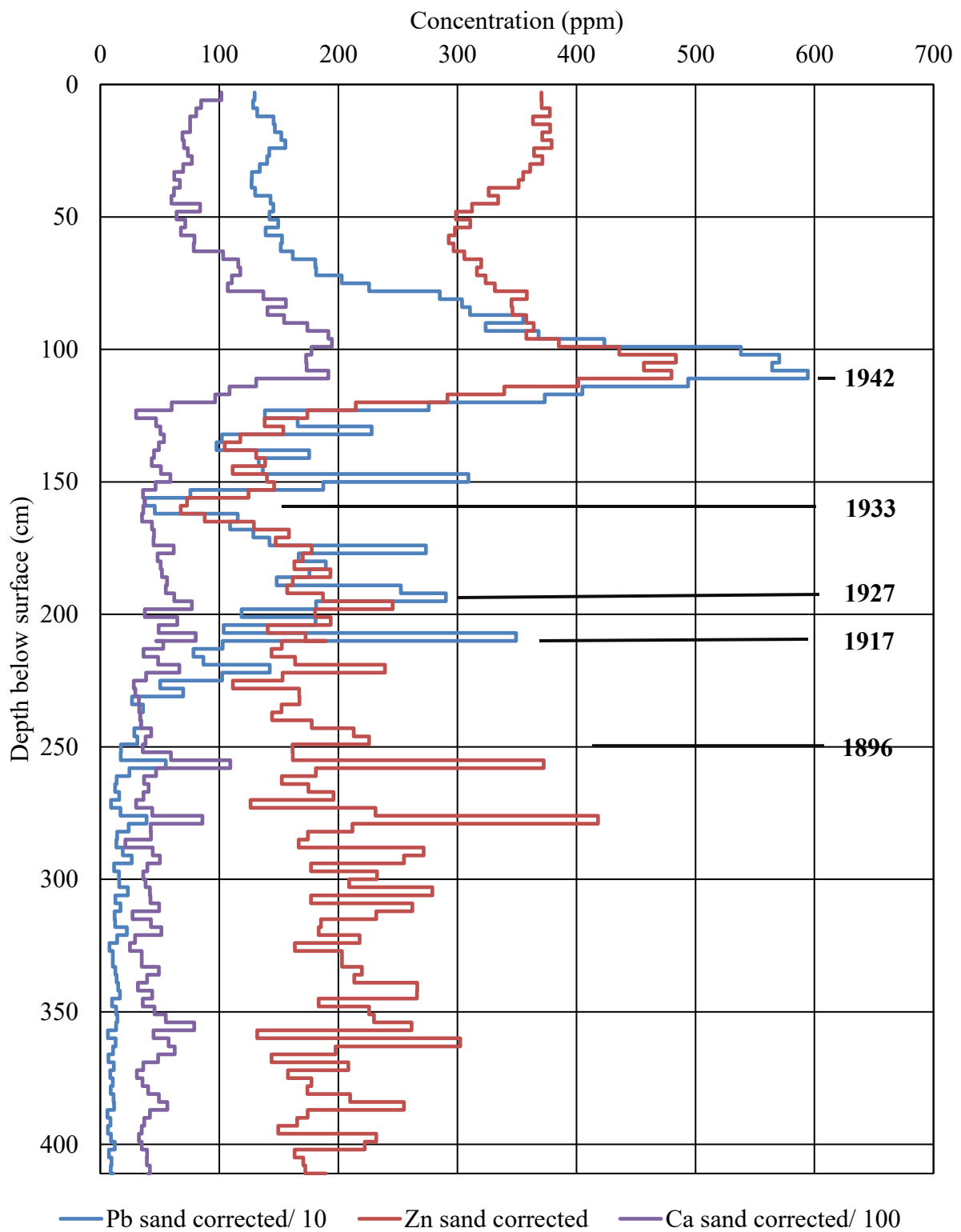
Figure 33. Geochemical results for core 12.
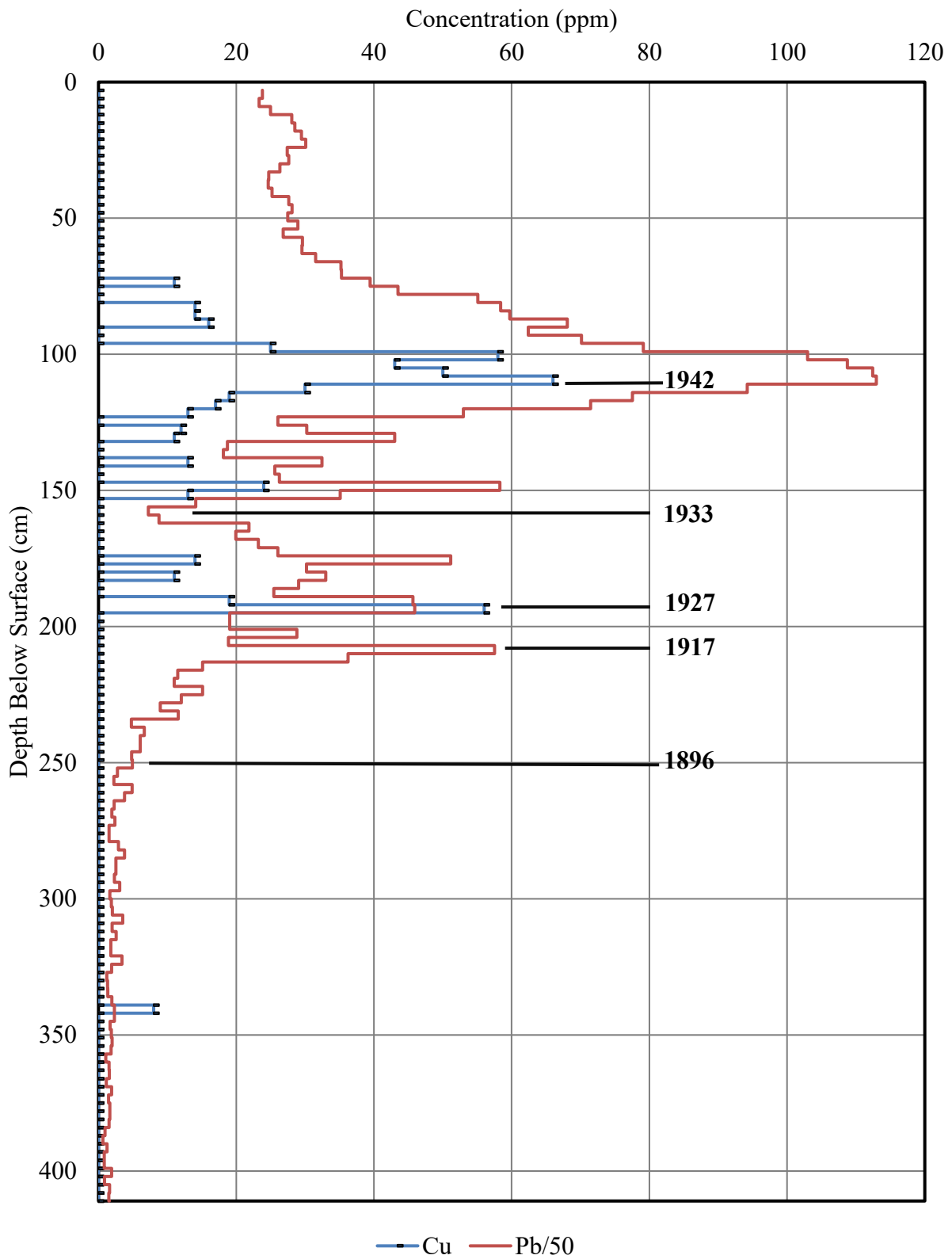
Figure 34. Cu and Pb/50 profile for core 12.
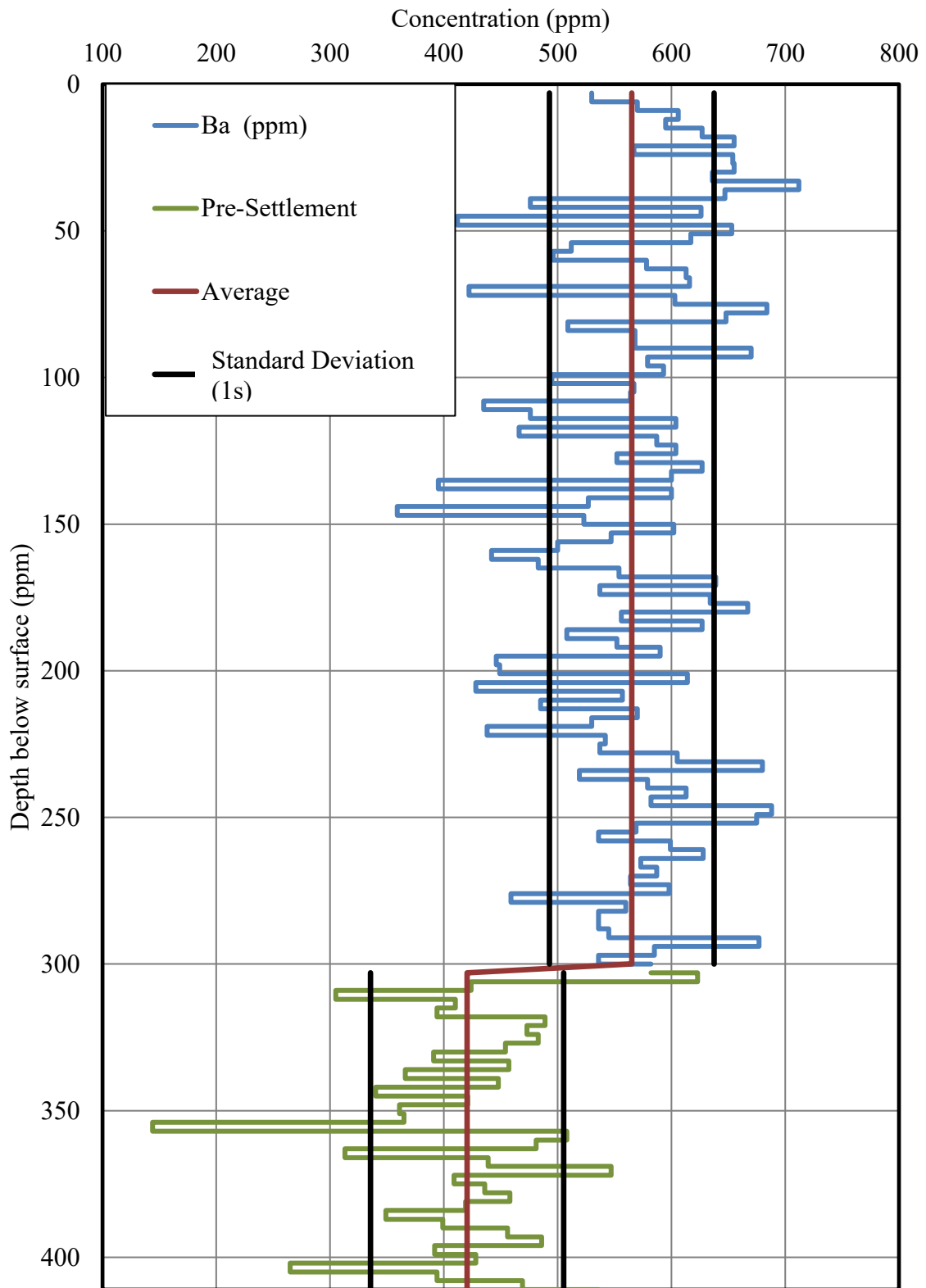
Figure 35. Ba concentration profile for core 12.
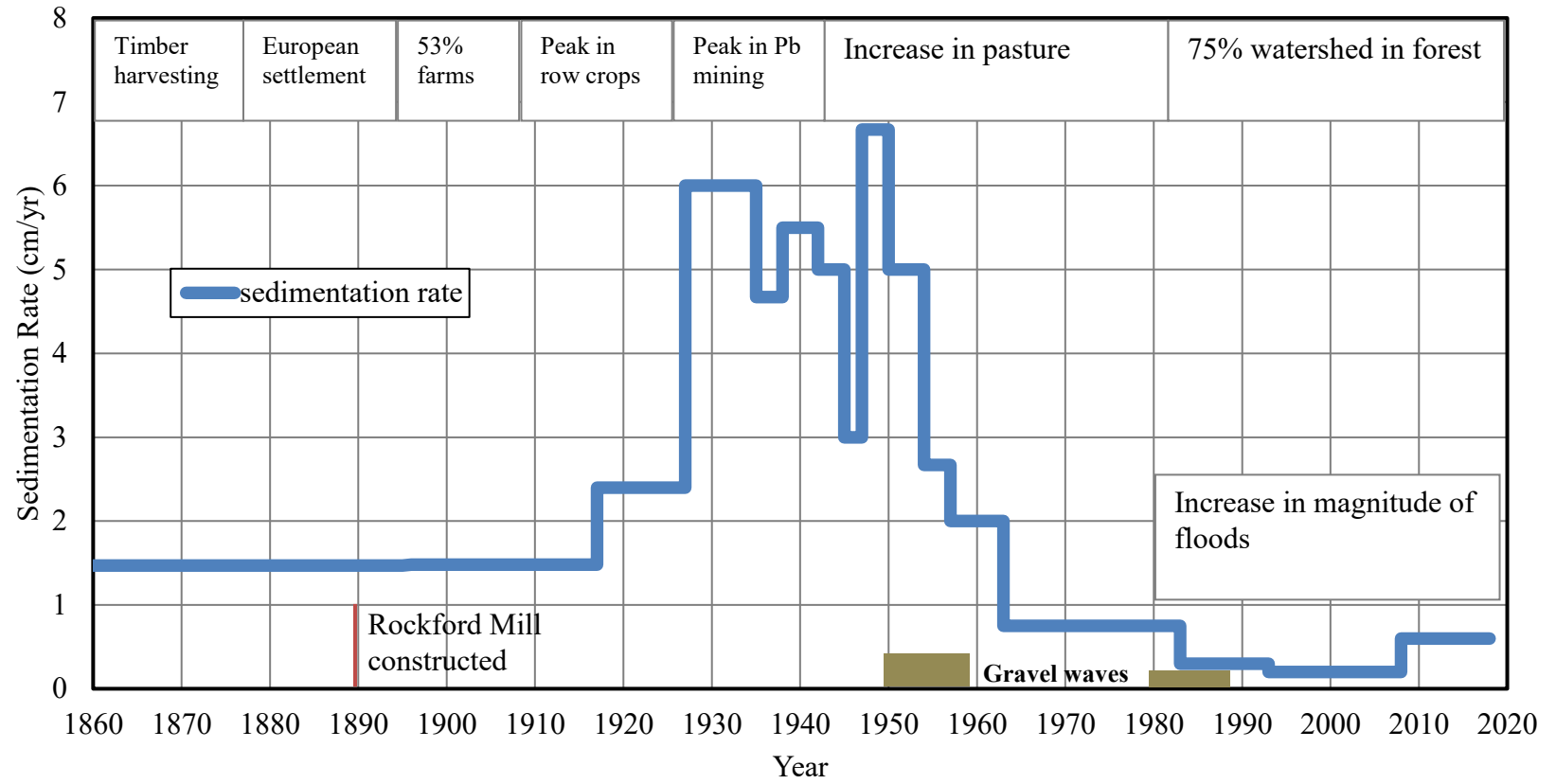
Figure 36. Sedimentation rates for core 12. Note: gravel wave peaks reported by Jacobson (1995)

CONCLUSIONS

Land use changes during European settlement starting before 1860 caused increased runoff and soil erosion resulting in the deposition of large volumes of sediment within floodplains along Big River. In addition, large-scale mining in the watershed from the late 1800s to 1972 discharged mine wastes to the river that were dispersed by fluvial processes downstream to contaminate floodplains with Pb and Zn along 171 km of Big River (Mosby et al., 2009; Pavlowsky et al., 2017). Once deposited on floodplains, these contaminated sediments have been stored in floodplain soils for over 120 years. Stratigraphic trends in contamination levels evaluated from core analyses reflect the production history of the Old Lead Belt. Thus, Pb profiles in floodplain cores can be used to date sediment layers using ore production records (Macklin, 1985; Knox, 1987). While Pb profiles are useful for geomorphological analysis, these floodplains pose a secondary pollutant source through bank erosion and weathering that can harm both terrestrial and aquatic dwelling organisms. Superfund projects and other management practices are being used to mitigate ecological damages (EPA, 2011, 2012). However, more information on legacy sediments in lower Big River watershed is needed to develop future remediation efforts.

The goal of this study was to determine historical trends in floodplain deposition rates and link them to disturbance factors in Big River watershed. LiDAR and published soil survey data were used to map the landforms present along a 327 m transect located about three km downstream from USGS gage at Byrnesville (07018500) along lower Big River. Twelve sediment cores and 27 surface soil samples were collected were analyzed for metals and other sediment properties. Core 12 was collected and divided into three cm segments for a total of 137

samples for high resolution analyses to examine vertical geochemical trends of legacy sediments.

Geochemical and textural results were then compared to historical records from mining, flood,

and census data to assign sedimentation dates to the core.

Results from this study produced four key findings:

1. **Legacy sediments occur on lower Big River floodplains.** Contaminated legacy sediment (post-1896) accumulated on the Big River floodplain transect to depths ranging from 2.2 m to 4.0 m. The most contaminated deposits were typically found at depths between 90 to 95 cm and contained 3,000 ppm Pb. Lead concentrations in surface soils (0-30 cm) were above toxic levels of 400 ppm on all landforms except for low terrace locations that were about 0.5 m higher in elevation compared to adjacent contaminated floodplains. The highest concentrations of Pb were found near the present channel in floodplain and bench deposits at depths between 50 cm and 150 cm with concentrations ranging from 1,100 to 5,412 ppm Pb. Anthropogenic material in the form of broken glass and microplastic beads were present in the top 3 cm of core 12.

2. **Sedimentation rates can be quantified using geochemical analyses and historical mining records.** Peaks in Pb mining production in 1917, 1927, and 1942 were correlated to Pb concentration peaks at 219 cm, 195 cm, and 111 cm in core 12. The decrease in Pb production in 1933 was also used to date the 159 cm depth. Lead mining dating indicates a period of rapidly increasing sedimentation rates on floodplains from 1917 to 1927 and sedimentation rates remained high (>5 cm/yr) until 1953. In core 12, ^{137}Cs activity results and 1993 flood deposits indicated a peak at 30 cm (1963) and first occurrence at (1954) at 50 cm indicating a sedimentation rate of 2.2 cm/yr from 1954 to 1963, 0.3 cm/yr from 1963 to 1993, and 0.6 cm/yr from 1993 to the 2018 surface.

3. **Sedimentation rates can be applied by linking sand peaks to historical flood events.** Sand percentages combined with flood records were used to fill in the gaps in sedimentation dates between the mining peaks and the ^{137}Cs dates. Sand percentage peaks at 9 cm, 12 cm, 15 cm, 42 cm, 70 cm, 90 cm, 96 cm, 111 cm, 133 cm, 147 cm and 195 cm were assigned the years 2008, 1993, 1983, 1957, 1950, 1947, 1945, 1942, 1938, 1935, and 1927, respectively. More work is needed to evaluate the precision of this method since sand percentages did not increase for all of the largest floods or those floods with the longest overbank duration.

4. **Land use and geomorphological factors have controlled floodplain deposition.** Land disturbance due to settlement and timber harvesting in the mid-1800s released excess runoff and sediment to the river system that resulted in peak legacy deposition rates on floodplains in the lower portion of the watershed 20 to 30 years later when sedimentation rates increased to > 5 cm/yr. The lag between land use "cause" and geomorphic "effect" has been observed in other watersheds and is believed to reflect the travel time for sediment and channel disturbances downstream from the headwaters. Peak land clearing for agricultural purposes occurred between 1880 and 1900 in the headwaters and

subsequent sedimentation rates increased in 1927 to 6 cm/yr in the lower portion of the watershed. Although flood frequency and magnitude have increased recently, floodplain sedimentation rates have generally decreases to <0.5 cm/yr since 1993. Decreased floodplain sedimentation may be attributed to a combination of variables such as geomorphic adjustments of the channel and alluvial landforms due to historical sediment waves as well as a decrease in disturbances in the upper portions of the watershed and tributaries. This geomorphic response shows that land use change in tributaries in the upper portions of the watershed affect sedimentation rates in lower portions of the watershed, although sediment delivery to downstream floodplain sinks on the main channel may take decades.

Results from this study provided a high-resolution study of a floodplain core in lower Big River and how land use change and historical events influenced sedimentation rates. Further, it showed that mining metal storage in floodplain deposits and mining-contaminated sediment profiles vary laterally across the valley floor of Big River. It is important to assess other floodplain sites along the lower Big River to better understand the ecological risks surrounding heavy metal contamination. Floodplain surface samples collected provided spatial information on the variation of metal concentrations relating low errors for Pb, Zn, and Ca at < 15 CV%. These low errors suggest that the results of core analyses reported in this study are representative of floodplain profiles within the study area. The results of this study will aid in remediation efforts throughout the watershed and will provide needed information on heavy metal transport throughout Big River and its floodplains. Finally, future studies should sample and date floodplain cores along upstream segments to test the hypothesis that watershed disturbances start in the headwaters and progress downstream overtime.

REFERENCES

Abella, S.R., and Zimmer, B.W., 2007, Estimating Organic Carbon from Loss-On-Ignition in Northern Arizona Forest Soils: Soil Science Society of America Journal, v. 71, p. 545–550, https://doi.org/10.2136/sssaj2006.0136.

Acosta, J., Faz, A., Martínez-Martínez, S., Zornoza, R., Carmona, D., and Kabas, S., 2011, Multivariate statistical and GIS-based approach to evaluate heavy metals behavior in mine sites for future reclamation: Journal of Geochemical Exploration, v. 109, p. 8–17, https://doi.org/10.1016/j.gexplo.2011.01.004.

Adamski, J.C., 1995, Environmental and hydrologic setting of the Ozark Plateaus study unit, Arkansas, Kansas, Missouri, and Oklahoma: Little Rock, Arkansas, National Water-Quality Assessment Program, 94.

Akpomie, K.G., Dawodu, F.A., and Adebowale, K.O., 2015, Mechanism on the sorption of heavy metals from binary-solution by a low cost montmorillonite and its desorption potential: Alexandria Engineering Journal, v. 54, p. 757–767, https://doi.org/10.1016/j.aej.2015.03.025.

Angel, J.R., and Huff, F.A., 1991, , Changes in heavy rainfall in midwestern United States': Journal of Water Resources Planning & Management, v. 123, p. 246, https://doi.org/10.1061/(ASCE)0733-9496(1997)123:4(246).

Arnt, R.H., 1979, The Mineral Industry of Missouri: US Geological Survey Report, p. 299–314.

Ashley, G.H., 1910, Drainage problems in Tennessee, Tennessee State Geological Survey.

Bain, D.J., and Brush, G.S., 2005, Early chromite mining and agricultural clearance: Opportunities for the investigation of agricultural sediment dynamics in the eastern piedmont (USA): American Journal of Science, v. 305, p. 957–981, https://doi.org/10.2475/ajs.305.9.957.

Baker, V.R., 2008, Paleoflood hydrology: Origin, progress, prospects: Geomorphology, v. 101, p. 1–13, https://doi.org/10.1016/j.geomorph.2008.05.016.

Bartley, R., and Rutherfurd, I., 2005, Re-evaluation of the wave model as a tool for quantifying the geomorphic recovery potential of streams disturbed by sediment slugs: Geomorphology, v. 64, p. 221–242, https://doi.org/10.1016/j.geomorph.2004.07.005.

Benn, D.W., and Ray, J.H., 1996, The Prospect Spring Site and the Problem of the Late Woodland/Mississippian Transition in the Western Ozarks: Midcontinental Journal of Archaeology, v. 21, p. 49–78, https://www.jstor.org/stable/20708385.

Bennett, H.H., 1931, The problem of soil erosion in the United States: Annals of the Association of American Geographers, v. 21, p. 147–170.

Blundell, A., Dearing, J., Boyle, J., and Hannam, J., 2009, Controlling factors for the spatial variability of soil magnetic susceptibility across England and Wales: Earth-Science Reviews, v. 95, p. 158–188, https://doi.org/10.1016/j.earscirev.2009.05.001.

Bradley, D.C., and Leach, D.L., 2003, Tectonic controls of Mississippi Valley-type lead-zinc mineralization in orogenic forelands: Mineralium Deposita, v. 38, p. 652–667, https://doi.org/10.1007/s00126-003-0355-2.

Brown, B.L., 1981, Soil Survey of St. Francois County, Missouri: U.S. Department of Agriculture, Soil Conservation Service and Forest Service, p. 142.

Buckley, E.R., 1908, Geology of the disseminated lead deposits of St. Francois and Washington Counties: Jefferson City, Mo, H. Stephens printing Company.

Carlson, J.L., 1999, Zinc mining contamination and sedimentation rates of historical overbank deposits, Honey Creek Watershed, Southwest Missouri [thesis].

Chen, L.M., Zhang, G.L., Rossiter, D.G., and Cao, Z.H., 2015, Magnetic depletion and enhancement in the evolution of paddy and non-paddy soil chronosequences: European Journal of Soil Science, v. 66, p. 886–897, https://doi.org/10.1111/ejss.12281.

Ciszewski, D., and Turner, J., 2009, Storage of sediment-associated heavy metals along the channelized Odra River, Poland: Earth Surface Processes and Landforms, v. 34, p. 558–572, https://doi.org/10.1002/esp.1756.

Coghill, W.H., and OMeara, R.G., 1932, Milling methods and costs at a Flat River (Mo.) mill: Washington, D.C., U.S. Dept. of Commerce, Bureau of Mines.

Constantine, J.A., Mclean, S.R., and Dunne, T., 2009, A mechanism of chute cutoff along large meandering rivers with uniform floodplain topography: Geological Society of America Bulletin, v. 122, p. 855–869, https://doi.org/10.1130/b26560.1.

Deacon, R.T., 1999, Deforestation and Ownership: Evidence from Historical Accounts and Contemporary Data: Land Economics, v. 75, p. 341, https://doi.org/10.2307/3147182.

Dean, D.J., Scott, M.L., Shafroth, P.B., and Schmidt, J.C., 2011, Stratigraphic, sedimentologic, and dendrogeomorphic analyses of rapid floodplain formation along the Rio Grande in Big Bend National Park, Texas: Geological Society of America Bulletin, v. 123, p. 1908–1925, https://doi.org/10.1130/b30379.1.

Dean, J.W.E., 1974, Determination of Carbonate and Organic Matter in Calcareous Sediments and Sedimentary Rocks by Loss on Ignition: Comparison With Other Methods: SEPM Journal of Sedimentary Research, v. Vol. 44, https://doi.org/10.1306/74d729d2-2b21-11d7-8648000102c1865d.

Downing, J.A., Cole, J.J., Middelburg, J.J., Striegl, R.G., Duarte, C.M., Kortelainen, P., Prairie, Y.T., and Laube, K.A., 2008, Sediment organic carbon burial in agriculturally eutrophic impoundments over the last century: Global Biogeochemical Cycles, v. 22, https://doi.org/10.1029/2006gb002854.

Easterling, D.R., Evans, J.L., Groisman, P.Y., Karl, T.R., Kunkel, K.E., and Ambenje, P., 2000, Observed Variability and Trends in Extreme Climate Events: A Brief Review*: Bulletin of the American Meteorological Society, v. 81, p. 417–425, https://doi.org/10.1175/1520-0477(2000)081<0417:ovatie>2.3.co;2.

Environmental Protection Agency (EPA), 2015, Regional Screening Levels (RSL) for Chemical Contaminants at Superfund Sites: http://www.epa.gov/region09/superfund/prg/index.html. (accessed 2018).

EPA, 2011, Record of decision Big River mine tailings superfund site: U.S. Environmental Protection Agency, p. 133.

EPA, 2012, Record of decision Luebbers – residential soils operable unit 2 Southwest Jefferson County Mining Site: U.S. Environmental Protection Agency.

Famera, M., Babek, O., Grygar, T.M., and Novakova, T., 2013, Distribution of Heavy-Metal Contamination in Regulated River-Channel Deposits: a Magnetic Susceptibility and Grain-Size Approach; River Morava, Czech Republic: Water, Air, & Soil Pollution, v. 224, https://doi.org/10.1007/s11270-013-1525-1.

Florsheim, J.L., and Mount, J.F., 2002, Restoration of floodplain topography by sand-splay complex formation in response to intentional levee breaches, Lower Cosumnes River, California: Geomorphology, v. 44, p. 67–94, https://doi/org/10.1016/s0169-555x(01)00146-5.

Foreman, A.T., 2014, Climate change influence on historical flood variability in Ozark highland rivers [thesis].

Gale, N.L., Adams, C.D., Wixson, B.G., Loftin, K.A., and Huang, Y.-W., 2004, Lead, Zinc, Copper, and Cadmium in Fish and Sediments from the Big River and Flat River Creek of Missouri's Old Lead Belt: Environmental Geochemistry and Health, v. 26, p. 37–49, https://doi.org/10.1023/b:egah.0000020935.89794.57.

Gallman, R.E., 1972, Changes in Total U.S. Agricultural Factor Productivity in the Nineteenth Century: Agricultural History, v. 46, p. 191–210, https://www.jstor.org/stable/3741570.

Gazdag, E.R., and Sipter, E., 2008, Geochemical background in heavy metals and human health risk assessment at an ore mine site, Gyöngyösoroszi (North Hungary): Carpathian Journal of Earth and Environmental Sciences, v. 3, p. 83–92.

Gilbert, G., 1917, Hydraulic-mining debris in the Sierra Nevada: Professional Paper, https://doi.org/10.3133/pp105.

Gomez, B., Eden, D.N., Hicks, D.M., Trustrum, N.A., Peacock, D.H., and Wilmshurst, J., 1999, Contribution of floodplain sequestration to the sediment budget of the Waipaoa River, New Zealand: Geological Society, London, Special Publications, v. 163, p. 69–88, https://doi.org/10.1144/gsl.sp.1999.163.01.06.

Goodbred, S.L., and Kuehl, S.A., 1998, Floodplain processes in the Bengal Basin and the storage of Ganges–Brahmaputra river sediment: an accretion study using 137Cs and 210Pb geochronology: Sedimentary Geology, v. 121, p. 239–258, https://doi.org/10.1016/s0037-0738(98)00082-7.

Gregg, J.M., and Shelton, K.L., 1989, Minor- and trace-element distributions in the Bonneterre Dolomite (Cambrian), southeast Missouri: Evidence for possible multiple-basin fluid sources and pathways during lead-zinc mineralization: Geological Society of America Bulletin, v. 101, p. 221–230, https://doi.org/10.1130/0016-7606(1989)101<0221:matedi>2.3.co;2.

Groisman, P.Y., and Easterling, D.R., 1994, Variability and Trends of Total Precipitation and Snowfall over the United States and Canada: Journal of Climate, v. 7, p. 184–205, https://doi.org/10.1175/1520-0442(1994)007<0184:vatotp>2.0.co;2.

Haddadchi, A., Ryder, D.S., Evrard, O., and Olley, J., 2013, Sediment fingerprinting in fluvial systems: review of tracers, sediment sources and mixing models: International Journal of Sediment Research, v. 28, p. 560–578, doi: 10.1016/s1001-6279(14)60013-5.

Hajic, E.R., Mandel, R.D., Ray, J.H., and Lopinot, N.H., 2007, Geoarchaeology of stratified paleoindian deposits at the Big Eddy site, Southwest Missouri, U.S.A.: Geoarchaeology, v. 22, p. 891–934, https://doi.org/10.1002/gea.20200.

Hammer, T.R., 1972, Stream channel enlargement due to urbanization: Water Resources Research, v. 8, p. 1530–1540, https://doi.org/10.1029/wr008i006p01530.

Happ, S.C., Rittenhouse, G., and Dobson, G.C., 1940, Some Principles of Accelerated Stream and Valley Sedimentation, US Department of Agriculture, v. 695.

Harrington, M.C., 2012, Stream discharge-drainage area relationships in Missouri [thesis].

Heimann, D.C., Holmes, R.R., and Harris, T.E. Flooding in the Southern Midwestern United States, April-May 2017.

Heiri, O., Lotter, A.F., and Lemcke, G., 2001, Loss on ignition as a method for estimating organic and carbonate content in sediments: reproducibility and comparability of results: Journal of paleolimnology, v. 25, p. 101–110.

Hill, R.J., 2016, Channel sediment and mining-lead storage in Flat River Creek, Old Lead Belt, Missouri [thesis].

Hocutt, C.H., Stauffer, J.R., and Mills, P.A., 1978, Influence of a barite tailings pond rupture on the fishes of Big River, Missouri: Washington, D.C., US Fish and Wildlife Service, FWS/OBS-78/81, p. 177.

Hudson, P.F., 2005, Historical floodplain sedimentation in the Galena River basin, Wisconsin and Illinois: Encyclopedia of water science, v. 10.

Huggins, D.B., 2016, Spatial distribution and geomorphic factors of lead contamination on floodplains affected by historical mining, Big River, S.E. Missouri [thesis].

Hughes, M.L., McDowell, P.F., and Marcus, W.A., 2006, Accuracy assessment of georectified aerial photographs: implications for measuring lateral channel movement in a GIS: Geomorphology, v. 74, p. 1–16.

Hupp, C., Schenk, E., Kroes, D., Willard, D., Townsend, P., and Peet, R., 2015, Patterns of floodplain sediment deposition along the regulated lower Roanoke River, North Carolina: Annual, decadal, centennial scales: Geomorphology, v. 228, p. 666–680, https://doi.org/10.1016/j.geomorph.2014.10.023.

Hupp, C.R., 2000, Hydrology, geomorphology and vegetation of Coastal Plain rivers in the south-eastern USA: Hydrological Processes, v. 14, p. 2991–3010, https://doi.org/10.1002/1099-1085(200011/12)14:16/17<2991::aid-hyp131>3.0.co;2-h.

Jackson, C.F., Knaebel, J.B., and Wright, C.A., 1935, Lead and zinc mining and milling in the United States: current practices and costs: Washington, D.C., U.S. Dept. of the Interior, Bureau of Mines.

Jacobson, R.B., 1995, Spatial controls on patterns of land-use induced stream disturbance at the drainage-basin scale—An example from gravel-bed streams of the Ozark Plateaus, Missouri: Geophysical Monograph Series Natural and Anthropogenic Influences in Fluvial Geomorphology, p. 219–239, https://doi.org/10.1029/gm089p0219.

Jacobson, R.B., 2004, Watershed sustainability: Downstream effects of timber harvest in the Ozarks of Missouri : Forest Service US Department of Agriculture, NC-239-6, p. 106–128.

Jacobson, R.B., and Coleman, D.J., 1986, Stratigraphy and Recent evolution of Maryland Piedmont flood plains: American Journal of Science, v. 286, p. 617–637, https://doi.org/10.2475/ajs.286.8.617.

Jacobson, R.B., and Primm, A.T., 1994, Historical land-use changes and potential effects on stream disturbance in the Ozark Plateaus, Missouri: Rolla, MO, U.S. Dept. of the Interior, US Earth Science Information Center, U.S. Geological Survey.

Jacobson, R.B., and Primm, A.T., 1997, Historical land-use changes and potential effects on stream disturbance in the Ozark Plateaus, Missouri: Rolla, MO, U.S. Dept. of the Interior, U.S. Geological Survey, v. 2484.

Jacobson, R.B., and Pugh, A.L., 1997, Riparian-vegetation controls on the spatial pattern of stream-channel instability, Little Piney Creek, Missouri: Washington, U.S. Dept. of the Interior, U.S. Geological Survey.

Jacobson, R.B., and Gran, K.B., 1999, Gravel sediment routing from widespread, low- intensity landscape disturbance, Current River Basin, Missouri: Earth Surface Processes and Landforms, v. 24, p. 897–917, https://doi.org/10.1002/(sici)1096-9837(199909)24:10<897::aid-esp18>3.3.co;2-y.

James, L.A., 1989, Sustained Storage and Transport of Hydraulic Gold Mining Sediment in the Bear River, California: Annals of the Association of American Geographers, v. 79, p. 570–592, https://doi.org/10.1111/j.1467-8306.1989.tb00277.x.

James, L.A., 2010, Secular Sediment Waves, Channel Bed Waves, and Legacy Sediment: Geography Compass, v. 4, p. 576–598, https://doi.org/10.1111/j.1749-8198.2010.00324.x.

James, L.A., 2013, Legacy sediment: Definitions and processes of episodically produced anthropogenic sediment: Anthropocene, v. 2, p. 16–26, https://doi.org/10.1016/j.ancene.2013.04.001.

James, L., and Lecce, S., 2013, 9.37 Impacts of Land-Use and Land-Cover Change on River Systems: Treatise on Geomorphology, p. 768–793, https://doi.org/10.1016/b978-0-12-374739-6.00264-5.

Jefferson County Geneaological Society, 2015, Jefferson County Missouri: History & Families: Acclaim Press, v. 17.

Junk, W.J., Bayley, P.B., and Sparks, R.E., 1989, The flood pulse concept in river-floodplain systems: Canadian special publication of fisheries and aquatic sciences, v. 106, p. 110–127.

Juracek, K.E., and Fitzpatrick, F.A., 2009, Geomorphic applications of stream-gage information: River Research and Applications, v. 25, p. 329–347, https://doi.org/10.1002/rra.1163.

Knox, J.C., 1987, Historical valley floor sedimentation in the Upper Mississippi Valley: Annals of the Association of American Geographers, v. 77, p. 224–244, https://www.jstor.org/stable/2562767.

Knox, J.C., and Daniels, J.M., 2013, Watershed Scale and the Stratigraphic Record of Large Floods: Water Science and Application Ancient Floods, Modern Hazards, p. 237–255, https://doi.org/10.1029/ws005p0237.

Knox, J.C., 1972, Valley Alluviation In Southwestern Wisconsin∗: Annals of the Association of American Geographers, v. 62, p. 401–410, https://doi.org/10.1111/j.1467-8306.1972.tb00872.x.

Knox, J.C., 1977, Human Impacts On Wisconsin Stream Channels∗: Annals of the Association of American Geographers, v. 67, p. 323–342, https://doi.org/10.1111/j.1467-8306.1977.tb01145.x.

Knox, J.C., 2006, Floodplain sedimentation in the Upper Mississippi Valley: Natural versus human accelerated: Geomorphology, v. 79, p. 286–310, https://doi.org/10.1016/j.geomorph.2006.06.031.

Koinig, K.A., Shotyk, W., Lotter, A.F., Ohlendorf, C., and M Sturm, 2003, 9000 years of geochemical evolution of lithogenic major and trace elements in the sediment of an alpine lake– the role of climate, vegetation, and land-use history: Journal of Paleolimnology, v. 30, p. 307–320.

Konare, H., Yost, R.S., Doumbia, M., McCarty, G.W., Jarju, A., and Kablan, R., 2010, Loss on ignition: measuring soil organic carbon in soils of the Sahel, West Africa: African Journal of Agricultural Research, v. 5, p. 3088–3095.

Kooistra, L., Wehrens, R., Buydens, L.M., Leuven, R.S., and Nienhuis, P.H., 2001, Possibilities of soil spectroscopy for the classification of contaminated areas in river floodplains: International Journal of Applied Earth Observation and Geoinformation, v. 3, p. 337–344, https://doi.org/10.1016/s0303-2434(01)85041-8.

Le Borgne, E., 1955, Abnormal magnetic susceptibility of the top soil: Ann, Geophys, v. 11, p. 399–419.

Lecce, S.A., and Pavlowsky, R.T., 1997, Storage Of Mining-Related Zinc In Floodplain Sediments, Blue River, Wisconsin: Physical Geography, v. 18, p. 424–439, https://doi.org/10.1080/02723646.1997.10642628.

Lecce, S.A., 1997, Spatial patterns of historical overbank sedimentation and floodplain evolution, Blue river, Wisconsin: Geomorphology, v. 18, p. 265–277, https://doi.org/10.1016/s0169-555x(96)00030-x.

Lecce, S.A., 2000, Seasonality of Flooding in North Carolina: Southeastern Geographer, v. 40, p. 168–175, https://doi.org/10.1353/sgo.2000.0004.

Lecce, S.A., and Pavlowsky, R.T., 2001, Use of mining-contaminated sediment tracers to investigate the timing and rates of historical flood plain sedimentation: Geomorphology, v. 38, p. 85–108, https://doi.org/10.1016/s0169-555x(00)00071-4.

Lecce, S.A., and Pavlowsky, R.T., 2004, Spatial and temporal variations in the grain-size characteristics of historical flood plain deposits, Blue River, Wisconsin, USA: Geomorphology, v. 61, p. 361–371, https://doi.org/10.1016/j.geomorph.2004.01.008.

Lecce, S.A., Pease, P.P., Gares, P.A., and Rigsby, C.A., 2004, Floodplain Sedimentation During an Extreme Flood: the 1999 Flood on the Tar River, Eastern North Carolina: Physical Geography, v. 25, p. 334–346, https://doi.org/10.2747/0272-3646.25.4.334.

Lecce, S., Pavlowsky, R., and Schlomer, G., 2007, Mercury contamination of active channel sediment and floodplain deposits from historic gold mining at Gold Hill, North Carolina, USA: Environmental Geology, v. 55, p. 113–121, https://doi.org/10.1007/s00254-007-0970-9.

Lecce, S.A., and Pavlowsky, R.T., 2014, Floodplain storage of sediment contaminated by mercury and copper from historic gold mining at Gold Hill, North Carolina, USA: Geomorphology, v. 206, p. 122–132, https://doi.org/10.1016/j.geomorph.2013.10.004.

Lecce, S.A., and Pavlowsky, R.T., 2014, Floodplain storage of sediment contaminated by mercury and copper from historic gold mining at Gold Hill, North Carolina, USA: Geomorphology, v. 206, p. 122–132, https://doi.org/10.1016/j.geomorph.2013.10.004.

Leigh, D.S., 2018, Vertical accretion sand proxies of gaged floods along the upper Little Tennessee River, Blue Ridge Mountains, USA: Sedimentary Geology, v. 364, p. 342–350, https://doi.org/10.1016/j.sedgeo.2017.09.007.

Macklin, M., Brewer, P., Hudson-Edwards, K., Bird, G., Coulthard, T., Dennis, I., Lechler, P., Miller, J., and Turner, J., 2006, A geomorphological approach to the management of rivers contaminated by metal mining: Geomorphology, v. 79, p. 423–447, https://doi.org/10.1016/j.geomorph.2006.06.024.

Macklin, M.G., 1985, Flood-Plain Sedimentation in the Upper Axe Valley, Mendip, England: Transactions of the Institute of British Geographers, v. 10, p. 235, https://doi.org/10.2307/621826.

Macklin, M.G., and Dowsett, R.B., 1989, The chemical and physical speciation of trace metals in fine grained overbank flood sediments in the Tyne basin, north-east England: Catena, v. 16, p. 135–151, https://doi.org/10.1016/0341-8162(89)90037-4.

Magilligan, F.J., 1985, Historical Floodplain Sedimentation in the Galena River Basin, Wisconsin and Illinois: Annals of the Association of American Geographers, v. 75, p. 583–594, https://doi.org/10.1111/j.1467-8306.1985.tb00095.x.

Magilligan, F.J., 1992, Sedimentology of a fine-grained aggrading floodplain: Geomorphology, v. 4, p. 393–408, https://doi.org/10.1016/0169-555x(92)90034-l.

Marsh, G.P., 1864, Man and Nature; or: Physical geography as modified by human action, p. 35.

Matschullat, J., Ellminger, F., Agdemir, N., Cramer, S., Lieβmann, W., and Niehoff, N., 1997, Overbank sediment profiles—evidence of early mining and smelting activities in the Harz mountains, Germany: Applied Geochemistry, v. 12, p. 105–114, https://doi.org/10.1016/s0883-2927(96)00068-6.

Mccall, P., Robbins, J., and Matisoff, G., 1984, ^{137}Cs and ^{210}Pb transport and geochronologies in urbanized reservoirs with rapidly increasing sedimentation rates: Chemical Geology, v. 44, p. 33–65, https://doi.org/10.1016/0009-2541(84)90066-4.

Mccomb, J.Q., Rogers, C., Han, F.X., and Tchounwou, P.B., 2014, Rapid Screening of Heavy Metals and Trace Elements in Environmental Samples Using Portable X-Ray Fluorescence Spectrometer, A Comparative Study: Water, Air, & Soil Pollution, v. 225, https://doi.org/10.1007/s11270-014-2169-5.

Mckean, J.A., Isaak, D.J., and Wright, C.W., 2008, Geomorphic controls on salmon nesting patterns described by a new, narrow-beam terrestrial–aquatic lidar: Frontiers in Ecology and the Environment, v. 6, p. 125–130, https://doi.org/10.1890/070109.

Mclarty, C., 2016, Saving Endangered Mussels in Missouri's Big River: EPA, https://blog.epa.gov/tag/lead-contamination/ (accessed 2018).

MDNR, 2003, Biological Assessment and Fine Sediment Study: Big River (lower): Irondale to Washington State Park, St. Francois, Washington, and Jefferson Counties, Missouri: Prepared by the Water Quality Monitoring Section, Environmental Services Program, Air and Land Protection Division of the Missouri Department of Natural Resources.

MDNR, 2007, Total Maximum Daily Load Information Sheet: Big River and Flat River Creek: http://www.dnr.mo.gov/env/wpp/tmdl/info/2074-2080-2168-big-r-info.pdf. (accessed April 2018).

MDNR, 2013, Our Missouri waters: Big River Watershed (HUC 07040104), https://dnr.mo.gov/omw/documents/omw-bigriver-factsheet.pdf (accessed 2018).

Meade, R.H., 1996, River-Sediment Inputs to Major Deltas: Coastal Systems and Continental Margins Sea-Level Rise and Coastal Subsidence, p. 63–85, https://doi.org/10.1007/978-94-015-8719-8_4.

Meneau, K.J., 1997, Big River basin inventory and management plan: House Springs, Missouri Dept. of Conservation.

Miller, J.R., 1997, The role of fluvial geomorphic processes in the dispersal of heavy metals from mine sites: Journal of Geochemical Exploration, v. 58, p. 101–118, https://doi.org/10.1016/s0375-6742(96)00073-8.

Minerals yearbook, All years, United States Geological Survey.

Mosby, D.E., and Klahr, F., 2009, Final phase I damage assessment plan for Southeast Missouri Lead Mining District: Big River Mine Tailings Superfund site, St. Francois County and Viburnum Trend Sites, Reynolds, Crawford, Washington, and Iron Counties: Columbia, Missouri, U.S. Fish and Wildlife Service U.S. Department of the Interior , p. 84.

Mugel, D.N., 2016, Geology and mining history of the Southeast Missouri Barite District and the Valles Mines, Washington, Jefferson, and St. Francois Counties, Missouri: U.S. Geological Survey and U.S. Environmental Protection Agency, 2016-5173.

Mullins, C.E., 1977, Magnetic Susceptibility Of The Soil And Its Significance In Soil Science - A Review: Journal of Soil Science, v. 28, p. 223–246, https://doi.org/10.1111/j.1365-2389.1977.tb02232.x.

Nanson, G.C., Young, R.W., Price, D.M., and Rust, B.R., 1988, Stratigraphy, sedimentology and late Quaternary chronology of the Channel Country of western Queensland: Fluvial geomorphology of Australia, p. 151–175.

Nanson, G., and Croke, J., 1992, A genetic classification of floodplains: Geomorphology, v. 4, p. 459–486, https://doi.org/10.1016/0169-555x(92)90039-q.

Nanson, G.C., 1986, Episodes of vertical accretion and catastrophic stripping: A model of disequilibrium flood-plain development: Geological Society of America Bulletin, v. 97, p. 1467, https://doi.org/10.1130/0016-7606(1986)97<1467:eovaac>2.0.co;2.

National Resources Conservation Services (NRCS), 2006, Official Soil Series Descriptions: Lincoln, Ne, USDA-NRCS.

Oldfield, F., Maher, B.A., Donoghue, J., and Pierce, J., 1985, Particle-size related, mineral magnetic source sediment linkages in the Rhode River catchment, Maryland, USA: Journal of the Geological Society, v. 142, p. 1035–1046, https://doi.org/10.1144/gsjgs.142.6.1035.

Owen, M.R., Pavlowsky, R.T., and Womble, P.J., 2011, Historical Disturbance and Contemporary Floodplain Development along an Ozark River, Southwest Missouri: Physical Geography, v. 32, p. 423–444, https://doi.org/10.2747/0272-3646.32.5.423.

Owens, P.N., Batalla, R.J., Collins, A.J., Gomez, B., Hicks, D.M., Horowitz, A.J., Kondolf, G.M., Marden, M., Page, M.J., Peacock, D.H., Petticrew, E.L., Salomons, W., and Trustrum, N.A., 2005, Fine-grained sediment in river systems: environmental significance and management issues: River Research and Applications, v. 21, p. 693–717, https://doi.org/10.1002/rra.878.

Ozarks Environmental and Water Resources Institute (OEWRI), 2007, Standard operation procedure for: organic matter in sediment, loss on ignition method: Standard Operating Procedure.

Ozarks Environmental and Water Resources Institute (OEWRI), 2007, Standard Operating Procedure for: X-MET3000TXS Handheld XRF Analyzer: Standard Operating Procedure.

Ozarks Environmental and Water Resources Institute (OEWRI), 2013, Standard Operating Procedure for Magnetic Susceptibility (Magnetic_Susceptibility_R01): Standard Operating Procedure.

Ozarks Environmental and Water Resources Institute (OEWRI), 2016, Set-up and operating the RTK. Field Manual. Standard Operating Procedure.

Page, K., Nanson, G., and Frazier, P., 2003, Floodplain Formation and Sediment Stratigraphy Resulting from Oblique Accretion on the Murrumbidgee River, Australia: Journal of Sedimentary Research, v. 73, p. 5–14, https://doi.org/10.1306/070102730005.

Pavlowsky, R.T., Owen, M.R., and Martin, D.J., 2010, Distribution, geochemistry, and storage of mining sediment in channel and floodplain deposits of the Big River System in St. Francois, Washington, and Jefferson Counties, Missouri: rep.

Pavlowsky, R.T., and Meyer, J.L., 2018, Human history, river response, and legacy deposits in the Ozark Highlands, Living Ozarks: the ecology and culture of a natural place: Ozarks Studies Institute and Library Services, p. 165–172.

Pavlowsky, R.T., Lecce, S.A., Owen, M.R., and Martin, D.J., 2017, Legacy sediment, lead, and zinc storage in channel and floodplain deposits of the Big River, Old Lead Belt Mining District, Missouri, USA: Geomorphology, v. 299, p. 54–75, https://doi.org/10.1016/j.geomorph.2017.08.042.

Petrovský, E., Kapička, A., Jordanova, N., and Borůvka, L., 2001, Magnetic properties of alluvial soils contaminated with lead, zinc and cadmium: Journal of Applied Geophysics, v. 48, p. 127–136, https://doi.org/10.1016/s0926-9851(01)00085-4.

Pizzuto, J.E., 1987, Sediment diffusion during overbank flows: Sedimentology, v. 34, p. 301–317, https://doi.org/10.1111/j.1365-3091.1987.tb00779.x.

Renschler, C.S., and Harbor, J., 2002, Soil erosion assessment tools from point to regional scales—the role of geomorphologists in land management research and implementation: Geomorphology, v. 47, p. 189–209, https://doi.org/10.1016/s0169-555x(02)00082-x.

Rodgers, W., 2005, Mercury contamination of channel and floodplain sediments in Wilson Creek Watershed, southwest Missouri [thesis].

Rosgen, D.L., 1996, Applied river morphology: Wildland Hydrology.

Saucier, R.T., 1983, Historic changes in Current River meander regime: River Meandering, p. 180–190.

Sauer, C.O., 1920, The geography of the Ozark highland of Missouri.

Schoolcraft, H.R., 1819, A view of the lead mines of Missouri: including some observations on the mineralogy, geology, geography, antiquities, and soil, climate, population, and productions of Missouri and Arkansaw, and other sections of the western country: New York, C. Wiley.

Schoolcraft, H.R., 1821, Narrative journal of travels through the northwestern regions of the United States, extending from Detroit through the great chain of American lakes, to the sources of the Mississippi River, performed as a member of the expedition under Governor Cass, in the year 1820: E. & E. Hosford.

Schulte, L., et al. "A 2600 Year History of Floods in the Bernese Alps, Switzerland: Frequencies, Mechanisms and Climate Forcing." Hydrology and Earth System Sciences Discussions, vol. 12, no. 3, 2015, pp. 3391–3448., https://doi.org/10.5194/hessd-12-3391-2015.

Seeger, C.M., 2008, History of mining in the southeast Missouri lead district and description of mine processes, regulatory controls, environmental effects, and mine facilities in the Viburnum Trend subdistrict. Hydrologic investigations concerning lead mining issues in southeastern Missouri: Rolla, Missouri, Missouri Department of Natural Resources, Division of Geology and Land Survey, 2008-5140, p. 5–30.

Shepherd, M., Mote, T., Dowd, J., Roden, M., Knox, P., Mccutcheon, S.C., and Nelson, S.E., 2011, An Overview of Synoptic and Mesoscale Factors Contributing to the Disastrous Atlanta Flood of 2009: Bulletin of the American Meteorological Society, v. 92, p. 861–870, https://doi.org/10.1175/2010bams3003.1.

Simmons, C.E., 1993, Sediment characteristics of North Carolina streams, 1970–1979: U.S. Geological Survey Water-Supply Paper, 2364, p. 84.

Skaer, D.M., 2004, Soil survey of Jefferson County, Missouri: Washington, D.C., Natural Resources Conservation Service.

Smith, B.J., 1988, Assessment of water quality in non-coal mining areas of Missouri: Rolla, MO, Dept. of the Interior, U.S. Geological Survey.

Smith, B.J., and Schumacher, J.G., 1991, Hydrochemical and sediment data for the Old Lead Belt, southeastern Missouri--1988-89: Rolla, MO, USGS Open File Report, p. 91–211.

Smith, B.J., and Schumacher, J.G., 1993, Surface-water and sediment quality in the Old Lead Belt, southeastern Missouri--1988-89, US Department of the Interior, US Geological Survey.

Smith, D.C., and Schumacher, J.G., 2018, Distribution of mining-related trace elements in streambed and flood-plain sediment along the middle Big River and tributaries in the Southeast Missouri Barite District, 2012–15: US Geological Survey, https://pubs.er.usgs.gov/publication/sir20185103.

Steel, R.J., 1974, New Red Sandstone Floodplain and Piedmont Sedimentation in the Hebridean Province, Scotland: SEPM Journal of Sedimentary Research, v. Vol. 44, https://doi.org/10.1306/74d72a27-2b21-11d7-8648000102c1865d.

Suggs, G.G., 2008, Water mills of the Missouri Ozarks: Norman, University of Oklahoma Press.

Surian, N., 1999, Channel changes due to river regulation: the case of the Piave River, Italy: Earth Surface Processes and Landforms, v. 24, p. 1135–1151, https://doi.org/10.1002/(sici)1096-9837(199911)24:12<1135::aid-esp40>3.3.co;2-6.

Swennen, R., and Sluys, J.V.D., 1998, Zn, Pb, Cu and As distribution patterns in overbank and medium-order stream sediment samples: their use in exploration and environmental geochemistry: Journal of Geochemical Exploration, v. 65, p. 27–45, https://doi.org/10.1016/s0375-6742(98)00057-0.

Thayer, J.B., and Ashmore, P., 2016, Floodplain morphology, sedimentology, and development processes of a partially alluvial channel: Geomorphology, v. 269, p. 160–174, https://doi.org/10.1016/j.geomorph.2016.06.040.

Thom, R.H., and Wilson, J.H., 1983, The natural divisions of Missouri: Natural Areas Journal, p. 44–51.

Thompson, H.C., 1992, Our Lead Belt Heritage: A Series of Articles:

Topcon, 2007, Instruction manual: Pulse Total Station GPT-7500. Manual: Topcon Positioning Systems, Inc. publication.

Trimble, J.C., 2001, Spatial patterns and floodplain contributions of mining-related contaminants in Chat Creek watershed, southwest Missouri [thesis].

Trimble, S.W., 1983, A sediment budget for Coon Creek basin in the Driftless Area, Wisconsin, 1853-1977: American Journal of Science, v. 283, p. 454–474, https://doi.org/10.2475/ajs.283.5.454.

Trimble, S.W., and Crosson, P., 2000, LAND USE: U.S. Soil Erosion Rates--Myth and Reality: Science, v. 289, p. 248–250, https://doi.org/10.1126/science.289.5477.248.

Trimble, S., and Lund, S., 1982, Soil conservation and the reduction of erosion and sedimentation in the Coon Creek basin, Wisconsin: Professional Paper, https://doi.org/10.3133/pp1234.

Turner, G.M., 1997, Environmental magnetism and magnetic correlation of high resolution lake sediment records from Northern Hawkes Bay, New Zealand: New Zealand Journal of Geology and Geophysics, v. 40, p. 287–298, https://doi.org/10.1080/00288306.1997.9514761.

Walling, D.E., and Woodward, J.C., 1992, Use of radiometric fingerprints to derive information on suspended sediment sources: , Erosion and sediment transport monitoring programmes in river basins, v. 210, p. 153–164.

Walling, D.E., and He, Q., 1993, Use of cesium-137 as a tracer in the study of rates and patterns of floodplain sedimentation: IAHS PUBLICATION, p. 319.

Walling, D.E., and He, Q., 1994, Rates of overbank sedimentation on the flood plains of several British rivers during the past 100 years: IAHS Publications-Series of Proceedings and Reports-Intern Assoc Hydrological Sciences, v. 78, p. 223.

Walling, D.E., and He, Q., 1999, Improved Models for Estimating Soil Erosion Rates from Cesium-137 Measurements: Journal of Environment Quality, v. 28, p. 611, https://doi.org/10.2134/jeq1999.00472425002800020027x.

Walling, D., and He, Q., 1998, The spatial variability of overbank sedimentation on river floodplains: Geomorphology, v. 24, p. 209–223, https://doi.org/10.1016/s0169-555x(98)00017-8.

Wang, L., and Leigh, D.S., 2012, Late-Holocene paleofloods in the Upper Little Tennessee River valley, Southern Blue Ridge Mountains, USA: The Holocene, v. 22, p. 1061–1066, https://doi.org/10.1177/0959683612437863.

Wilkinson, B.H., and McElroy, B.J., 2007, The impact of humans on continental erosion and sedimentation: Geological Society of America Bulletin, v. 119, p. 140–156, https://doi.org/10.1130/b25899.1.

Wohl, E., 2014, A legacy of absence: Progress in Physical Geography: Earth and Environment, v. 38, p. 637–663, https://doi.org/10.1177/0309133314548091.

Wolman, M.G., and Leopold, L.B., 1957, River flood plains: Some observations on their formation: Professional Paper, p. 87–109, https://doi.org/10.3133/pp282c.

Wolman, M.G., and Miller, J.P., 1960, Magnitude and Frequency of Forces in Geomorphic Processes: The Journal of Geology, v. 68, p. 54–74, https://doi.org/10.1086/626637.

Wolman, M.G., and Brush, L.M., 1961, Factors controlling the size and shape of stream channels in coarse noncohesive sands: Professional Paper, p. 183–210, https://doi.org/10.3133/pp282g.

Wolman, M.G., 1967, A Cycle of Sedimentation and Erosion in Urban River Channels: Geografiska Annaler. Series A, Physical Geography, v. 49, p. 385, https://doi.org/10.2307/520904.

Wolman, M.G., and Schick, A.P., 1967, Effects of construction on fluvial sediment, urban and suburban areas of Maryland: Water Resources Research, v. 3, p. 451–464, https://doi.org/10.1029/wr003i002p00451.

Wuebbles, D.J., and Hayhoe, K., 2004, Climate Change Projections for the United States Midwest: Mitigation and Adaptation Strategies for Global Change, v. 9, p. 335–363, https://doi.org/10.1023/b:miti.0000038843.73424.de.

Young, B.M., 2011, Historical channel change and mining-contaminated sediment remobilization in the lower Big River, eastern Missouri [thesis].

Zhang, L., Zhang, Z., Chen, Y., and Fu, Y., 2015, Sediment characteristics, floods, and heavy metal pollution recorded in an overbank core from the lower reaches of the Yangtze River: Environmental Earth Sciences, v. 74, p. 7451–7465, https://doi.org/10.1007/s12665-015-4733-8.

APPENDICES

Appendix A. Annual peak frequency.

Annual Exceedance Probability	Recurrence Interval	EMA Estimate		For EMA Estimate with Reg skew		
		With Reg Skew (cfs)	Without Reg skew (cfs)	Log variance of estimate	confidence limits	
					5% lower (cfs)	95% upper (cfs)
0.995	1.005	3122	2652	0.0033	2289	3974
0.99	1.01	3673	3235	0.0029	2757	4597
0.95	1.05	5726	5460	0.0019	4569	6866
0.9	1.1	7254	7134	0.0014	5961	8530
0.8	1.25	9661	9759	0.0011	8185	11150
0.6667	1.5	12620	12940	0.0009	10930	14420
0.5	2	16710	17210	0.0008	14640	19070
0.4292	2.33	18770	19310	0.0009	16460	21490
0.2	5	28910	29140	0.0012	25060	34030
0.1	10	38500	37770	0.0016	32750	46690
0.04	25	52250	49220	0.0022	43320	65800
0.02	50	63650	58030	0.0027	51790	82300
0.01	100	76010	67010	0.0032	60760	100800
0.005	200	89410	76180	0.0038	70280	121300
0.002	500	108900	88610	0.0045	83780	152100

Appendix B. Core locations and analyses.

Core number	Latitude	Longitude	Number of samples	Core length (cm)	Field XRF	XRF <2mm	XRF <250 um	Magnetic susceptibility	sand%	LOI
7	38.2437618	-90.370634	9	100	X					
1	38.243853	-90.371253	12	120	X					
8	38.2439199	-90.373024	16	210	X					
2	38.2439712	-90.375542	22	370	X					
9	38.2440355	-90.376078	18	315	X					
3	38.2440691	-90.377056	19	320	X					
10	38.2441348	-90.378271	17	310	X					
4	38.2441974	-90.379116	20	385	X					
5	38.2443104	-90.379697	14	270	X					
12	38.2443556	-90.3710362	137	411		X	X	X	X	X
11	38.2443556	-90.3710362	19	400	X					
6	38.2443895	-90.3711495	16	330	X					

Appendix C. Geochemical results Cores 1 – 11.

Core number	Depth (cm)	XRF concentration (ppm)		
		Pb	Zn	Ca
1	1	376	174	2996
1	5	401	178	3712
1	10	391	172	3191
1	10	368	153	1762
1	15	352	176	1865
1	17.5	306	163	2690
1	20	155	124	3656
1	20	222	146	3848
1	30	52	118	1783
1	30	63	114	1584
1	40	39	111	1921
1	50	27	95	0
1	70	28	99	0
1	90	0	106	0
1	120	0	115	1753
2	1	659	209	3319
2	5	642	200	3397
2	35	797	213	4000
2	35	750	196	4394
2	70	806	168	3088
2	70	838	175	3025
2	90	892	199	3707
2	105	1182	135	2854
2	105	1173	138	2976
2	115	1146	137	2550
2	120	1313	187	4416
2	125	791	91	1806
2	130	1952	195	4533
2	130	3699	294	7511
2	130	3813	268	7941
2	135	4087	341	7481
2	140	3476	294	5399
2	150	1615	186	1897
2	160	1523	164	2156
2	190	1036	70	0

Appendix C- continued

Core number	Depth (cm)	XRF concentration (ppm)		
		Pb	Zn	Ca
2	210	688	100	0
2	220	327	157	0
2	250	79	136	0
2	280	41	143	0
2	295	0	110	0
2	310	0	74	0
2	370	0	116	0
3	5	752	234	2974
3	35	831	196	3125
3	70	1264	175	3991
3	70	1167	194	4488
3	80	1142	144	3133
3	87	1172	178	3497
3	90	996	139	2763
3	95	3037	222	5017
3	100	3264	303	6262
3	100	3664	265	6945
3	110	3672	286	5955
3	120	2580	225	7028
3	130	1240	121	2706
3	160	279	124	0
3	190	222	196	1408
3	220	55	118	0
3	250	49	115	0
3	280	41	112	0
3	300	275	73	1313
3	310	420	88	1762
3	320	0	32	0
4	5	747	246	3257
4	35	739	246	2653
4	70	733	185	3005
4	100	1523	181	4726
4	100	1546	192	4477
4	110	1501	178	3545
4	120	2084	256	6197
4	125	1932	221	4670
4	130	3286	265	7485

Appendix C- continued

Core number	Depth (cm)	XRF concentration (ppm)		
		Pb	Zn	Ca
4	160	938	120	0
4	180	1546	116	1659
4	180	1594	122	2000
4	210	1353	115	1962
4	230	516	155	0
4	260	133	140	0
4	290	85	135	0
4	300	68	121	0
4	320	55	143	0
4	347	67	140	0
4	347	38	121	0
4	355	55	98	0
4	365	35	83	0
4	385	19	81	0
5	5	742	207	1808
5	5	1122	227	2361
5	35	1073	209	2110
5	35	1056	207	2740
5	40	1105	199	3075
5	60	1768	218	5216
5	70	3713	296	7856
5	70	3691	294	7871
5	80	3817	293	5982
5	90	2215	190	2741
5	100	1056	81	1803
5	100	1242	97	1581
5	130	1116	125	1556
5	160	105	149	0
5	190	107	138	0
5	220	37	101	0
5	260	0	49	0
5	270	40	95	0
6	5	665	204	2526
6	35	784	224	2483
6	70	1243	225	3959
6	100	798	175	2698
6	100	870	170	3696
6	110	2250	208	7172

Appendix C- continued

Core number	Depth (cm)	XRF concentration (ppm)		
		Pb	Zn	Ca
6	120	5412	408	12320
6	125	488	199	3366
6	125	3418	333	10088
6	130	3057	304	7877
6	130	3497	309	8631
6	135	2750	237	11578
6	160	1370	161	3053
6	190	965	104	2106
6	220	1589	105	1899
6	250	1193	88	1500
6	280	824	86	2497
6	310	423	57	0
6	330	882	77	1742
6	330	954	76	2897
7	1	381	159	1446
7	5	355	153	1261
7	10	355	158	1532
7	10	259	133	1443
7	20	177	106	1445
7	25	81	82	1212
7	25	104	102	1309
7	30	0	80	1364
7	30	0	86	1484
7	35	0	82	3285
7	35	30	78	1361
7	70	0	85	6014
7	100	0	98	1276
8	5	676	215	2713
8	20	721	234	3411
8	30	604	153	0
8	35	664	109	0
8	35	690	108	0
8	50	763	98	0
8	60	811	114	1316
8	65	1010	112	0
8	70	771	116	0
8	70	946	115	1443

Appendix C- continued

Core number	Depth (cm)	XRF concentration (ppm)		
		Pb	Zn	Ca
8	75	691	126	1696
8	80	416	120	0
8	100	109	170	0
8	110	75	166	0
8	130	54	143	0
8	160	0	110	0
8	190	0	75	0
8	210	51	120	0
8	210	43	131	0
9	5	767	233	3872
9	35	881	202	2713
9	50	998	198	2311
9	60	1207	209	3010
9	70	2174	254	7627
9	70	2090	217	4839
9	80	2695	224	5263
9	85	3054	275	7046
9	90	3406	299	5059
9	95	2069	217	2398
9	100	1654	145	2051
9	100	1467	115	1667
9	110	1179	110	1480
9	120	608	202	3382
9	130	168	185	0
9	130	189	164	0
9	160	66	116	0
9	190	56	131	0
9	220	34	101	0
9	255	38	112	0
9	315	19	65	0
10	5	700	235	3367
10	35	776	211	2040
10	70	632	145	2215
10	100	1026	147	1886
10	100	1013	141	2414
10	110	1126	147	3603
10	110	966	146	2196

Appendix C- continued

Core number	Depth (cm)	XRF concentration (ppm)		
		Pb	Zn	Ca
10	120	1670	179	2935
10	125	2984	215	4958
10	125	2565	196	2954
10	130	2682	215	3517
10	140	2847	223	4644
10	145	3084	246	3810
10	150	2339	193	3170
10	160	1380	126	1490
10	190	1303	116	1503
10	220	102	171	0
10	250	80	128	0
10	280	47	105	0
10	310	24	76	0
11	5	773	215	2744
11	35	983	215	2645
11	70	1599	238	3331
11	70	1598	231	5086
11	90	2442	237	6754
11	100	3956	349	9060
11	100	4537	327	9611
11	110	3388	267	5940
11	130	1383	94	1448
11	130	1473	96	1949
11	160	251	59	1149
11	170	719	133	1337
11	180	1291	110	1438
11	190	1262	111	1879
11	200	1196	82	0
11	220	773	113	0
11	250	140	123	0
11	280	87	102	0
11	310	50	102	0
11	340	51	84	0
11	370	40	74	0
11	400	0	80	0

Appendix D. Surface sample geochemistry.

Surface sample Number	Latitude	Longitude	XRF concentrations (ppm)			Sand %	Magnetic susceptibility	LOI
			Pb	Zn	Ca			
1a	38.2438307	-90.371499	700	270	5356	6.80	5E-04	5.50
1b	38.2438474	-90.371311	579	251	6586	8.41	5E-04	6.71
1c	38.2437644	-90.3712	709	259	7273	8.56	5E-04	6.49
2a	38.2439519	-90.375753	1118	343	14841	9.45	4E-04	5.26
2b	38.2439674	-90.375591	1120	348	9402	10.25	4E-04	4.86
2c	38.2439932	-90.375469	997	309	10355	8.54	4E-04	5.48
9a	38.244034	-90.376284	1151	318	7978	6.97	4E-04	4.65
9b	38.2440386	-90.376178	1142	338	9014	8.33	4E-04	5.66
9c	38.2440455	-90.376063	1095	314	7851	8.70	4E-04	5.66
3a	38.2440365	-90.377156	1183	370	7075	7.12	4E-04	5.68
3b	38.2440569	-90.377097	1238	366	7440	5.21	4E-04	4.67
3c	38.244071	-90.376935	1235	342	7408	6.06	4E-04	4.85
10a	38.2441137	-90.378344	1154	360	6772	11.52	4E-04	5.86
10b	38.2441238	-90.378236	1143	349	17021	10.97	4E-04	4.92
10c	38.2441438	-90.377959	1167	360	8657	10.51	4E-04	5.87
4a	38.2441958	-90.379181	1136	339	8466	6.82	4E-04	5.87
4b	38.2442122	-90.379175	1161	343	8772	8.60	4E-04	6.09
4c	38.2442316	-90.378933	1128	351	9514	14.26	4E-04	6.90
5a	38.2443187	-90.379891	1246	338	7596	6.22	4E-04	5.05
5b	38.2443128	-90.379657	1153	325	7702	10.22	4E-04	6.48
5c	38.2443255	-90.379513	1244	357	9898	8.68	4E-04	5.25
11/12a	38.2443541	-90.3710411	1172	314	7683	8.64	4E-04	4.85
11/12b	38.2443647	-90.3710216	1104	334	8932	12.11	4E-04	5.25
11/12c	38.2443843	-90.3710053	994	317	8006	14.29	4E-04	5.86
6a	38.2443732	-90.3711671	984	316	8093	17.81	4E-04	5.25
6b	38.2443811	-90.3711537	1006	310	7544	11.93	4E-04	5.47
6c	38.2443897	-90.3711368	945	310	8231	13.41	4E-04	4.83

Appendix E. Geochemical and textural results for core 12.

Sample number	Pb	Zn	Ca	Ba	Magnetic susceptibility	LOI	Sand %
					Core 12 Sample Analyses		
	XRF <250						
1	1213	392	10562	530	4E-04		8.2
2	1108	332	8495	570		8.87	9.1
3	1248	337	7589	606	4E-04		5.2
4	1379	354	6356	595		5.53	3.7
5	1370	354	7233	627	5E-04		2.9
6	1548	395	8120	655		5.44	3.0
7	1504	342	6167	567	5E-04		3.2
8	1389	353	6558	654		5.85	3.4
9	1329	346	6473	655	5E-04		1.5
10	1164	286	4548	636		5.44	1.7
11	1279	340	5579	712	5E-04		2.9
12	1287	341	5905	647		5.09	3.0
13	1309	331	5616	476	5E-04		3.1
14	1474	360	6539	626		6.73	3.4
15	1477	322	5335	412	5E-04		3.3
16	1392	298	5635	653		4.43	3.2
17	1443	299	6833	617	5E-04		3.2
18	1525	325	6808	512		4.83	3.3
19	1577	290	6919	496	5E-04		3.0
20	1605	284	8223	578		4.84	2.6
21	1603	295	8131	613	5E-04		2.5
22	1826	315	10486	616		4.44	2.5
23	1842	313	11100	422	5E-04		2.7
24	2242	345	13042	603		4.85	2.7
25	2195	343	10809	684	5E-04		3.8
26	2791	361	13416	648		5.23	3.4
27	2932	355	14254	509	5E-04		3.9
28	3127	364	13202	568		4.22	3.8
29	3581	366	14311	568	4E-04		4.2
30	3506	381	15544	670		3.83	3.6
31	3621	364	15101	579	4E-04		4.7
32	4276	380	16483	593		3.61	6.6
33	5401	447	15998	495	4E-04		4.3
34	5833	469	15175	567		4.23	4.7
35	5702	439	15744	564	5E-04		4.5

Appendix E - continued

Sample number	Pb	Zn	Ca	Ba	Magnetic susceptibility	LOI	Sand %

Core 12 Sample Analyses

XRF <250

Sample number	Pb	Zn	Ca	Ba	Magnetic susceptibility	LOI	Sand %
36	5561	444	13610	435		5.26	5.0
37	4848	408	11318	476	5E-04		4.6
38	4071	334	7912	604		4.66	4.3
39	3464	272	7743	466	4E-04		4.3
40	2784	222	4331	587		4.44	4.0
41	1353	162	2870	604	5E-04		5.8
42	1638	134	4624	552		3.83	8.8
43	2183	152	3929	627	5E-04		5.7
44	1099	127	4090	600		3.22	8.2
45	1003	104	3539	395	4E-04		7.2
46	1574	130	4059	600		4.23	7.5
47	1251	131	4551	527	5E-04		3.9
48	1300	111	3368	359		4.02	3.8
49	2922	138	4227	523	5E-04		5.8
50	1845	148	4316	602		4.23	6.2
51	716	120	3206	547	4E-04		6.8
52	344	69	2338	500		3.61	3.8
53	504	69	2835	442	4E-04		3.8
54	1020	82	3311	483		4.24	5.4
55	956	104	3527	554	3E-04		8.6
56	1153	162	3249	639		3.62	9.8
57	1224	132	3310		3E-04		8.4
58	2298	155	4986	634		4.84	6.5
59	1413	157	3894	667	4E-04		9.4
60	1767	174	5427	556		3.42	12.9
61	1458	147	3890	627	4E-04		17.3
62	1224	140	4971	508		4.03	14.1
63	2197	155	4256	552	4E-04		9.6
64	2256	141	4713	590		4.23	20.9
65	907	141	3935	446	2E-04		47.5
66	945	146	3401	449		3.82	19.7
67	1311	158	3972	614	3E-04		20.4
68	916	136	4897	428		4.64	8.9
69	2303	127	4864	557	3E-04		17.7

Appendix E - continued

					Core 12 Sample Analyses		
	XRF <250						Sand
Sample number	Pb	Zn	Ca	Ba	Magnetic susceptibility	LOI	%
70	1696	182	4692	485		4.44	16.3
71	837	128	3090	570	3E-04		26.3
72	585	119	3648	530		3.43	36.5
73	434	96	2453	438	2E-04		46.9
74	627	114	2633	542		4.03	41.2
75	590	101	2488	537	2E-04		7.6
76	466	104	2627	605		3.22	16.9
77	611	163	3001	680	2E-04		10.3
78	234	136	2664	519		5.73	7.4
79	285	145	2023	579	2E-04		9.3
80	299	145	3954	613		4.03	11.6
81	274	166	2879	582	1E-04		15.9
82	225	176	3275	688		8.94	20.3
83	211	175	2799	675	2E-04		20.8
84	144	138	2978	569		3.21	34.4
85	112	106	4019	536	2E-04		55.5
86	235	156	3910	599		3.82	22.7
87	194	159	4513	628	2E-04		17.3
88	118	145	3328	573		3.42	22.2
89	92	134	2463	587	2E-04		24.9
90	132	179	3423	564		4.23	14.4
91	76	108	2565	598	1E-04		53.9
92	77	105	1981	459		2.81	62.7
93	145	156	3199	560	3E-04		20.2
94	190	169	3379	536		5.03	11.1
95	126	155	3781	594	4E-04		5.8

Appendix E - continued

Sample number	Pb	Zn	Ca	Ba	Magnetic susceptibility	LOI	Sand %
			Core 12 Sample Analyses				
	XRF <250						
96	127	157	1984	545		4.84	38.5
97	116	167	2708	677	3E-04		41.6
98	154	149	2924	585		3.82	28.9
99	83	126	2810	536	3E-04		40.2
100	93	139	2162	582		3.61	36.4
101	101	133	2413	623	3E-04		23.6
102	177	213	3190	424		5.44	22.1
103	99	138	3278	305	3E-04		24.1
104	128	199	3747	410		9.73	25.4
105	90	173	2017	394	4E-04		28.3
106	89	133	3045	489		3.82	23.1
107	171	141	3954	473	3E-04		32.5
108	95	147	1978	483		4.23	19.8
109	61	131	2001	454	3E-04		36.9
110	66	128	2191	391		2.81	49.5
111	67	117	2615	457	3E-04		46.8
112	97	151	2782	366		4.64	29.2
113	116	207	2458	448	2E-04		22.3
114	116	188	3076	340		7.27	29.4
115	84	155	3004	421	2E-04		15.6
116	93	159	3212	361		7.68	29.6
117	99	158	3785	365	2E-04		7.47	31.3
118	91	178	5366	144		14.20	32.0
119	52	108	3665	508	2E-04		5.43	18.0
120	76	178	3380	481		5.44	41.1

Appendix E - continued

Sample number					Core 12 Sample Analyses		
					XRF <250		
	Pb	Zn	Ca	Ba	Magnetic susceptibility	LOI	Sand %
121	79	146	4623	313	2E-04	6.25	26.1
122	56	118	3977	439		5.84	18.0
123	96	175	3027	547	3E-04	5.43	16.0
124	73	137	2661	409			13.1
125	83	140	2788	436	3E-04	4.62	21.1
126	82	161	3725	458		6.06	7.4
127	76	142	3330	419	3E-04	4.65	32.4
128	48	106	2342	349		2.61	58.5
129	32	93	2221	399	2E-04	3.85	46.6
130	62	121	2711	456		4.43	26.8
131	41	95	2212	486	3E-04	3.02	36.5
132	41	105	1470	392		3.01	54.7
133	95	174	2731	428	3E-04	5.44	21.7
134	44	100	2403	265		5.24	38.7
135	80	145	3316	394	3E-04	5.63	15.0
136	75	148	3586	469		5.66	14.1
137	78	135	2863	536	3E-04	4.23	28.7